Resilience-based Facade Design Framwework

Kyujin Kim

MSc Thesis in Building Technology

Building Technology Graduation Studio
MSc Architecture, Urbanism & Building Sciences

Title:

Resilience-based Facade Design Framework
A case study on facade systems under seismic and heat hazard

Author:

Kyujin Kim
5570743
July 3, 2023

Mentors:

Simona Bianchi *Structural Design & Mechanics, TU Delft*
Alessandra Luna Navarro *Facade & Product Design, TU Delft*

External Adviser:

Jonathan Ciurlanti *Arup Amsterdam*

Delft University of Technology

Acknowledgements

Reflecting on my master's studies in the Building Technology track at TU Delft, I am grateful for the positive reception I received from the faculties AE+T. They recognized the value of my work and provided me with the right input to grow. Additionally, I experienced the Dutch way of education, which emphasizes clear pitching of ideas and reflecting on and improving them.

Although I did not expect to delve into the topic of facade resilience, I am glad to have discovered a field that aligns with many of my interests. Working on this thesis was a genuinely enjoyable experience, largely thanks to my mentors. I would like to thank Simona Bianchi for all the fruitful sessions where she shared her knowledge and provided practical guidance. Alessandra Luna Navarro, I am thankful for the questions you asked during our mentoring sessions, which broadened my perspective on the approach. I would also like to express my gratitude to external adviser Jonathan Ciurlanti for his consultations and for giving me the opportunity to present this thesis at Arup. This experience reminded me of the practical applicability of my work.

I am grateful to all my friends in Delft and Seoul for their constant support and concern. Last but not least, I want to thank my family for their unwavering support that made all of this possible.

Abstract

With the increasing number and diversity of disruptive events imposed on the built environment, it is becoming more important to identify a system's resilience. Quantifying resilience is crucial because it enables effective preparation, recovery, and adaptation to the uncertainties that lie ahead. This study focuses on the resilience of building facades, which play an integral role in a building's various functions, including environmental, structural, and operational performance. Facades contribute significantly to the total building damage, yet their resilience is not sufficiently addressed in current discourse. This research aims to bridge this research gap by addressing the question: How can the integrated resilience of a facade system to multiple hazards be identified? A methodology was developed with two objectives: 1) evaluating facade resilience, and 2) integrating this methodology into the facade design process.

The Resilience-based Facade Design Framework assesses the impact of multiple hazards on a building facade, taking into account its fragility. The framework provides a quantitative approach to decision-making regarding facades, both in the early design stage and in retrofitting. Users can input project location, building geometry, and existing facade specifications to create a facade package. This package is then assessed for resilience under different hazards, including seismic and heat hazards. The resilience performance, defined in terms of resilience loss and economic loss, is integrated into a multi-attribute decision-making tool. This tool allows users to select a facade package based on its integrated resilience performance value, or to configure a facade package based on individual enhancements to resilience attributes.

Keywords: Facade Resilience, Multi-hazard Approach, Quantitative Resilience Assessment, Resilience-based Design, Multi-attribute Decision Making

Contents

List of Figures

List of Tables

1 Research Framework

1.1 Background

Sustainable Development: Building for Resilience

Designing structures to accommodate the increasingly frequent and severe disturbances is a way of developing not only for the present but also for future generations (Brundtland & Khalid, 1987). Resilience is deeply linked to sustainable development. As the frequency and severity of disturbances increase, it is essential that local governments adopt multi-hazard approaches to building resilience. This is particularly important given the systemic and cascading nature of risk, which is often fueled by climate change (United Nations, 2022). The Sustainable Development Goals 11.b target aims to "By 2020, substantially increase the number of cities and human settlements adopting and implementing integrated policies and plans towards inclusion, resource efficiency, mitigation and adaptation to climate change, resilience to disasters, and develop and implement, in line with the Sendai Framework for Disaster Risk Reduction 2015-2030, holistic disaster risk management at all levels" (United Nations, 2022).

1.2 Problem Statement

The current procedure for designing facades does not ensure resilience under multi-hazards, despite the significant damage and danger posed by the fragility of facades. This is due to a lack of tools that can apply hazard to the performance analysis and induce design factors that determine resistance to proposed risks. To address this issue and facilitate the resilience-based design of facades, a quantitative resilience assessment procedure needs to be implemented. This requires evaluating the complete range of building performance that the facade contributes to, including thermal and structural characteristics, during disruptive events and the recovery phase that follows.

Additionally, there is a lack of available tools that can solve the multi-hazard problem, as existing procedures do not consider the combined effect of multi-hazards. It is difficult to understand how the performance of various building components of the façade work together to form overall resilience to multiple hazards.

With the increasing number and diversity of disruptive events imposed on the built environment, the need for robust methods that allow for the quantification of resilience is becoming increasingly important. However, existing frameworks are mostly qualitative, which has limited applicability in emergency cases or retrofit scenarios with high uncertainties and lack of time for broad assessments. This issue is further compounded by the fact that indices that express the degree of hazard and performance metrics that assess building performance vary from study to study.

1.3 Research Objective

The purpose of the research is to promote facade resilience, to facilitate resilience based design decision making. More specifically, is to identify the design/decision parameters that impact the resilience of a facade system under two or more hazard factors. With more knowledge of these determinants will allow facade resilience to be included in early decision making, enable a more integrated approach to facade design.

The proposed research outcome is the ”Resilience-based Facade Design Framework”. This framework serves as a digital workflow for a design decision support tool that employs quantitative resilience assessment. It takes hazard and facade fragility properties as input parameters and generates the resilience levels of facade systems in response to multi-hazards as output variables.

The framework aims to address the complexity of facade design by utilizing a multi-hazard approach. By considering the potential impact of different hazards on the facade and presenting design solutions that address those hazards, the framework helps architects and engineers make informed decisions about the design of the building's facade that enhance its overall resilience.

1.4 Research Question

The main research question is:

> **What methodology can be developed to assess the resilience of facade systems under multiple hazards and integrate into the facade design process?**

The main research question can be further refined into domain-specific subquestions, which will be addressed through state-of-the-art research:

- What are the different types of hazards that impact the resilience of a building's facade, and what intensity indices are commonly used to quantify these hazards?
- Which performance domains of a facade need to be evaluated to determine its resilience, and what performance indices can be employed for quantification?

Questions related to the design and implementation of an actual framework through a case study approach are as follows:

- How to assess the integrated resilience of a facade system to multiple hazards?
- What metrics can be employed to compare the resilience of different facade systems?
- How can resilience-based framework be implemented in design decision making?

1.5 Methodology

The thesis aims to deliver a digital tool that aids in facade design decision making through quantitative resilience assessment. The research draws upon multiple domains of knowledge, including 1) Facade Resilience, 2) Facade Design Process, and 3) Quantitative Resilience Assessment, which are integrated throughout the research process. The methodology of the thesis follows the process of a digital tool development, including the following steps :

Domain Analysis In order to establish the overall framework of the design tool, a state-of-the-art research is conducted on the three sections of the research. The *Application Scenario* of the tool is researched to define the problem domain that the tool should be able to address. The goal is to identify the major risks posed to facades and their impact on the facade. The *Potential Users* of the tool are investigated to define the priorities of the functions the tool should serve. Specifically, the research focuses on robust methods where it can make use of existing databases while still providing quasi-design solutions during the preliminary facade design stage. *Measurable Resilience* is explored to identify all the input and output variables that are necessary to quantify the resilience of a specific system. The research examines what intensity indexes, performance indicators, and resilience metrics are relevant for measuring facade resilience.

Framework Design Based on the key features identified from the domain analysis, the framework for the design tool is developed, which includes the general architecture and digital data flow chart. *Multi-Hazard Approach* investigates the impact of multiple hazards on the performance of the functional layer of the facade. *Design Decision Support Tool* configures facade packages with different seismic and thermal fragility aspects. Then, screen the packages to identify those with lower resilience loss. *Quantitative Resilience Assessment* utilizes metrics: Seismic and Heat (hazard); Interstorey Drift and Outdoor Temperature (impact); Structural Stability and Indoor Thermal Condition (performance); Functionality and Recovery Curve (resilience)

Implementation The focus is on implementing the framework in a digital environment, which is composed of different modules that stem from various data types and simulation engines. The *Hazard Analysis* module select the hazard model and analyze the building response. The *Facade / Building Model* module construct a finite element model of RC structural frames and dynamic thermal model of multi thermal zones. The *Resilience Analysis* module processes the simulation of sturctural / thermal performance and the calculation of resilience metrics (functionality loss, economic loss).

Case Study A case study of 18-story office building loated in Izmir, Turkey is used to validate the framework proposed by the research. Response spectrum with 475 return periods and weather data including extreme heat events in Izmir is used for the case study. A decision tree is employed to configure a facade package with a high / low probability of damage. For each facade package, a radar chart is used to plot a set of performance attributes related to resilience loss and economic loss.

Evaluation The evaluation of the tool aims to identify areas for future research and potential changes to be applied. The effectiveness of using a multi-hazard approach in comparison to single hazard analysis, the ease of integration of the design tool into current facade design processes in terms of accessibility and usability, and the efficiency of the digital tool's architecture in data management and consistency of simulation results across domains will be evaluated.

The summary of the methodology is illustrated in Figure 1.1.

1. DOMAIN ANALYSIS	State of Art		
	APPLICATION SCENARIO	POTENTIAL USER	MEASURABLE RESILIENCE
	research question What are the types of risks posed to facade, and how can they be incorporated into the design process to reduce potential damage?	research question How can the facade system be configured for comparative analysis of various performance? How can a tool provide intuitive results while also allowing for fine-tuning?	research question What intensity indexes, performance indicators, and resilience metrics should be used to analyze failure behavior of facade over time?
2. FRAMEWORK DESIGN	Key Feature of the Design Tool		
	MULTI HAZARD APPROACH	DESIGN DECISION SUPPORT TOOL	QUANTITATIVE RESILIENCE ASSESSMENT
	Investigate the impact of multiple hazards on the performance of the functional layer of the facade.	Configure facade packages with different seismic and thermal fragility aspects. Then, screen the packages to identify those with lower resilience loss.	Use the following metrics: - Seismic and Heat (hazard) - Interstorey Drift and T_out (impact) - Structural Stability and Indoor Thermal Condition (performance) - Functionality and Recovery Curve (resilience)
3. IMPLEMENTATION	Module based on Python Scripting Language		
	HAZARD ANALYSIS	FACADE / BUILDING MODEL	RESILIENCE ANALYSIS
	• Select hazard model • Analyze building response	• Finite element model of RC structural frame • Dynamic thermal model of multi thermal zone • Fragility database of seismic / thermal model	• Simulation of sturctural / thermal performance • Calculation of resilience metrics (functionality loss, economic loss)
4. CASE STUDY	Case study of an 18-story Office Building in Izmir, Turkey		
	Response spectrum with 475 return periods and weatherdata including extreme heat events in Izmir is used for the case study	A decision tree is employed to configure a facade package with a high / low probability of damage.	For each facade package, a radar chart is used to plot a set of performance attributes related to resilience loss and economic loss.
5. EVALUATION	Effectiveness Does using a multi-hazard approach result in greater resilience than single hazard analysis?	Accessibility How easily can the design tool be integrated into current facade design processes in terms of accessibility and ease of use?	Efficiency Is the digital tool's architecture efficient in data management and consistent in simulation results across domains?

Figure 1.1: Research Methodology for Framework Development

1.6 Boundary Condition

Resilience can be conceptualized as encompassing four interrelated dimensions: technical, organizational, social and economic (Bruneau et al., 2019). This study is limited to the technical dimension of resilience which refers to the ability of physical systems. Resilience analysis of individual structural units only, interaction with other structure and community as a whole is outside the scope of the study.

This study employs simplified methods to analyze risk and resilience in facade components. These methods rely on an available database, which limits the scope of configurations that can be examined. Additionally, the research is based on a combined method that does not use a single, coherent real-world scenario for data. As a result, the risk intensity, actual impact, and recovery time obtained in this research may not reflect actual values. Despite these limitations, the study aims to provide the most accurate approximation within the given constraints.

2 State of Art on Multi-Hazard Facade Resilience

2.1 Framework for Resilient Facade System

2.1.1 Concept of Facade Resilience

The concept of resilience has arisen as a result of a shift in focus from preventing climate change to preparing for and accepting the future uncertainties brought about by the inevitability of climate change. The National Academy of Sciences defines resilience as "the ability to prepare and plan for, absorb, recover from, and more successfully adapt to adverse events" (National Research Council, 2012, p.16). Thus, the resilience of a system can be engineered by implementing predictive risk assessment and mitigation strategies for focused disturbances.

The growing discourse on resilience in the built environment is largely due to increasing frequency and intensity of external environmental hazards imposed by climate change. This study focuses on a specific aspect of building systems, specifically the resilience of facades. Located on the layer between the exterior and interior of the building, the façade delivers a collection of complex functions including environmental, structural, and operational performance of the building. Therefore, enhancement of facade resilience is directly linked to the overall resilience of the building. Patterson et al. (2017) address the scalability of resilience and argues that targeted exploration to define specific resilience characteristics of a façade system can not only improve the resilience of the façade itself, but also enhance the overall resilience of the larger built environment.

Patterson et al. (2017) provide a pioneering examination of the principles of facade resilience, by demonstrating how principles of resilience adopted at the city level can be interpreted within the context of a building envelope. Environmental factors such as flood, extreme temperature, extreme wind, and fire, as well as factors related to security, durability, adaptability, recovery, and health and comfort, are identified as important attributes in achieving facade resilience.

Despite the potential impact that facade resilience could have on the overall resiliency of the built environment, it is a topic that is not yet sufficiently addressed in current discourse. According to the current building code, ASCE 7, facade components are classified as non structural elements. The façade design criteria for seismic design can be found in the section Seismic Design Requirements for Non Structural Components (American Society of Civil Engineers, 2010). However, non structural elements can turn out to be more vulnerable to disruptive events compared to the primary structure because resilient technology is not sufficiently considered in the design process. The resulting structural damage can can lead to even greater economic losses. A study of the 1994 Northridge earthquake showed that 75% of buildings were susceptible to damage to non structural elements (Charleson, 2008).

Technical design solutions, such as designing a proper connection between facade and the primary structure, can significantly reduce damage from earthquakes as it determines the interaction between the two systems (Baird et al., 2011).

Facade resilience not only enables enhancement of a single performance of the facade, but also facilitates improvements in multiple performance domains associated with it. Bianchi et al. (2022) investigate the resilience of building envelope design solutions under long-term impacts of climate change and the immediate impact associated with an earthquake. Energy efficient and earthquake resistant systems were applied to verify the efficacy of integrated resilience enhanced solutions and the results show that the reduction of resilience loss was further enhanced when an integrated solution was applied. Facade resilience strategy can address multiple performance issues, but not all cases are complementary. Thus, it is crucial to conduct a comparative analysis to balance performance and resilience aspects before reaching a final decision.

2.1.2 Resilience-based Frameworks

The current state of research on viewing facades from the perspective of resilience is limited, with few studies having been conducted. These studies use a qualitative assessment approach, which employs conceptual frameworks and expert assessments to measure resilience. However, a quantitative approach, which uses numerical measurements, is needed to directly compare buildings and quantify potential improvements in order to promote the direct adoption of facade resilience in the design process.

Favoino et al. (2022) presents a qualitative evaluation framework, known as the Façade Resilience Evaluation Framework (FREF), for assessing the risks associated with specific facade designs in specific geographical and social contexts, and for identifying measures and mitigation strategies to reduce such risks in a climate change scenario. The framework is applied to a case study of a 41-storey high-rise building with a fully glazed facade, located in an area that poses both climate and geo-topographical risks. The study explores different mitigation measures at different design stages, both pre- and post-contract, and finds that implementing resilience reviews in the early stages of design can have a greater impact and lower costs of mitigation. Attia et al. (2021) conducted a literature review on the qualitative performance of cooling technologies during extreme events, and found that direct comparison between technologies is needed. To address this limitation, a quantitative assessment approach with specific boundary conditions was proposed as a future study.

Resilience-based frameworks are analyzed with a focus on how the framework is structured. The comparison of various resilience frameworks in the Figure 2.1 highlights their differences in focus, scale, and hierarchy. The outcomes of these frameworks are either the resiliency measurements or design solutions. For example, City Resilience Framework (The Rockefeller Foundation & Arup, 2014) measures the resiliency of a target project through indicators, Resilient Cooling Strategies Assessment Framework (Zhang & Kazanci, 2021) measures the resiliency of a cooling technology, and Facade Resilience Evaluation Framework (Favoino et al., 2022) calculates the risk of a stressor on a facade. In Resilience-based Engineering Design Initiative Framework (Almufti & Willford, 2013), the outcome is a design solution that meets resilience-based criteria.

Arup's Resilience-based Engineering Design Initiative (REDi™) Rating System is a framework for implementing Resilience-based design (RBD) in building projects. The framework

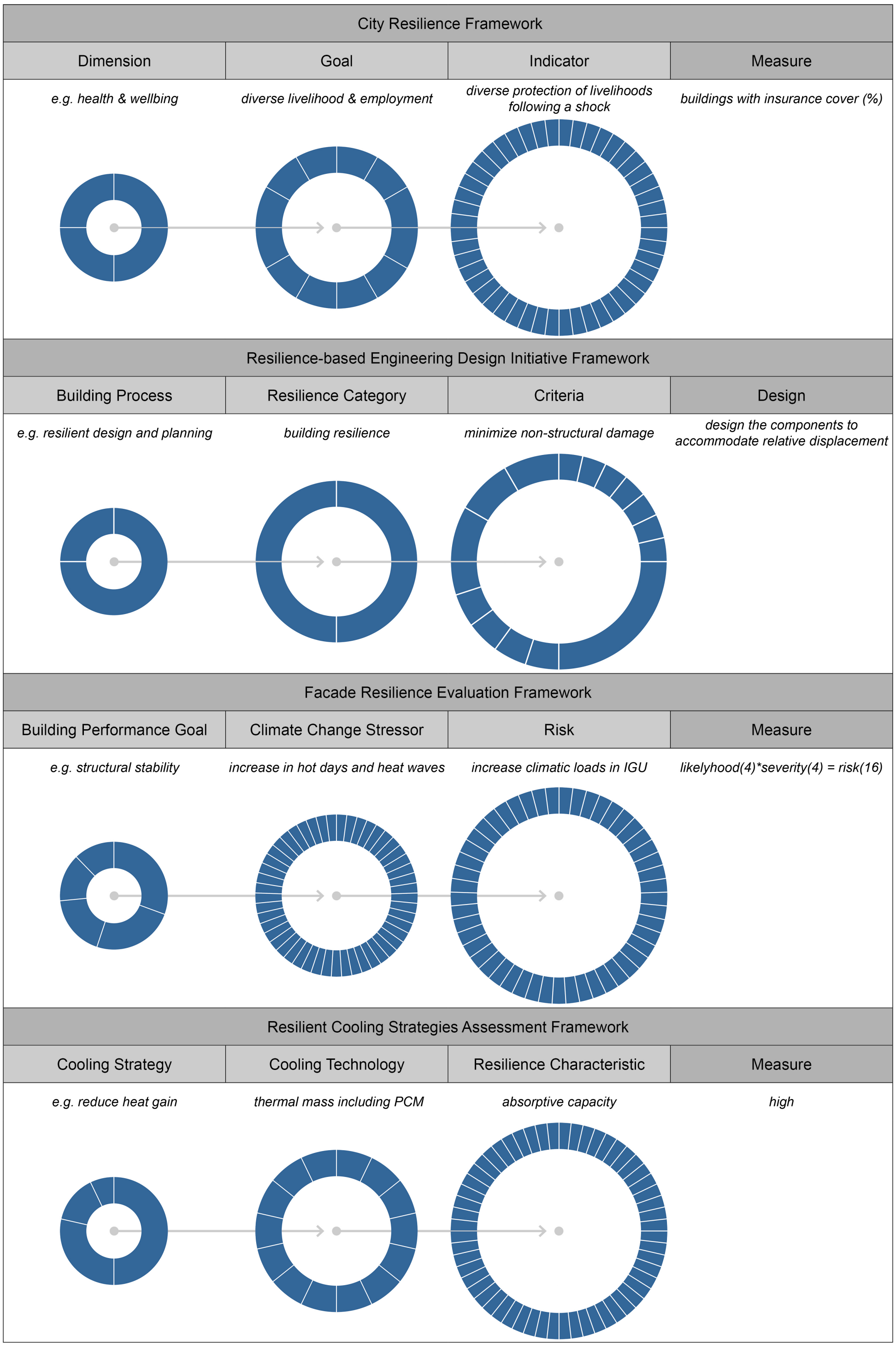

Figure 2.1: Comparison of Resilience Frameworks

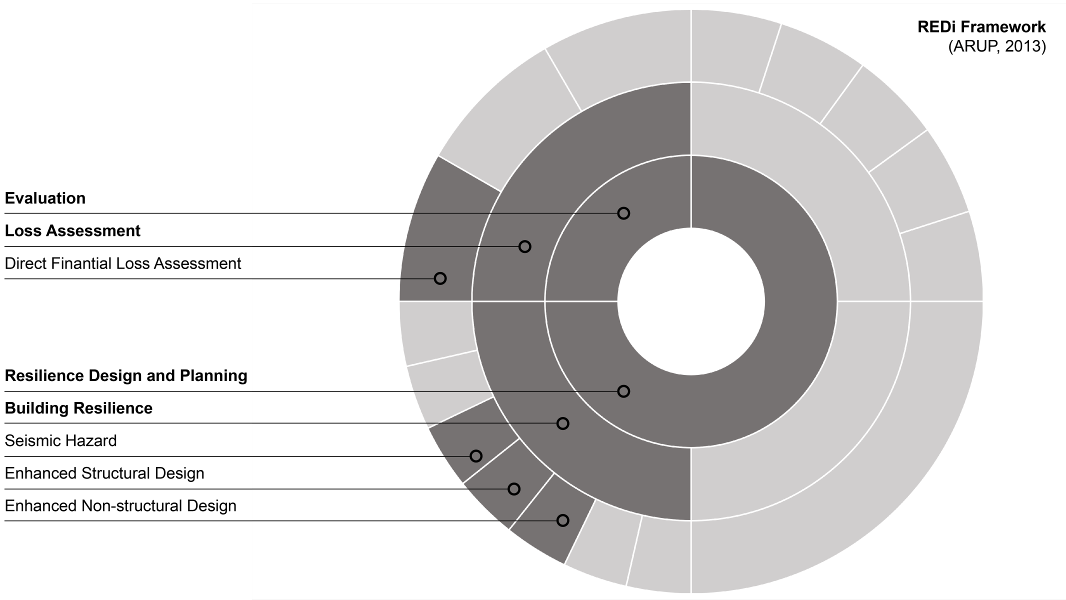

Figure 2.2: Resilience-based Design for Facades

is divided into four categories: Building resilience, which focuses on minimizing damage to structural, architectural, and MEP components; Organizational resilience, which deals with contingency planning for utility disruption and business continuity; Ambient Resilience, which addresses external hazards that could damage the building; and Loss Assessment, which evaluates the financial losses and downtime resulting from the design measures to evaluate their effectiveness.

RBD is a holistic process that involves identifying and mitigating risks. It incorporates code-based and performance-based design approaches to minimize damage in case of disruptive events. Code-based design provides guidelines for design solutions, while performance-based design uses simulations to explicitly demonstrate the project's performance. RBD goes beyond code and performance-based designs by taking into account all relevant building components, external factors, and post-damage contingency planning (Almufti & Willford, 2013). The RBD approach achieves the goal of sustainability and resilience by minimizing disruption impact and facilitating prompt recovery to operational status.

Adopting a RBD approach in the facade design process can enhance the overall building resilience especially with respect to ”Building Resilience” and ”Loss Assessment”. As mentioned in Section 2.1.1, facade is exposed to multiple hazards at the forefront, involves non-structural building components, and significantly contributes to economic loss during disruptive events. It encompasses not only structural performance, but also thermal and operational functions. By expanding the existing RBD framework to include specific factors for facades, facade resilience can be addressed as part of the broader goal of creating a resilient built environment (illustrated in Figure 2.2).

2.2 Multi-Hazard Approach

2.2.1 Multi-Hazard in Facade

A multi hazard approach is essential in defining resilience, in order to comprehensively address the diverse range of challenges that buildings encounter. The city resilience framework developed by Arup shows that the recent resilience concept has shifted from traditional disaster risk management that relate to specific hazards to enhancing the performance in the face of multiple hazards, acknowledging the possibility of a wide range of disruptive events (The Rockefeller Foundation & Arup, 2014). The Facade Resilience Principle also emphasizes the importance of building design that anticipates future uncertainty, i.e., building design that is not limited to specific weather conditions but can adapt to a variety of circumstances (Patterson et al., 2017).

Multi-hazard is defined as "(1) the selection of multiple major hazards that the country faces, and (2) the specific contexts where hazardous events may occur simultaneously, cascadingly or cumulatively over time, and taking into account the potential interrelated effects" (UNDRR, 2019, p53). This indicates that the origins and effects of hazards can be diverse, they can stem from one cause and have a singular impact, or from multiple causes with multiple impacts.

According to the division made by UNDDR (2020), hazards are classified into 8 types (e.g., meteorological, extraterrestrial, geohazard, environmental, chemical, biological, technological, societal) depending on how they originate. According to this classification, heatwave is categorized in this hazard list as a meteorological / temperature-related hazard, and earthquake as geohazard / seismogenic hazard.

The impact of multi hazards on buildings can be interpreted as "relative risks posed by multiple hazards and the synergies or trade-offs in protecting for different hazards" (Padgett & Kameshwar, 2016, p.41). The impact of multi hazards varies depending on the interrelation between hazards and how they interact through structural performance. Padgett and Kameshwar (2016) present a classification of multi-hazard combinations based on three distinct criteria: hazard occurrence (non-concurrent, concurrent, cascading), influence on design parameter selection (competing, complementary), and influence on fragility and risk (amplifying, diminishing). This classification of multi hazards helps to have a structure on which hazards in the project are seen as the main determinants of design and how mitigation strategies should be proposed.

In a case of a warehouse building facade (Dimitar et al., 2019), inter-storey drifts produced by relatively weak earthquakes increased the vulnerability of panel fastenings to subsequent wind suction effects. From this we can infer that Earthquake and Wind have some degree of joint probability of occurrence, and that Earthquake was Wind's amplifying hazard. Therefore, in order to reduce overall risk to the facade, it can be seen that complementary connection design for both hazards needs to be improved. The multi hazard approach therefore means taking into account both the individual impact of two or more hazards on a building and the combined impact resulting from the interaction between hazards.

Multi-hazard on a facade level imposes extreme loading configurations, including natural, accidental, or human-induced events (Favoino et al., 2022). The hazards mainly associated with facades are blast, wind, seismic and heat. Studies on how each of these hazards affects facades are as follows: blast enhancement of glazing curtain walls (Bedon & Amadio, 2018), wind risk assessment for cladding and glazing (Beers, 2011), seismic performance enhancement of facade systems (Baird et al., 2011), heat stress risk mitigation with PCM (Ramakrishnan et al., 2017). In facade engineering field, these hazards are interpreted as exceptional loadings applied to the facade, and design regulations provide minimum acceptable standards, not based on the quantification of risk as in earthquake engineering. According to Eurocode 8, Seismic requirements for nonstructural components aim to ensure adequate clearance gaps to accommodate the relative horizontal displacements of primary buildings (European Comitee for Standardisation, 1998). In US FEMA 450, specific interstory drift value are given for 'glazed curtain walls', 'storefronts' and 'partitions' (Building Seismic Safety Council, 2003). Blast requirements for facade components are indicated in UFC 4-010-01 which aims to ensure dynamic material strength (US Department of Defense, 2018). Components are expected to undergo inelastic deformation, and connections are designed for the out-of-plane ultimate flexural capacity of the attached components.

A summary of how multi-hazards are addressed for which structural types and for which hazards are covered in the review paper (Jami et al., 2022). For high-rise buildings, wind and seismic are commonly set as hazard factors for assessing multi-hazard effects on building. Frameworks that standardize and unify existing probabilistic hazard assessment methods used for different natural actions are pointed as a challenging task. Multi-hazards effects on facades is a relatively new field of research. Table 2.1 shows that few studies have shown frameworks that use combined hazard models to evaluate the performance of building envelopes. Multi-hazards applied in the literature consists of a combination between natural events (Ouyang et al., 2020), a combination of natural and human-induced (Bedon & Amadio, 2018), or a combination of natural and climate condition (Bianchi et al., 2022).

Table 2.1: Overview of Multi-Hazard Framework

Literature	Hazards	Assessment
(Ouyang et al., 2020)	Directional Wind, Rain	Building Envleope
(Joyner & Sasani, 2018)	Seismic, Wind	RC Building
(Bedon & Amadio, 2018)	Seismic load, Blast event	Glass Curtain Walls
(Bianchi et al., 2022)	Seismicity, Weather Condition	Precast Concrete Panels, Glazed Curtain Walls

2.2.2 Multi-Hazard Design of Facades

In structural engineering, the risk-based design approach is a method of identifying the likelihood and severity of risks to a structure and establishing design criteria that are resistant to those risks. Typically, individual risk assessments are carried out for a single hazard, which allows us to determine the necessary structural performance for that particular hazard. However, it is important to note that while designing to seismic performance criteria can secure a structure's ability to withstand earthquakes, it does not ensure its resistance against wind. To address this, a multi-hazard approach can be implemented, which can enhance the structure's reliability in areas that are exposed to multiple hazards (Chiu & Chock, 1998).

When designing facades for multiple hazards, several design criteria-sometimes in conflict-must be satisfied. This is because the favorable resisting behavior differs depending on the hazard. In the common approach for designing facades for multiple hazards, the design

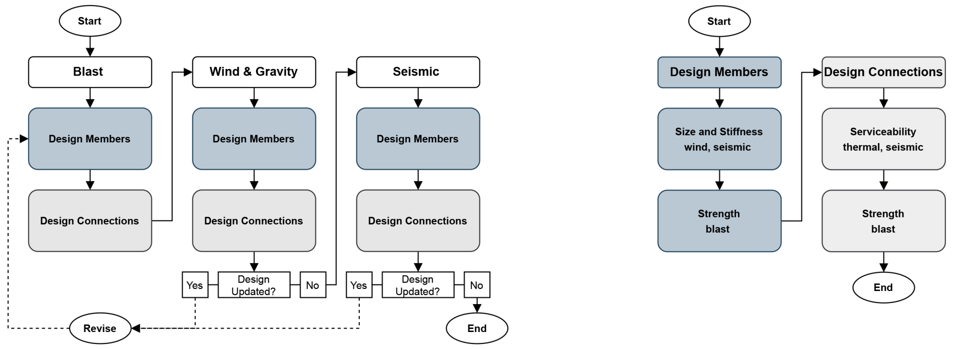

(a) Compartmentalized by discipline

(b) Compartmentalized by task

Figure 2.3: Facade design process for multiple hazards, adapted from Mckay et al. (2015)

process is compartmentalized by load case (illustrated in Figure 2.3). For each load case, size of all members and connections are determined in an individual sequential steps. For this reason, synergies and conflicts between load cases are often overlooked, causing unnecessary iterations to reach the final design (Mckay et al., 2015). As a complement to this, a holistic approach, with a rather simple structure in which design members are proceeded and design connections are determined, all criteria and their interactions associated with multiple hazards are integrated and applied at each steps. When coordinating design criteria for multiple hazards, it is necessary to focus to the facade system features, which have the opposite effect depending on the load case. A design decision made in connection with a particular building performance can affect performance in other area; a tradeoff in the resistance to the hazard.

Table 2.2 provides a comparative analysis of how certain features of the facade system require different design criteria depending on the hazard. One of the most controversy feature is the weight of the facade system; The added mass provides increased inertial resistance to the blast load, and resists the heat load by flattening the fluctuating heat flow, but this increased mass can rather impose an additional seismic load on the supporting structure. By concentrating on these special features, the integrated design criteria-ranging from facade system selection, design detailing to elements and connections sizing-can be determined at a reasonable consensus that considers the multiple hazards.

Multi-hazard design of facades indicates that a different design process is taken into account than when only a single hazard is considered, and that a design decision is made under a design objective that satisfies multiple design requirements.

Table 2.2: Influence on selection of design parameters as competing or complementary hazards

Design Criteria	Blast	Seismic	Wind	Heat
Weight of the System	Added mass provides increased inertial resistance to blast loads (Mckay et al., 2015)	Light weight systems result in lower connection forces and lower imposed loads on the supporting structure (Mckay et al., 2015)		Adding thermal mass locks the heat away and prevents overheating (H. Sun et al., 2022)
Flexural Strength and Stiffness	Reinforcement can lead to unnecessary high blast reations (Mckay et al., 2015)		Additional flexural stiffness provides resistance to wind loads (Mckay et al., 2015)	
Impact Resistance	Laminated lazing can transfer high reaction forces into supporting structural elements (Mckay et al., 2015)		Laminated glazing resist impact from a wind-borne debris missile (Mckay et al., 2015)	
Gap between panel and frame		Seismic gaps thus aim to prevent the infill panel from interacting with the frame (Baird et al., 2011)		Point thermal bridge effect can occur which can lead to a actual thermal loss from the envelope (Theodosiou et al., 2014)

2.3 Quantitative Resilience Assessment

2.3.1 Engineering Resilience

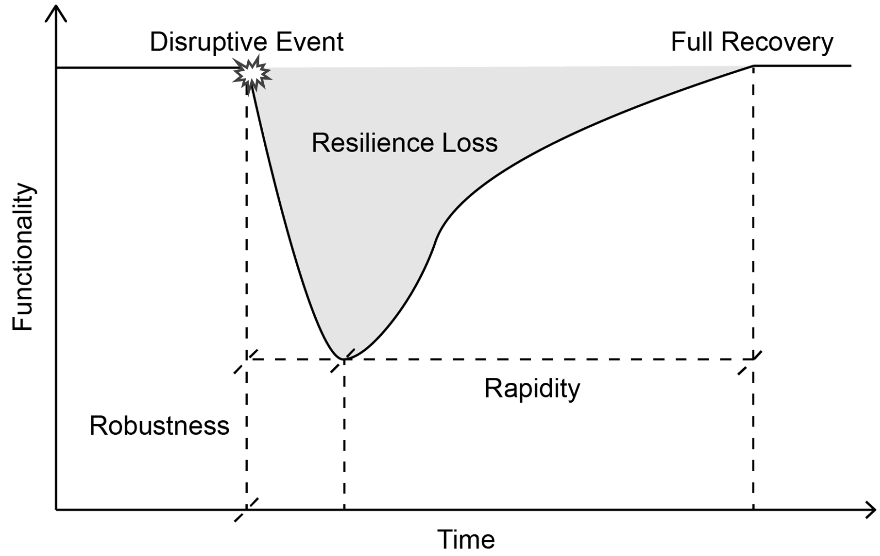

Figure 2.4: Engineering Resilience

Resilience of a system can be achieved by reducing the probability of failure, minimizing the consequences of failures, and shortening the time to recovery (Bruneau & Reinhorn, 2006). The resilience function, illustrated in Figure 2.4, explains the time variation of functionality and its relationship to response and recovery. Engineering resilience entails enhancing the system's robustness and rapidity to decrease its vulnerability (loss). Robustness refers to the ability to withstand a given demand, mathematically applied to the residual functionality right after a disruptive event. Rapidity refers to the capability to achieve recovery in a timely manner, which applies to the slope of the functionality curve.

Damage-resistant technologies aim to reduce the damage associated with hazards. To reduce earthquake damage, design solutions that disconnect the facade system from the primary structure can be achieved. This can be done by introducing seismic gaps between the infill panel and the frame, as well as using tie-back connections that minimize the interaction between the cladding systems and the frame (Baird et al., 2011). A partial disconnection is also possible by utilizing energy dissipative connections that are designed to yield before the facade yields. The resistivity of overheating is tested in cooling technologies that fall under the categories of reducing heat gain, removing sensible heat, enhancing personal comfort, and removing latent heat (Attia et al., 2020). These cooling technologies can be both passive and active, achieved by utilizing advanced glazing and shading, as well as evaporative and ventilative envelope surfaces.

2.3.2 Resilience Assessment Process

The resilience assessment process follows the same basic structure as the probabilistic risk assessment methodology. Risk is defined as the product of hazard, exposure, and vulnerability. Hazard is a potential stressor expressed as a hazard curve, which shows the probability of an event happening during a given period. Exposure is the number of people, buildings, or monetary value of exposed elements at risk specific to a location. Vulnerability refers to the system's ability to withstand the impacts of hazards on elements at risk given the intensity of the hazard. The total expected loss is determined probabilistically as a function of hazard, exposure, and vulnerability.

Probabilistic resilience assessment supplements risk analysis by considering the entire time range from functionality drop to recovery. The process of probabilistic assessment is illustrated in Figure 2.5. The resilience function, known as the functionality function, includes functional loss, determined by the vulnerability function, and functional recovery. Vulnerability is determined by the mean value of distributed functionality loss, which varies based on the system's resistance to stressors and the extent of resulting damage. The fragility function breaks down the building system into several limit states that the system may go through and quantifies the probability of exceeding such limit states. Information on the damage loss of each limit state is used together to calculate the overall loss.

In summary, the hazard intensity measure (IM) of a particular facade system is determined by its location. Each system has its own unique fragility function, associated damage, and recovery path, which ultimately creates a unique functionality function.

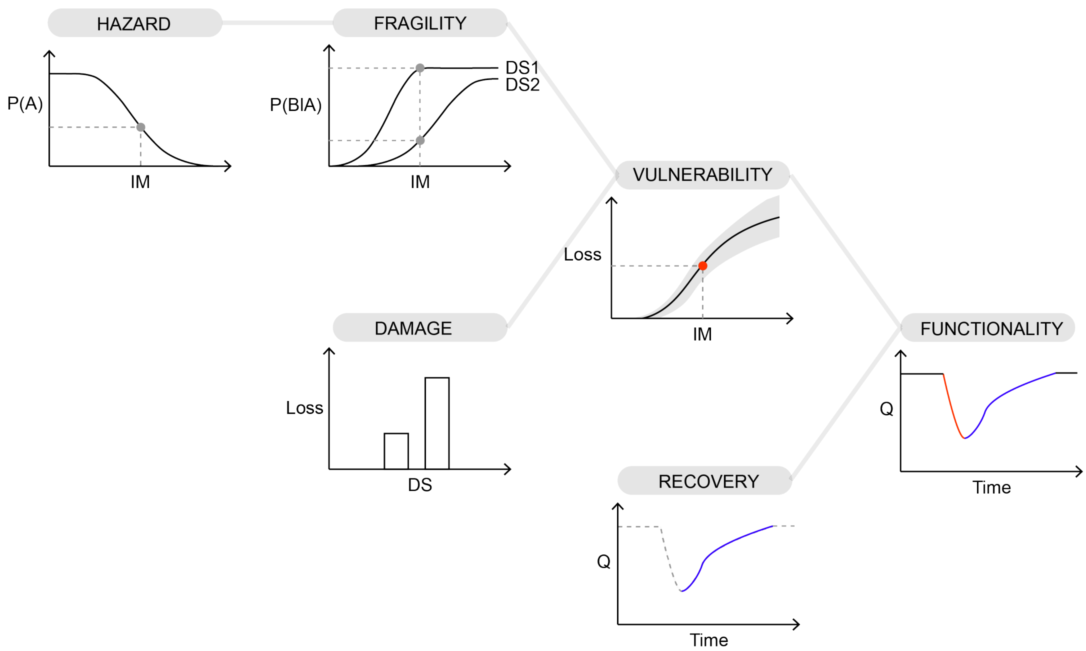

Figure 2.5: Probabilistic resilience assessment

2.3.3 Building Performance Evaluation

The risks imposed on a façade are complex as it serves as a structural barrier between the interior and exterior and is also responsible for maintaining climate control within the building. The impact of hazards on a façade can be analyzed through different aspects of building performance such as structural stability, thermal performance, indoor thermal comfort, and energy efficiency. Table 2.3 illustrates the possible combinations of hazards and building performance and the performance indicators used in literature to measure performance.

When comparing different configurations, it is important to consider how the building responds to the exceptional load that caused the change in performance. Direct exposure to heat can impact the facade components in terms of expansion (Wûest & Luible, 2016) or their thermal inertia (Ramakrishnan et al., 2017). Additionally, the heat can act as a thermal load on indoor conditions, potentially leading to overheating (Hamdy et al., 2017) or an increase in energy intensity (S. Sun et al., 2016). Seismic loads on buildings act as lateral loads, causing inter-story drift (Baird et al., 2011) on the facade level. Additionally, damage to a facade component due to a seismic event can affect its thermal performance, as well as its impact on indoor conditions in terms of thermal quality (Vailati et al., 2017) and energy demand (Milovanovic et al., 2022).

When assessing the resilience of facades to multiple hazards, it is necessary to select the building performance that will be evaluated, since it is not feasible to examine all the building performance associated with the facade. The selection can be based on the following criteria: Is the building performance related to the primary functionality of the facade? Has there been any previous discussion on the standards of risk and their thresholds for measurement? Does the performance being examined relate to both the opaque and window parts of the facade system?

Table 2.3: Exceptional Loading in Facade and its Impact on Building Performance

Exceptional Load	Building Performance	Performance Indicator
Seismic	Structural Stability	**Inter-storey Drift** (Baird et al., 2011) **Shear Stress** (Nardini & Doebbel, 2016)
Seismic	Thermal Performance	**Thermal Transmittance** (Vailati et al., 2017)
Seismic	Indoor Thermal Comfort	**Indoor Microclimatic Quality PI** (de Rubeis et al., 2020)
Seismic	Energy Efficiency	**Annual Heating/Cooling Energy Demand** (Milovanovic et al., 2022) **Energy Performance Index** (Vailati et al., 2017)
Heat	Structural Stability	**Thermal Expansion** (Wûest & Luible, 2016) **Plane Displacement** (Wang et al., 2013)
Heat	Thermal Performance	**Thermal Inertia** (Ramakrishnan et al., 2017) **Energy Storage** (Pomianowski et al., 2013)
Heat	Indoor Thermal Comfort	**Overheating Index** (Hamdy et al., 2017) **Heat Index** (Flores-Larsen & Filippín, 2021)
Heat	Energy Efficiency	**Energy Use Intensity** (S. Sun et al., 2016)

2.3.4 Resilience Metrics

Seismic resilience can be evaluated using the FEMA P-58 method, which is based on probabilistic seismic performance assessments. This method predicts building resilience metrics in terms of repair cost, repair time, life safety, occupancy, and environmental impacts. There is currently no uniform methodology for assessing thermal resilience, as it is a relatively new field. Siu et al. (2023) classifies metrics based on their focus on measuring a) the ability to prevent buildings from reaching critical levels, b) reducing exposure to thermal stress, or c) recovering to a habitable state. Metrics aim to measure time a) to reach the threshold, b) spent exceeding the threshold, and c) required to return to the threshold.

Table 2.4 discusses resilience metrics and their measurement scenarios in literature. Power outages during the inspection period were assumed in all cases. Passive survivability measures the time a building can remain habitable without power. Longer passive survivability indicates a more resilient system. Active survivability involves appropriately sizing batteries to allow flexibility in case of power outages. Thermal resilience can be measured in terms of survivable time as well as the amount of uncomfortable or uninhabitable time; the lesser the time above the threshold, the more resilient it is. Metrics such as the Discomfort Index (DI), Predicted Percent Dissatisfied (PPD), and Occupant Hours Lost (OHL) measure degree hours above the discomfort threshold. More complex metrics account for thermal behavior diversity and zone differences during the measurement period. The Indoor Overheating Degree (IOD) accounts for thermal comfort limits for different zones, while the Weighted Unmet Thermal Performance (WUTP) applies different weights to the pre-, during-, and post-heatwave periods. The Thermal Resilience Index (TRI) accounts for resilience levels with respect to the relative improvement from the original indoor thermal conditions.

Table 2.4: Thermal Resilience Metrics in Literature

Literature	Application Scenario	Resilience Metrics
(Katal et al., 2019)	Power outage due to historical snowstorm	**Passive Survivability**
(O'Brien & Bennet, 2016)	Power failure during winter and summer	**Passive Survivability, Thermal Autonomy**
(Ozkan et al., 2019)	Power outage during extreme weather	**Passive Survivability, Thermal Autonomy**
(White & Wright, 2020)	Power outage during resilience design week	**Passive Survivability**
(Homaei & Hamdy, 2021a)	Power outage during coldest and warmest periods	**Active Survivability**
(Baniassadi & Sailor, 2018)	Power outage during extreme heat episodes	**Discomfort Index**
(Sailor, 2014)	Global/local warming, Power outage, Failed AC operations	**Predicted Percent Dissatisfied**
(Mathew et al., 2021)	Power outage with 5 oudoor temperature conditions	**Occupant Hours Lost Degree Hours**
(Hamdy et al., 2017)	Historical and future climate scenairo, Ventilative cooling	**Indoor Overheating Degree**
(Ji et al., 2023)	Heatwave during summertime, Natural ventilation	**Thermal Resilience Index**
(Homaei & Hamdy, 2021b)	Power failure during 5 days	**Weighted Unmet Thermal Performance**

3 Resilience-based Facade Design Framework

3.1 Framework Design

The Resilience-based Facade Design Framework assesses the impact of multiple hazards on a building facade, taking into account its fragility. The multi-hazard resilience assessment provides quantitative attributes for decision-making regarding facades, both in the early design stage and in retrofitting.

The framework allows users to input project location, building geometry, and existing facade specifications. Using this information, a facade package is created that contains data on the fragility, construction type, and material properties of each facade component. The facade package is then assessed for resilience under different hazards, including seismic and heat hazards. The resilience performance, which is defined in terms of resilience loss and economic loss, is integrated into a multi-attribute decision-making tool. This tool provides users with the option to select a facade package based on its integrated resilience performance value, or to configure a facade package based on individual enhancements to resilience attributes.

The framework consists of five modules: a facade package, multi-hazard input modules, resilience assessment as the primary evaluation tool, and multi-attribute decision-making as the output of the framework. Figure 3.1 illustrates the framework scheme.

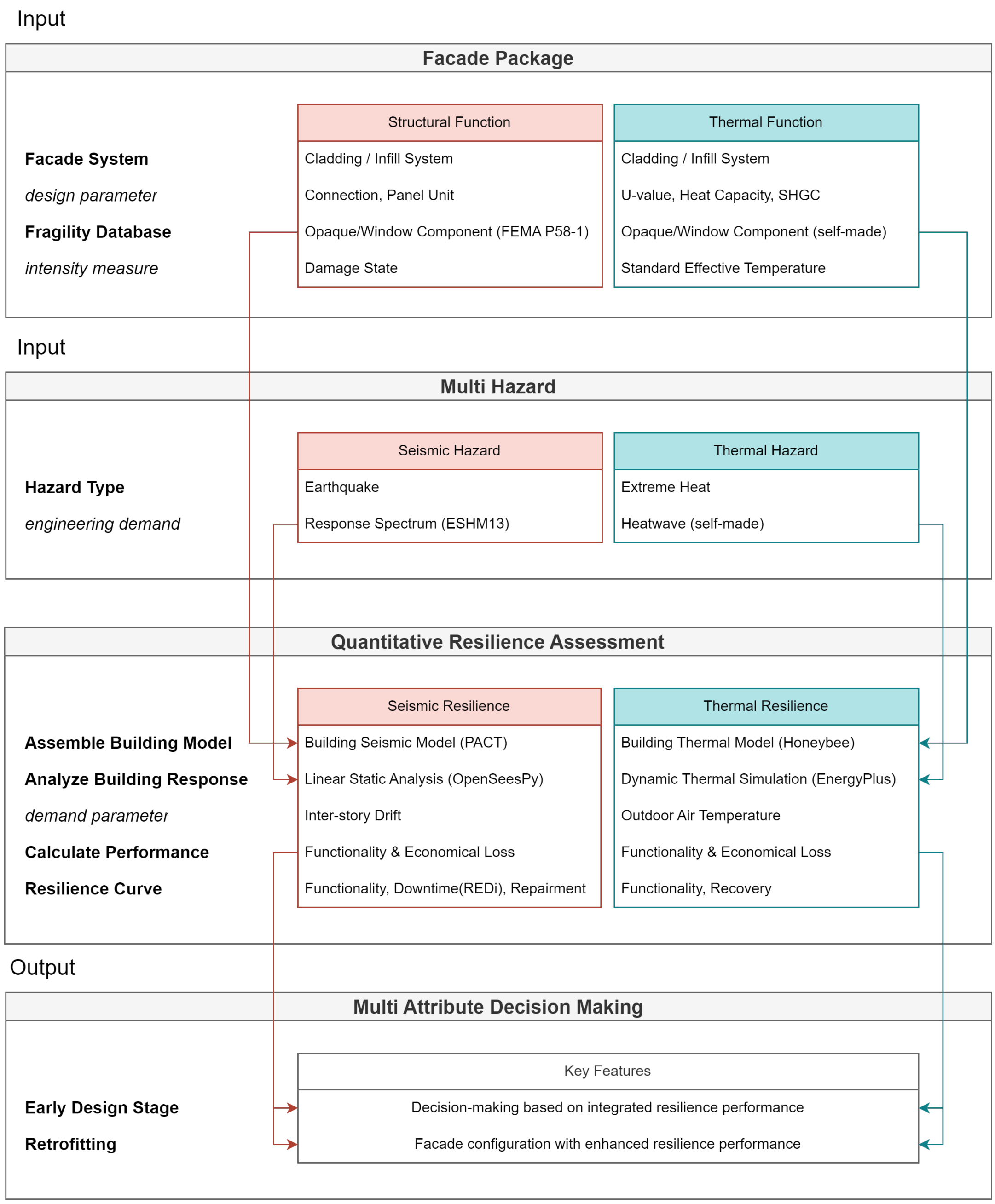

Figure 3.1: Resilience-based facade design framework

3.1.1 Multi Hazard

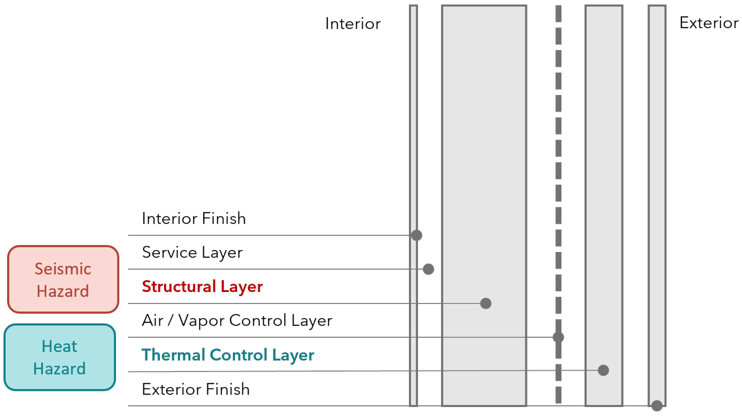

Figure 3.2: Facade functional layer

The framework aims to address the complexity of facade design by considering multiple hazards that may impact a building's performance. It employs a multi-hazard approach that takes into account the combined effects of two or more hazards during the design process. The two main hazards assigned are earthquakes and extreme heat, as they impact the structural and thermal functions of the facade layers. The hazards are assumed to occur independently, and are therefore defined separately. The impact of these hazards on the building is defined using the response spectrum of six different return periods for earthquake hazard. The response spectrum data is extracted for Izmir using the ESHM13 model. An extreme heat hazard is defined as a heatwave with a 5-degree increase in maximum outdoor temperature for seven consecutive days. The heatwave weather data is generated in this research using the existing TMY weather data of Izmir provided by EnergyPlus.

Following a disruptive event, the resilience performance of a facade is measured through its functional layer response. A facade system comprises multiple functional layers, as shown in Figure 3.2. Each theoretical functional layer serves a unique purpose for the facade. The distinction between layers does not always correspond to a material distinction; for example, concrete also provides insulation alongside rock wool. Components are not always arranged in the order described in the layer section; for instance, in a composite wall, all structural studs and insulation infill may be placed in the same location.

As researched in the Section 2.3.3, hazards can impact multiple domains of facade functionality. For example, seismic hazards can affect both the structural integrity and thermal performance of the component. However, for the purposes of this research, the focus is narrowed to inspect only major performance related to the hazard. For seismic hazards, the facade's structural layer is analyzed by degree of damage to the facade component. For heat hazards, the facade's thermal control layer is inspected for its capability to mitigate indoor thermal conditions, measured by degree hours of unmet SET hours. Performance measures that relate to building-level loss were selected, as the level of structural damage and level of unmet SET relate to the building's safety for occupancy.

3.1.2 Facade Package

A facade package is used to represent a facade typology for resilience assessment. Figure 3.3 illustrates a configuration of a facade package. The package is made up of two parts: one for an opaque wall and one for a window, which could either be an infill system or a cladding system. Each of these parts contains both structural and thermal fragility data. To determine the structural functionality of a facade system, the fragility data provided by the FEMA P-58 fragility database is analyzed. The thermal fragility function of a facade system is generated by running a dynamic thermal simulation in EnergyPlus and using a maximum likelihood fitting procedure.

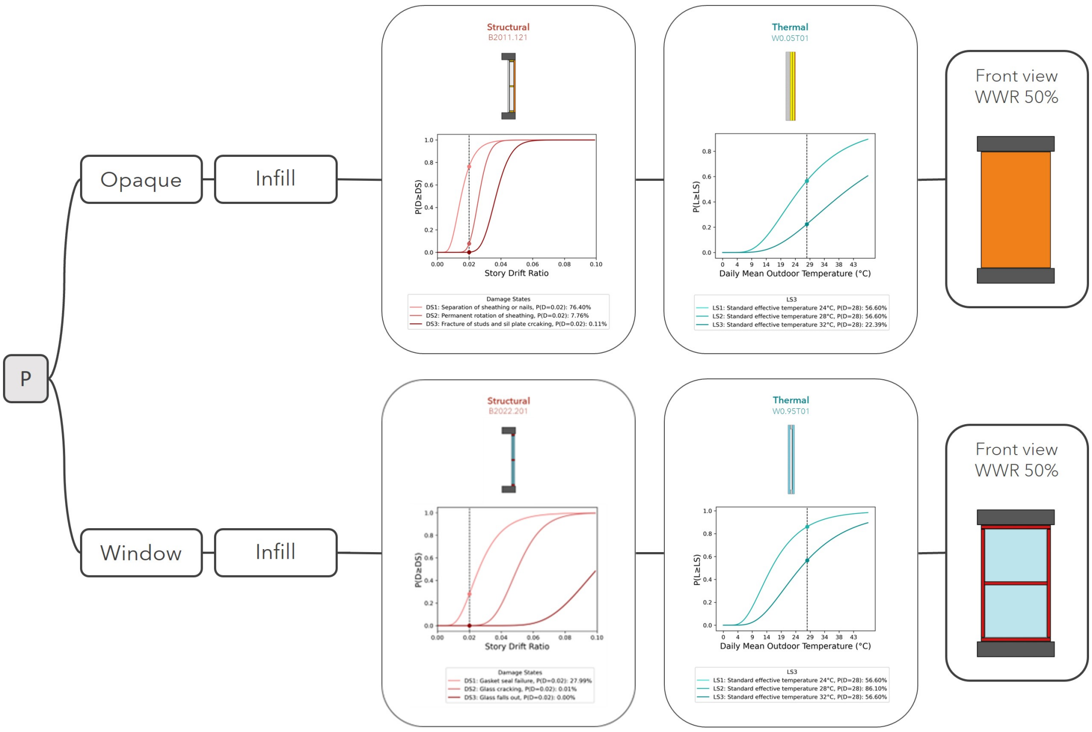

Figure 3.3: Facade package

3.1.3 Quantitative Resilience Assessment

Resilience of facade packages is quantified using the FEMA P-58 methodology for seismic performance assessment. FEMA P-58 methodology is adapted for assessing thermal performance. By using a coherent assessment process for multiple hazards, a comprehensive and systematic assessment of the facade design can be achieved.

Seismic resilience is quantified through an intensity-based assessment using damage state as a performance measure. The seismic building model is assembled using PACT, and the building's response is analyzed through linear static analysis using OpenSeesPy. Resilience loss and economic loss are calculated from the PACT intensity-based results. A resilience

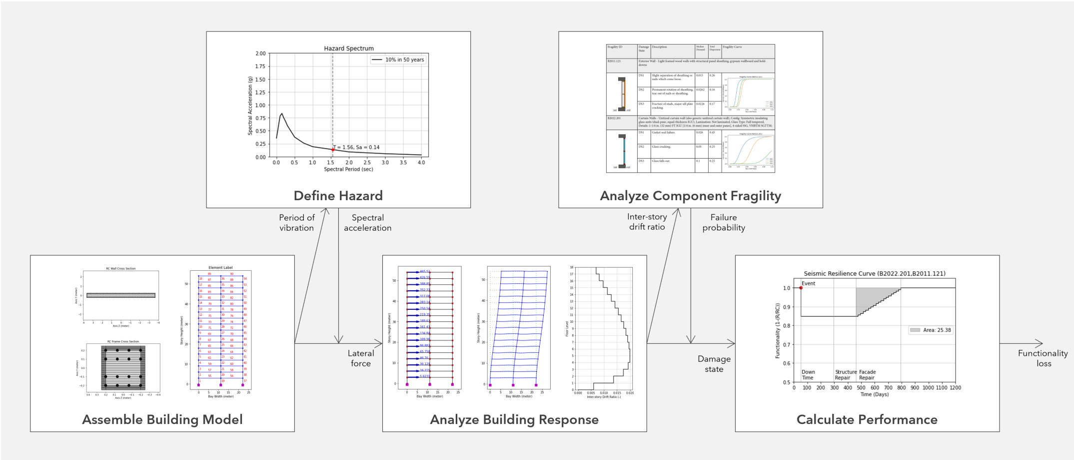

(a) Data flow of analysis modules

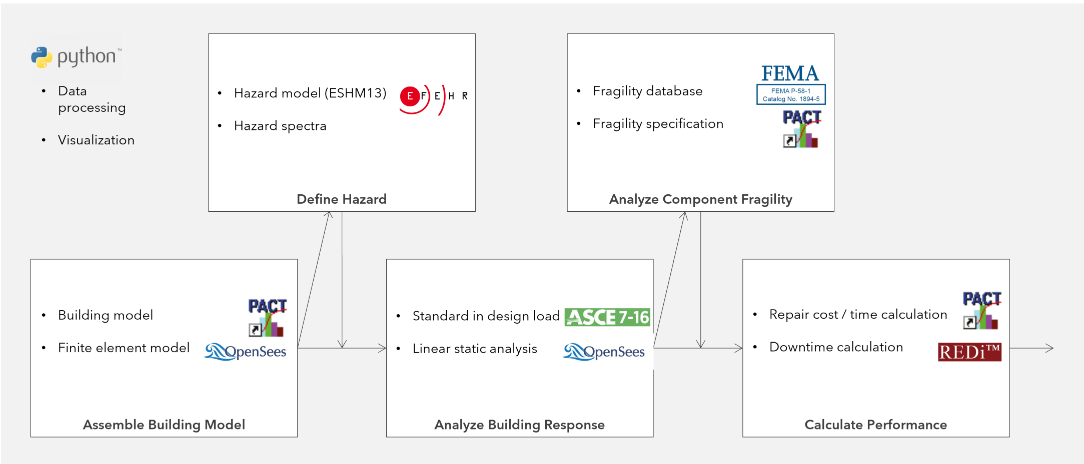

(b) Digital workflow of analysis modules

Figure 3.4: Seismic resilience assessment process

curve is formed, which includes functionality drop, downtime, and repairment. The downtime estimates are obtained from REDi. Figure 3.4 summarizes the data flow and digital workflow of the analysis modules.

Thermal resilience is quantified through an intensity-based assessment using standard effective temperature as a performance measure. The thermal building model is assembled using Honeybee, and the building's response is analyzed through dynamic thermal simulation using EnergyPlus. Resilience loss and economic loss are calculated from EnergyPlus SQL output. A resilience curve is formed, which includes functionality drop and recovery. Figure 3.5 summarizes the data flow and digital workflow of the analysis modules.

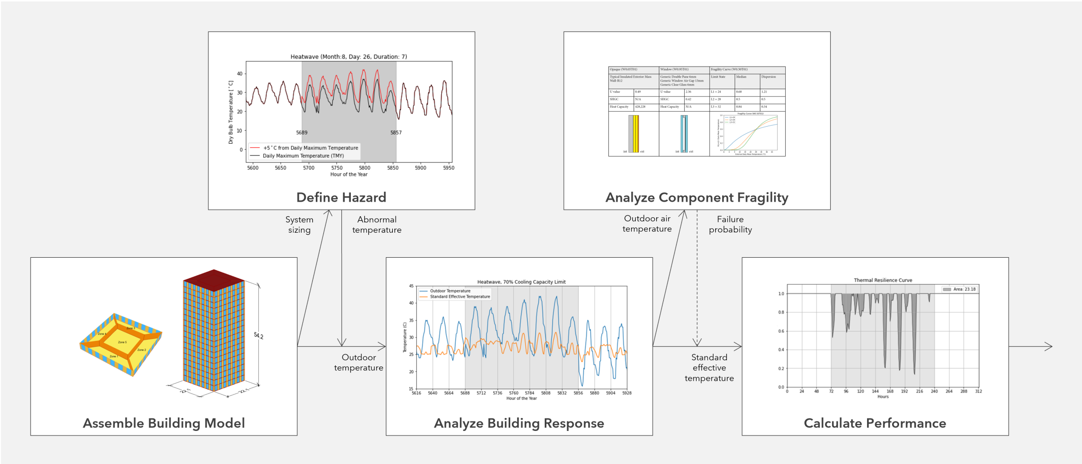

(a) Data flow of analysis modules

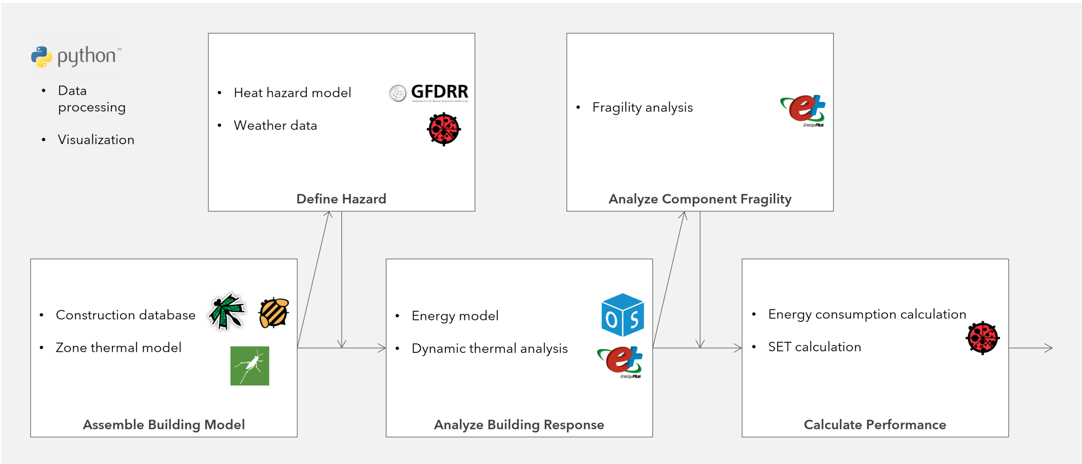

(b) Digital workflow of analysis modules

Figure 3.5: Thermal resilience assessment process

3.1.4 Multi-attribute Decision Making

The resilience assessment produces a set of resilience performance attributes (resilience loss, economic loss) that can aid decision-making. These four attributes are plotted on a radar chart for each facade package. This information can be used to make informed decisions during two different phases of building design.

During the early design phase, a facade package that has the highest score on integrated resilience (performing well on all four attributes) can be used to set a resilience-based design scope of the project. In the case of retrofitting, the decision-making tool can be used to configure a facade package with enhanced performance of a specific weighted attribute.

3.2 Case Study

Figure 3.6: Case study building description

To validate the framework, the Resilience-based Facade Design Framework is tested using a case study. The case study assumes a building structural system, and diverse facade systems are applied to assess their resilience to multiple hazards. Figure 3.6 illustrates the case study for this research, which considers an 18-story office building with seismic and heat hazards.

To carry out the case study, certain factors must be predefined to establish boundary conditions. The first input factor is the building location, which defines the seismic and thermal hazards. The second factor is the building type and structure, from which fragility is determined. With these two factors, the design range of a facade system in terms of seismic and thermal properties can be established. This chapter provides general information about the building and its facade.

The following chapters presents the process and results of the resilience assessment for the case study. Chapter 4 outlines the overall process and methodology for quantifying seismic resilience, while Chapter 5 focuses on quantifying the thermal resilience of a facade system. Both seismic and thermal assessments are conducted individually, but based on the same baseline building and facade system. Chapter 6 is dedicated to multi-attribute decision making for the various facade systems analyzed.

3.2.1 Project Location

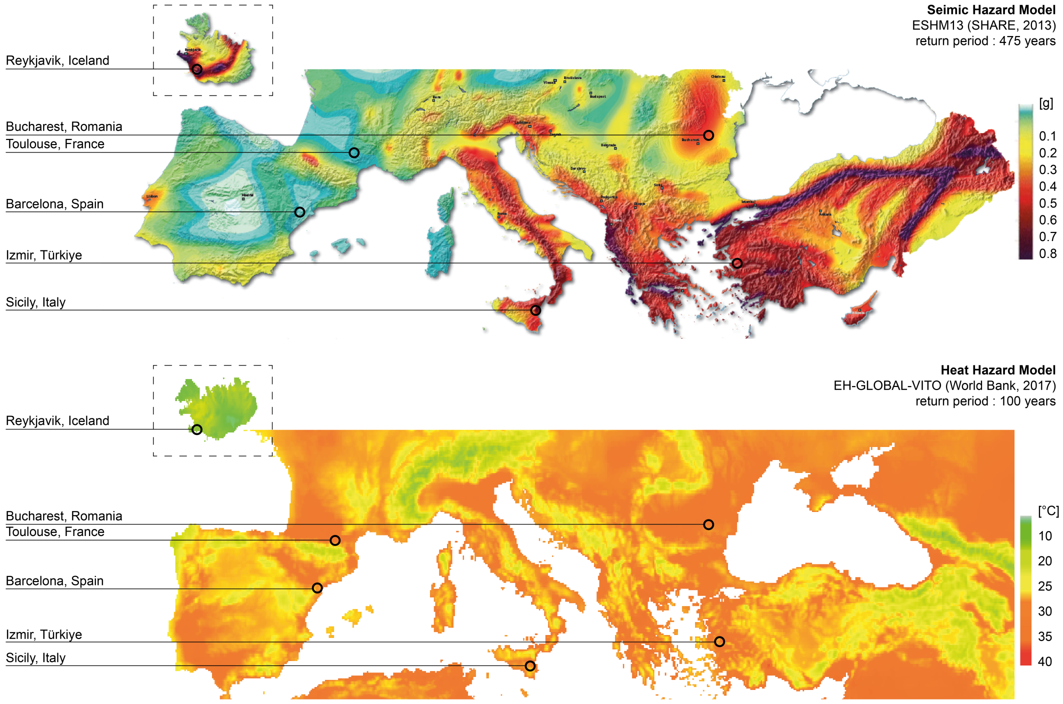

Figure 3.7: Multi Hazards in Europe

The location for a case study was chosen by comparing the hazard levels of cities in terms of seismic and extreme heat hazards. The weight assigned to a particular hazard in later decision-making phases will depend on the hazard level of the chosen location. If the location has a higher level of seismic hazard compared to heat hazard, then a higher weight will be given to seismic resilience performance. The ESHM13 (SHARE, 2013) seismic hazard model and EH GLOBAL VITO (World Bank, 2017) heat hazard model were used for the location selection.

Figure 3.7(top) shows a seismic hazard model, ESHM13 (SHARE, 2013). ESHM13 map displays peak ground acceleration (PGA) for 10% probability of exceedance in 50 years in units of standard gravity (g) for reference rock soil (vs30=800m/s). This corresponds to PGA-values that return on average every 475 years.

Figure 3.7(bottom) shows a heat hazard map for a hazard set EH-GLOBAL-VITO (World Bank, 2017). The map displays the extreme heat hazard for a 100-year return period. It is important to note that a return period of 100 years is too long to average out yearly variations in temperatures. The 100-year return period is mainly used to study locations with few heat waves over the long term. The Wet Bulb Globe Temperature (WBGT), measured in degrees Celsius, is used as a heat stress indicator. Heat stress risk is classified using WBGT thresholds of 28°C and 32°C. Slight/low heat stress is defined as WBGT below 28°C, moderate/high as 28-32°C, and severe/very high as above 32°C.

Since the models are based on different return periods, the hazard level was compared instead of directly comparing the hazard intensity values. Izmir, Turkey has a high level of seismic hazard and a medium level of extreme heat hazard. Reykjavik, Iceland has a high level of seismic hazard and a low level of extreme heat hazard. Barcelona, Spain, and Toulouse, France have a low level of seismic hazard and a medium level of extreme heat hazard. Izmir, which has a medium to high level of hazard for both hazards, was chosen to inspect the facade design criteria for maximum capacities.

3.2.2 Baseline Building

The building is an 18-story structure designed with a dual system of RC moment-resisting frames (MRFs) and RC shear walls. The structure's plan dimensions measure 22.5m by 22.5m, with three bays. All 18 stories have a floor-to-floor height of 3m. The building is an office that will mainly be occupied during daytime hours, from 8am to 6pm. Figure 5.7 illustrates the building's 3D view.

The research project aims to examine the performance of a building's facade under extreme hazards. Therefore, masonry construction, where the facade also acts as a loadbearing structure and there is no clear distinction between the structure and facade, was not the optimal system for the research. Instead, an RC frame structure was selected due to the clear distinction between the structure and facade.

For the facade configuration, a window to wall ratio of 0.5 was used for all four orientations of the building. This ratio allows for multiple facade configurations, depending on the number of opaque walls and windows placed next to each other. The decision to use this ratio was made to maintain an equal quantity of opaque and window components. This allows for a combined result and comparison of their contribution to the overall resilience of the building.

Both the opaque and window wall components span the entire story; a facade system with a window frame enclosed within an opaque wall is not a design option. This limitation is mainly due to the availability of more data for curtain walls in the seismic fragility database compared to unitized facade systems.

4 Quantification of Seismic Resilience

4.1 Select Assessment Type and Performance Measure

This case study evaluates a building's probable performance based on a specified earthquake shaking intensity. A response spectrum with six different return periods is applied to the building. The building's performance under earthquake shaking is measured using the damage state of the components. The damage state resulting from the disruptive event is used to calculate the extent of functionality loss. Finally, the seismic resilience of the facade package is evaluated using seismic resilience metrics.

4.1.1 Damage Intensity Measure

According to FEMA P58-1 (2018), damage state is the condition of damage associated with a unique set of consequences for a particular component or the building as a whole. Discrete damage states characterize different levels of damage that can occur for a component. Each damage state is associated with performance measures, as different damage states can result in varying performance measures. For example, an exterior cladding component may experience damage state 1, where there is cracking of the sealant joint, which requires relatively short repair cost and time. On the other hand, damage state 2, where there is cracking of the panel, would require replacement that has higher repair cost and time.

The average damage state (DS) weights the number of components that are damaged on a particular floor in a particular direction (i.e. performance group) against the extent of their damage, calculated using the following equation (FEMA,2013a):

$$\overline{DS} = \frac{\sum_{i=1}^{n} i \cdot DS_i}{n} \tag{4.1}$$

The damage of a component is determined by calculating the probability of reaching a damage state through a fragility function, given a demand. Performance measures such as repair actions, repair cost, and repair times that are associated with each of the damage states can then be deduced accordingly.

4.1.2 Seismic Resilience Metrics

Th seismic performance of a building is expressed with measures such as causalities, repair cost, repair time, unsafe placarding, and environmental impacts. Repair refers to the cost or time required to restore a damaged building to its pre-earthquake condition. Replacement becomes necessary in cases of total loss, where a new structure of comparable design and construction must be constructed.

In this study, repair cost and repair time are used as metrics to assess the impact of earthquakes on facades. The aim of the research is to analyze the structural performance of the facade component in the event of an earthquake. By analyzing repair cost and time, the value of a specific building component, such as the facade, can be extracted independently, as performance is assessed per performance group.

4.2 Define Component Fragility

4.2.1 Fragility Function

In vulnerability assessments of a structural system, the fragility function is used to identify the type and extent of damage that a component will experience. Assuming that the probability of incurring damage at different values of demand follows a lognormal distribution, the mathematical form for a fragility function is as follows:

$$F_i(D) = \Phi\left(\frac{\ln(D/\theta_i)}{\beta_i}\right) \tag{4.2}$$

where $F_i(D)$ is the conditional probability that the component will be damaged to damage state i as a function of a demand parameter D; Φ denotes the standard normal cumulative distribution function; θ_i denotes the median value of the probability distribution; and β_i denotes the logarithmic standard deviation. Both θ and β are established for each component type.

Figure 4.1 illustrates the fragility curve for sequential damage states. This curve can be used to determine the failure probability for the "i" damage state and a more severe "$i+1$" damage state, given a demand parameter equal to "d".

The python script for plotting fragility can be found in Appendix A.

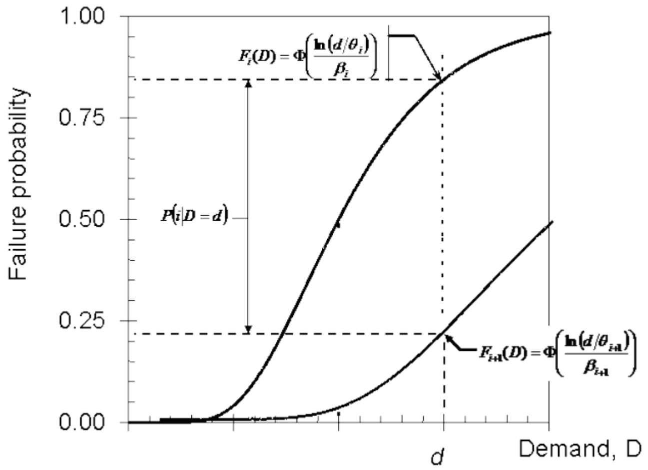

Figure 4.1: Fragility curve for sequential damage states (FEMA P-58, 2018)

4.2.2 Structural / Nonstructural Fragility Specifications

The FEMA P-58 Volume 3 includes a fragility database with over 700 individual fragility specifications. If a component is not included in the database, a custom component can be added using the PACT Fragility Specification Manager.

Structural fragility specifications

Figure 4.2 shows the fragility specifications of structural components and a fragility curve plotted based on the fragility database. Both steel moment-resisting frames (B1035.052) and reinforced concrete moment-resisting frames (B1041.013) are capable of withstanding seismic loads to a certain extent. However, they differ mainly in their failure mechanisms, which can be identified through the damage states. In a steel frame, failure is often due to the fracture of the welds connecting the beam and column. In a reinforced concrete frame, the beam-column joints are designed to transfer forces through reinforcement. Failure in such structures is often due to the crushing or cracking of the concrete, or the yielding or fracture of the reinforcement.

Nontructural fragility specifications

Figure 4.3 and Figure 4.4 displays the fragility specifications for non-structural components. The fragility database contains a wide range of data for curtain wall cladding. However, it lacks data on facade materials such as masonry or concrete. To supplement the missing data, information was gathered from the literature. Fragility specifications for concrete panels with U-shaped flexural plate connections (B2011.302a) and tie-back connections (B2011.302) were obtained from Bianchi and Pampanin (2022) where it derived the data from the test reports of Baird et al. (2013). Information on masonry infill walls (B2011.301) was obtained from Cardone and Perrone (2015).

When comparing the functionality curves of nonstructural components, it becomes clear that glazing components perform better than opaque exterior wall components. Among glazing systems, curtain wall systems (B2022.091, B2022.011) quickly reach damage state 1, which is gasket seal failure, in comparison to unitized systems (B2023.002, B2022.201), indicating that curtain wall systems are relatively more vulnerable. Of all the exterior wall components, masonry infill (B2011.301) and concrete panel (B2011.302) are more vulnerable compared to the steel-framed composite wall (B2011.001a). Among concrete cladding panels, the dissipative connection (B2011.302a) outperforms the tie-back connection (B2011.302). This is supported by the fact that cladding failures are primarily governed by the connection type.

Fragility ID	Damage State	Description	Median Demand	Total Dispersion	Fragility Curve
B1035.052	Pre-Northridge WUF-B beam-column joint, beam both sides of column, beam depth >= W30				
	DS1	Fracture of lower beam flange weld and failure of web bolts (shear tab connection)	0.017	0.4	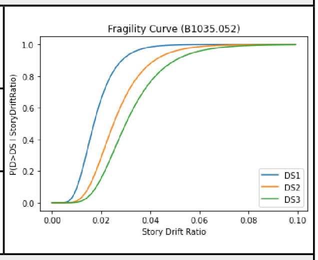
	DS2	Fracture is confined to beam flange region.	0.025	0.4	
	DS3	Fracture initiating at weld access hole and propagating through beam flange.	0.03	0.4	
B1041.013a	MF with SMF-conforming beam and column flexural and confinement reinforcement but weak joints , Conc Col & Bm = 36” x 36”, Beam one side				
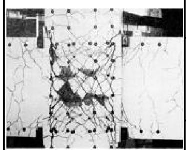	DS1	No significant spalling. No fracture or buckling of reinforcing.	0.02	0.4	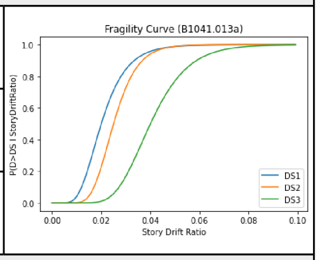
	DS2	Spalling of cover concrete exposes beam and joint transverse reinforcement.	0.025	0.3	
	DS3	Fracture or buckling of reinforcing requiring replacement may occur.	0.04	0.3	
B1044.091	Slender Concrete Wall, 12” thick, 12’ high, 15’ long Slender concrete shear wall with aspect ratio greater than or equal to 2.0. Costing assumes a 144 ft^2 wall panel.				
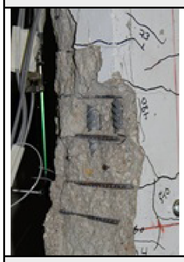	DS1	Spalling of cover, vertical cracks greater than 1/16 inch.	0.0093	0.5	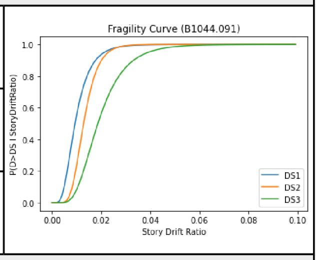
	DS2	Exposed longitudinal reinforcing.	0.0128	0.35	
	DS3	Core concrete damage, buckled reinforcing, fractured reinforcing, shear failure.	0.0186	0.45	
B1051.003	Ordinary reinforced masonry walls with partially grouted cells, 4” to 6” thick, flexure dominated up to 12’ tall				
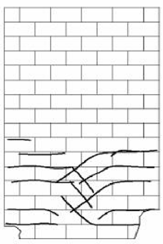	DS1	A few flexural and shear cracks with hardly noticeable residual crack widths.	0.0018	0.73	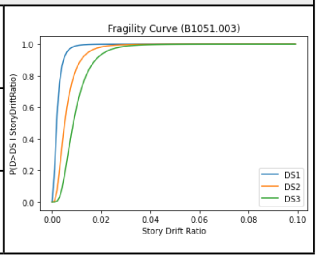
	DS2	Numerous flexural and diagonal cracks with residual crack widths less than 1/64 in.	0.0051	0.65	
	DS3	Severe flexural cracks with residual crack widths greater than 1/32 in.	0.0086	0.56	

Figure 4.2: Structural components fragility curves

Fragility ID	Damage State	Description	Median Demand	Total Dispersion	Fragility Curve
B2011.121	Exterior Wall - Light framed wood walls with structural panel sheathing, gypsum wallboard and hold-downs				
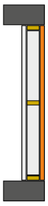 int ext	DS1	Slight separation of sheathing or nails which come loose.	0.015	0.26	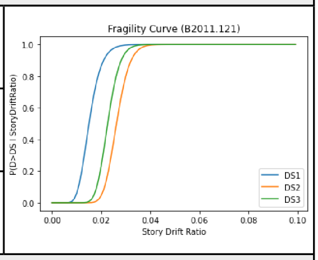
	DS2	Permanent rotation of sheathing, tear out of nails or sheathing.	0.0262	0.16	
	DS3	Fracture of studs, major sill plate cracking.	0.0226	0.17	
B2011.301	Exterior Wall - Masonry infills with French window and Partitions with door				
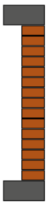 int ext	DS1	Detachment of infill, Light diagonal cracking	0.0015	0.5	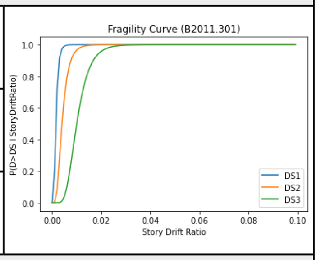
	DS2	Extensive diagonal cracking	0.004	0.5	
	DS3	Corner crushing and sliding of mortar joints	0.01	0.4	
B2011.302a	Exterior Wall - Precast concrete cladding panel U-shaped Flexural Plate connection, 120x8mm steel plate				
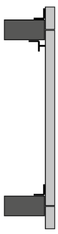 int ext	DS1	Pre-yielding	0.002	0.2	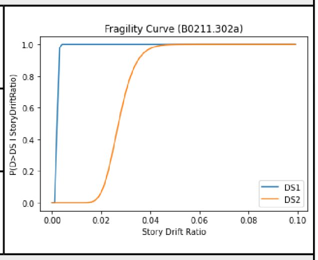
	DS2	Post-yielding	0.027	0.2	
	DS3	N/A	N/A	N/A	
B2011.302	Exterior Wall - Precast concrete cladding panel Tie-back connection Threaded rod with 20mm diameter and 250 mm length				
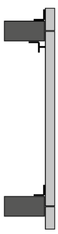 int ext	DS1	Pre-yielding	0.002	0.2	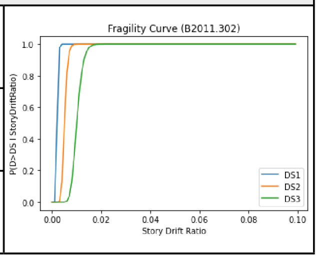
	DS2	Post-yielding	0.005	0.2	
	DS3	Severe damage to connections	0.010	0.2	

Figure 4.3: Non-structural components fragility curves - Opaque

Fragility ID	Damage State	Description	Median Demand	Total Dispersion	Fragility Curve
B2022.201	Curtain Walls - Unitized curtain wall (also generic unitized curtain wall), Config: Symmetric insulating glass units (dual-pane, equal-thickness IGU), Lamination: Not laminated, Glass Type: Full tempered, Details: 1-1/4 in. (32 mm) FT IGU [1/4 in. (6 mm) inner and outer panes], 4-sided SSG, VHBTM SGTTM;				
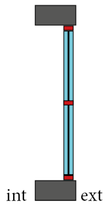	DS1	Gasket seal failure.	0.026	0.45	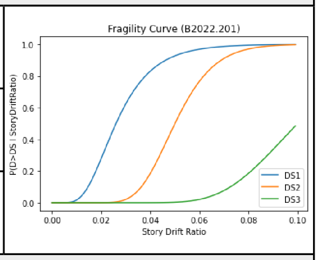
	DS2	Glass cracking.	0.05	0.25	
	DS3	Glass falls out.	0.1	0.25	
B2023.002	Generic Storefront, Config: IGU, Lamination: Unknown, Glass Type: Unknown, Details: Aspect ratio = 6:5, Other details Unknown				
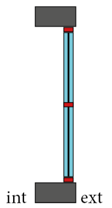	DS1	Gasket seal failure.	0.0423	0.3	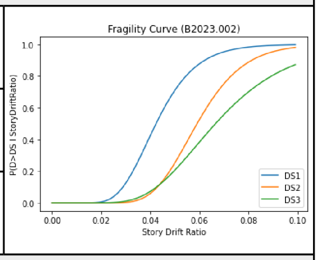
	DS2	Glass cracking.	0.059	0.25	
	DS3	Glass falls out.	0.0665	0.35	
B2022.011	Midrise stick-built curtain wall, Config: Asymmetric insulating glass units (dual-pane, unequal-thickness IGU), Lamination: Laminated, Glass Type: Annealed, Details: 1/4 in. (6 mm) inner AN / 1/2 in. (13 mm) outer AN LAM (0.030 PVB) IGU; glass-frame clearance = 0.43 in. (11 mm); aspect ratio = 6:5 sealant = dry				
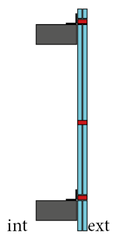	DS1	Gasket seal failure.	0.026	0.25	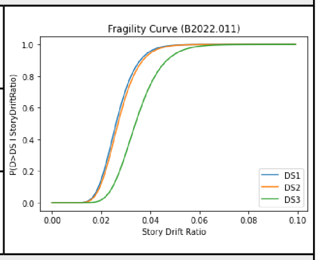
	DS2	Glass cracking.	0.0268	0.25	
	DS3	Glass falls out.	0.0339	0.25	
B2022.091	Midrise stick-built curtain wall, Config: Symmetric insulating glass units (dual-pane, equal-thickness IGU), Lamination: Not laminated, Glass Type: Full tempered, Details: 1 in. (25 mm) FT IGU [1/4 in. (6 mm) inner and outer panes]; glass-frame clearance = 0.43 in. (11 mm); aspect ratio = 6:5 sealant = dry				
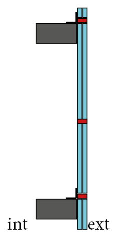	DS1	Gasket seal failure.	0.026	0.11	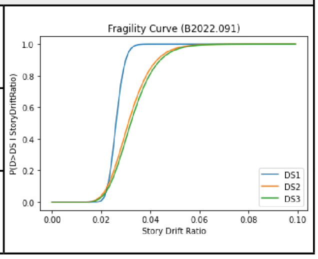
	DS2	Glass cracking.	0.031	0.25	
	DS3	Glass falls out.	0.032	0.25	

Figure 4.4: Non-structural components fragility Curves - Window

4.3 Assemble Building Performance Model

4.3.1 Building Information

18-story Reinforced Concrete Structure

The building is an 18-story structure designed with a dual system of RC moment-resisting frames (MRFs) and RC shear walls. The structure's plan dimensions measure 22.5m by 22.5m, with three bays. All 18 stories have a floor-to-floor height of 3m. Figure 4.5 provides an illustration of the building's floor plan and section.

For the research project, the building's facade's performance under extreme hazards was examined. Therefore, masonry construction, which doesn't have a clear distinction between the structure and facade, was not the optimal system for the research. Instead, an RC frame structure was selected due to the clear distinction between the structure and facade.

Given that the building is a medium to high-rise structure with 18 stories, a supplementary structure was required to resist the lateral load. The dual system of frame and shear walls is a commonly used seismic design practice. Patel and Amin (2015) study on a 20-story building using an RC dual system showed that the shear wall carried a higher percentage of lateral loads than the frame at lower stories. However, as the story increases, the frame resisted higher lateral forces.

To resist lateral loads in both Direction 1 (North-South) and Direction 2 (East-West), four shear walls were placed in the center of the building's floor plan. The placement of the shear walls was designed to maximize the surface area assigned for facade components. All surfaces along the perimeter were designated as facade components, with half being opaque exterior wall components and the other half being transparent window components.

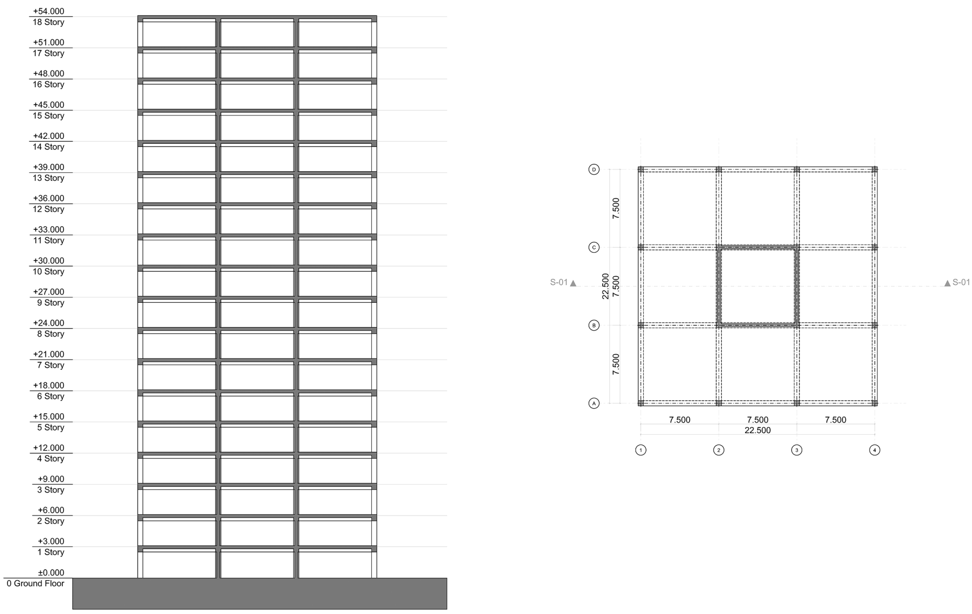

Figure 4.5: Floor plan and section of 18-story office building

Project Description (PACT Input)

To perform an analysis, PACT requires information about the entire building system, in addition to its structural inputs. A simplified building system was modeled, which includes the structural scheme, facade specifications, interior components, and building service system. Only the result pertaining to the facade components was later processed and analyzed. Table 1 contains common project information that applies to all building systems when calculating their performance.

In PACT, the damage state for each component is defined, and the corresponding repair cost is determined. Replacement occurs mainly when there is a system failure that cannot be repaired. However, there is a point at which the accumulated repair cost is so high that it is more cost-effective to replace the system than to repair it. This is referred to as the Total Loss Threshold, which is the ratio of repair cost to replacement cost at which the decision to replace the building is typically made. The value of the Total Loss Threshold is user-defined. FEMA P58-1 Volume 1 suggests that when repair costs exceed 40% of replacement costs, many owners will choose to demolish the existing building and replace it with a new one. A recent research conducted by Cardone and Perrone (2017) proposed a higher range from 60% to 75% of replacement costs, based on the reconstruction following the 2009 L'Aquila earthquake in Italy. PACT uses a default value of 1.0 to maximize the amount of assessment information that will be obtained in an assessment. For this project, a total loss threshold of 60% was selected, based on the different threshold values assumed in literature. The total replacement cost was determined using the formula provided by PACT, which defines the cost per total surface area.

Table 4.1: PACT building information tab

Input	**Value**
Number of Stories	18
Floor Area (m^2)	486.20
Floor Height (m)	3
Total Loss Threshold (ratio)	0.6
Total Replacement Cost ($)	$250/sf $\times$ sf $= 250 \times 18 \times 486.20$ $2,187,900
Core and Shell Replacement Cost ($)	$100/sf $\times$ sf $= 100 \times 18 \times 486.20$ $875,160
Replacement Time (days)	520
Maximum Workers per Square Meter	0.00018580608
Carbon Emissions Replacement (kg)	9,600,000
Embodied Energy Replacement (MJ)	130,000,000

4.3.2 Building Performance Group

PACT divides building components into performance groups. Facade components are categorized as non-structural, while beams, columns, and shear walls are categorized as structural. Table 1 lists the components assigned for analysis, including their performance group and the number of components in the PACT unit.

B1041.013a and B1041.013b are RC beam and column components. B1041.013a is used for a structural node where there is a one-sided beam column, and B1041.013b is used for a node where there is a two-sided beam column. There are 16 beam and column nodes per floor, with 8 nodes accounting for one-sided beams and 8 for two-sided beams each.

The unit of measurement for B201 exterior nonstructural walls is SF100 in PACT units. SF100 is a PACT unit for 100 components per surface area in square feet. The surface area allocated for the facade is 2790 sq ft, which is equivalent to 27.9 SF100. Since opaque walls take up half of the total facade area, it is divided by 2. Additionally, since the component is directional and the quantity per axis direction is separately indicated, the value is divided by 2 again, resulting in a final quantity value of 6.975 for the component. The same calculation applies for the B202 exterior window systems, but this time the PACT unit is SF30. 2790 square feet is equivalent to 93 SF30 units. By going through the same process, the result is a quantity value of 23.25 per component.

For other performance groups, such as interior partitions and building service systems, the quantities were defined using the Normative Quantity Estimation Tool provided in FEMA P58-1 Volume 3. This tool is an Excel sheet that calculates the common components and quantity per floor for an office building by defining the floor specifications and building usage.

Table 4.2: Performance group quantities per floor (482.2 sqm)

Performance Group	**Component**	**Input**	**Quantity**	**Quantity Unit**	**Direction**
B10 Super Structure	B1041.013a	8	16	EA1	D
	B1041.013b	8	16	EA1	D
B20 Exterior Opaque	B2011.201a	6.975	27.9	SF100	D
	B2011.301	6.975	27.9	SF100	D
	B2011.302a	6.975	27.9	SF100	D
	B2011.302	6.975	27.9	SF100	D
B20 Exterior Window	B2023.002	23.25	93	SF30	D
	B2022.201	23.25	93	SF30	D
	B2022.091	23.25	93	SF30	D
	B2022.011	23.25	93	SF30	D
C10 Interior Construction	C1011.001a	2.615	5.23	LF100	D
C30 Interior Finishes	C3027.001	39.25	39.25	SF100	Non-D
	C3032.001a	18.84	18.84	SF250	Non-D
D30 HVAC	D3041.011a	0.39	0.39	LF1000	Non-D
D40 Fire Protection	D4011.031a	0.47	0.47	EA100	Non-D

4.4 Construct Building Analytical Model

4.4.1 Seismic Force Resisting System

Design coefficients from ASCE/SEI 7-16

The structural design of the RC dual system was carried out by referencing ASCE/SEI 7-16, "Minimum Design Loads and Associated Criteria for Buildings and Other Structures"

(ASCE, 2010). This document proposes minimum safety-related seismic performance criteria for diverse structural systems. The structural system used in the research falls under Category B.5 Building frame systems, specifically Ordinary Reinforced Concrete Shear Walls. Chapter 12 provides a table (Table 12.2-1) that contains design coefficients and factors for this system. For Category B.5, the Response Modification Coefficient (R) is defined as 5, the Overstrength Factor (Ω) as 2½, and the Deflection Amplification Factor (Cd) as 4 for this structure.

The seismic mass of the building is designed to be 736 tons per floor. This value is based on research by Ciurlanti et al. (2019), where the structural type and area dimensions are equivalent to those of this building's design.

Material Properties and Dimensions

The beam and column elements have a uniform cross-section of 500 mm x 500 mm. Within the beam section, rebar with a diameter of 30mm was placed, as shown in Figure 4.6. The shear wall was simplified as a bundle of columns, using the same modeling technique as for the column element. Its length is the same as that of the column, and its width spans the whole bay.

Uniaxial material models predefined in OpenSees were used to describe the material behavior. The concrete component of the RC structure utilized the Concrete02 uniaxial model, with a compressive strength of 28 MPa. The reinforcement component used the Steel02 uniaxial model, with a yield strength of 420 MPa.

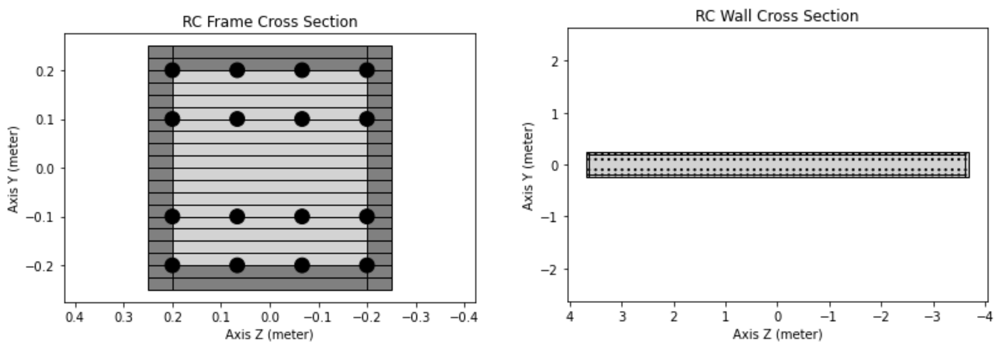

Figure 4.6: RC Element Cross Section

4.4.2 Finite Element Model

Finite element models were constructed using OpenSees. OpenSeesPy provides example files for analyzing a 2D steel portal frame. This example file was used as a base, and modified to create a multi-story, multi-bay frame structure with reinforced concrete cross-section elements.

The 2D beam-column elements have three degrees of freedom at each node: two translations and one rotation. The columns were assumed to be fixed at the base, and the beam-column intersection was modeled as a rigid connection. The node and element labels can be found in Figure 4.7.

The original structural layout had 3 bays, but it was reduced to 2. Instead of placing a shear wall between the columns, the design was simplified by placing the shear wall at the center of the node without columns on either side. The nodes at the building edge are assigned columns (elements 1 18, 37 54), whereas the nodes in the center are assigned walls (elements 19 36).

Both RC frame and wall were modeled using Force beam-column elements defined in the OpenSees library. The integration along the element section was based on Lobatto integration, which places an integration point at each end of the element. For a geometric transformation from the basic system to the global coordinate system, a linear transformation was applied for the beam element, while a P-Delta transformation was applied for the column and wall elements.

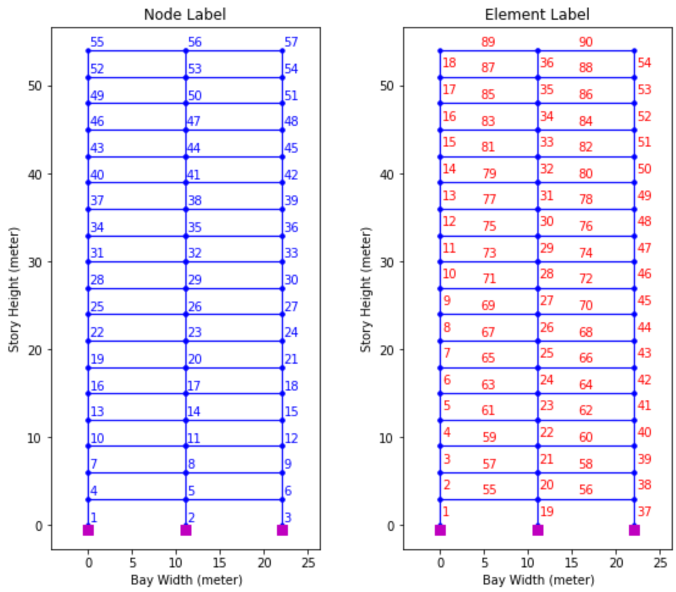

Figure 4.7: Finite element model

4.5 Define Seismic Hazard

4.5.1 Response Spectrum

Hazard Model

The EFEHR web platform provides seismic hazard data through the selection of a site location and a hazard model available on the platform. To define the hazard, the 2013 European Seismic Hazard Model (ESHM13) was used. ESHM13 was developed as part of the SHARE Project (Giardini et al, 2014), which was funded by the European Union under the Seventh Framework Programme for Research (FP7).

The building site is located in Izmir, Turkey, with a latitude and longitude of 27.143°N and 38.424°E, respectively. The site is classified as “rock vs30 800ms 1”and the aggregation type is the arithmetic mean. Figure 4.8 shows the hazard spectrum with spectral acceleration as the intensity measure plotted over six different probabilities of exceedance (POE).

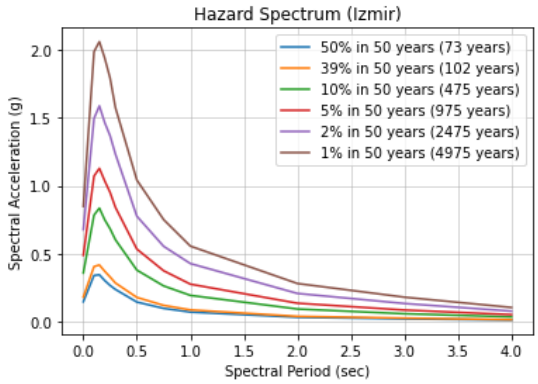

Figure 4.8: Hazard spectrum of 6 intensities (Izmir)

Fundamental Period of vibration

The fundamental period of vibration is at which the structure tends to vibrate most significantly when subjected to dynamic loading. This period is influenced by the mass, stiffness, and geometry of the building. The fundamental period of vibration can be calculated using the simplified formula provided by the design code ATC3-06, which relates the period to the height of the building for moment-resisting reinforced concrete frames.

$$T = C_t H^{3/4} \tag{4.3}$$

where C_t is a regression coefficient and H is the height of the building. The period-height formula presented here assumes a uniform story drift under linearly distributed lateral forces. Eurocode 8 adopts a coefficient of C_t=0.075, with the height measured in meters. The height of the building is H=57. This results in an estimated value T=1.56 for the fundamental period of the structure.

The target intensity is set to earthquake ground shaking with a return period of 475 years. At this return period, $S_a(T)$ is the ordinate of the hazard spectrum at the fundamental period of vibration. As shown in the Figure 4.9, spectral acceleration is $S_a(T = 1.56)$ = 0.14g.

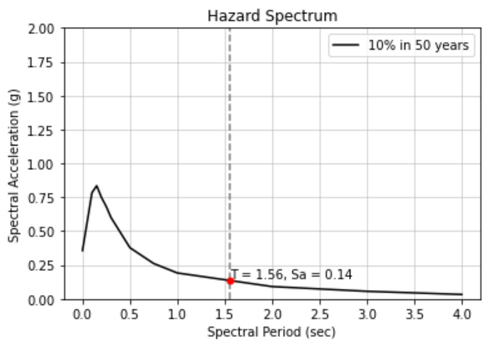

Figure 4.9: Fundamental period on response spectrum

4.6 Analyze Building Response

Equivalent Lateral Force Procedure

Linear static analysis was conducted using the equivalent lateral force method, as described in Chapter 12 of ASCE 7-16. This method provides a simple way to incorporate the effects of inelastic dynamic response into a linear static analysis, but is only valid in cases where the dominant response to ground motions is in the horizontal direction without significant torsion. The procedure involves first determining the seismic base shear, and then distributing the shear force along the height of the structure.

Seimic Base Shear

The seismic base shear is an estimate of the maximum expected lateral force on the base of a structure. It is expressed as the product of the absolute acceleration and the mass of the structure. The seismic base shear, denoted by V, is determined by the following equation:

$$V = C_s W \tag{4.4}$$

where W is the effective seismic weight; Seismic Response Coefficient C_s is determined in as follows:

$$C_s = \frac{S_{DS}}{\left(\frac{R}{I_e}\right)} \tag{4.5}$$

where S_{DS} is the design spectral response acceleration parameter, equivalent to S_a = 0.14g. R is the response modification factor determined as 5 from section 3. I_e is the importance factor determined as 1. This gives a value of C_s=0.027. Given the effective seismic weight previously defined as W=131035 kN, the seismic base shear V=3550 kN.

Vertical Distribution of Seismic Forces

The lateral seismic force, F_x at floor level x is determined from the following equation:

$$F_x = C_{vx} V \tag{4.6}$$

where C_{vx} is a vertical distribution factor given by:

$$C_{vx} = \frac{w_x h_x^k}{\sum_{i=2}^{N+1} w_i h_i^k} \tag{4.7}$$

Here, w_i is the portion of the total effective seismic weight assigned to level i. The seismic weight per floor is uniform for all the floors, w=7380 kN (736 tons). h_i is the height from the base to level i; and k is equal to 2.0 for a first mode period greater than 2.5 seconds, or equal to 1.0 for a first mode period less than or equal to 0.5 seconds. Since T=1.56 was previously defined, linear interpolation results in k=1.53. The lateral seismic force, F_x for an 18-story building is calculated as shown in Table 1.

Table 4.3: Vertical Distribution of Seismic Force

Node	x	h_x (m)	C_{vx}	F_x (kN)
4	1	3	0.002	6
7	2	6	0.005	16
10	3	9	0.008	30
13	4	12	0.013	47
16	5	15	0.019	66
19	6	18	0.024	87
22	7	21	0.031	110
25	8	24	0.038	135
28	9	27	0.045	161
31	10	30	0.053	190
34	11	33	0.062	219
37	12	36	0.071	251
40	13	39	0.080	283
43	14	42	0.089	317
46	15	45	0.099	352
49	16	48	0.110	389
52	17	51	0.120	427
55	18	54	0.131	466

4.6.1 Linear Static Analysis

To form a 2D load pattern, the seismic load derived from the equivalent lateral force procedure is passed through the Plain Pattern object in OpenSees. Afterwards, nodal loads are applied to each floor level in the Fx direction. For the analysis command, we select the 'Static' object and the solution algorithm 'Linear'. Figure 4.10 presents the lateral load distribution across the floors and the deformation response of the RC dual structure.

4.6.2 Inter-story Drift Ratio

After then later loads are applied to the nodes, the inter-story drift is calculated from the nodal displacement in the Fx direction. Inter-story drift ratio θ, which is the relative translational displacement between two consecutive floors is defined as:

$$\theta_i = \frac{\delta_i - \delta_{i-1}}{h_i - h_{i-1}} \tag{4.8}$$

where $\delta_i - \delta_{i-1}$ denotes the difference in displacement at floor level i, and $h_i - h_{i-1}$ denotes the story height of floor level i. The inter-story drift ratio obtained is then corrected for inelastic behavior and higher modes using FEMA P-58 Volume 1 Equation 5-10. The correction factor for each story is assigned based on the first mode of period and the total building height.

The actual building response is likely to vary from the estimated median response due to uncertainty in ground motion, mathematical modeling, and material property variability.

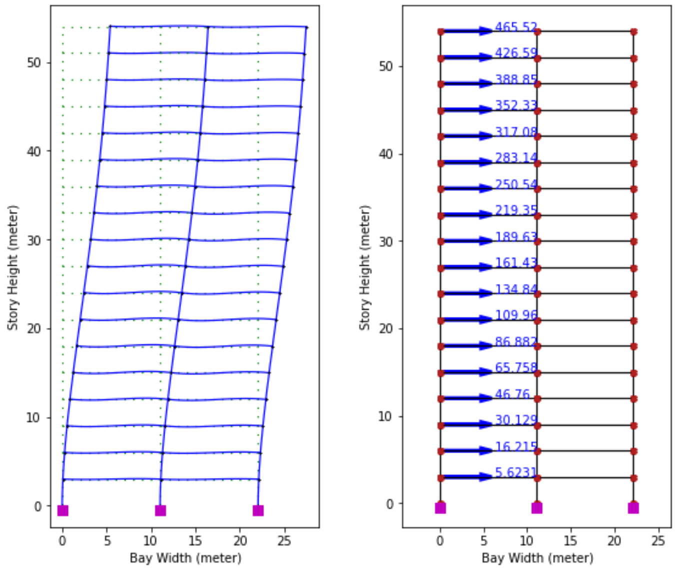

Figure 4.10: RC dual system load pattern and deformation

The total dispersion for story drift are found in FEMA P-58 Volume 1 Table 3-4. For T=1.56s and S=5.5, the dispersion value is β_{SD}=0.43.

Figure 4.11 shows the displacement in each floor and the story drift ratio for 6 intensities, as well as one intensity (return period of 475 years). This allows us to observe the impact of different hazard intensities on the structure. At a return period of 457 years, the inter-story drift ratio is at a maximum of 2%, whereas at a return period of 4975 years, it is at a maximum of 6%.

4.6.3 Intensity-based Results

PACT estimates for repair time of all the building performance group are plotted in Figure 4.12. The repair time is plotted across different intensities, where parallel time is used to repair all floors simultaneously. From the plot, it can be inferred that non-structural components like partitions and facade components become damaged at intensities 1 and 2, whereas structural component damage begins at intensity 3 and beyond. In lower intensity hazards, non-structural components are the major source of damage, as they require the most repair time.

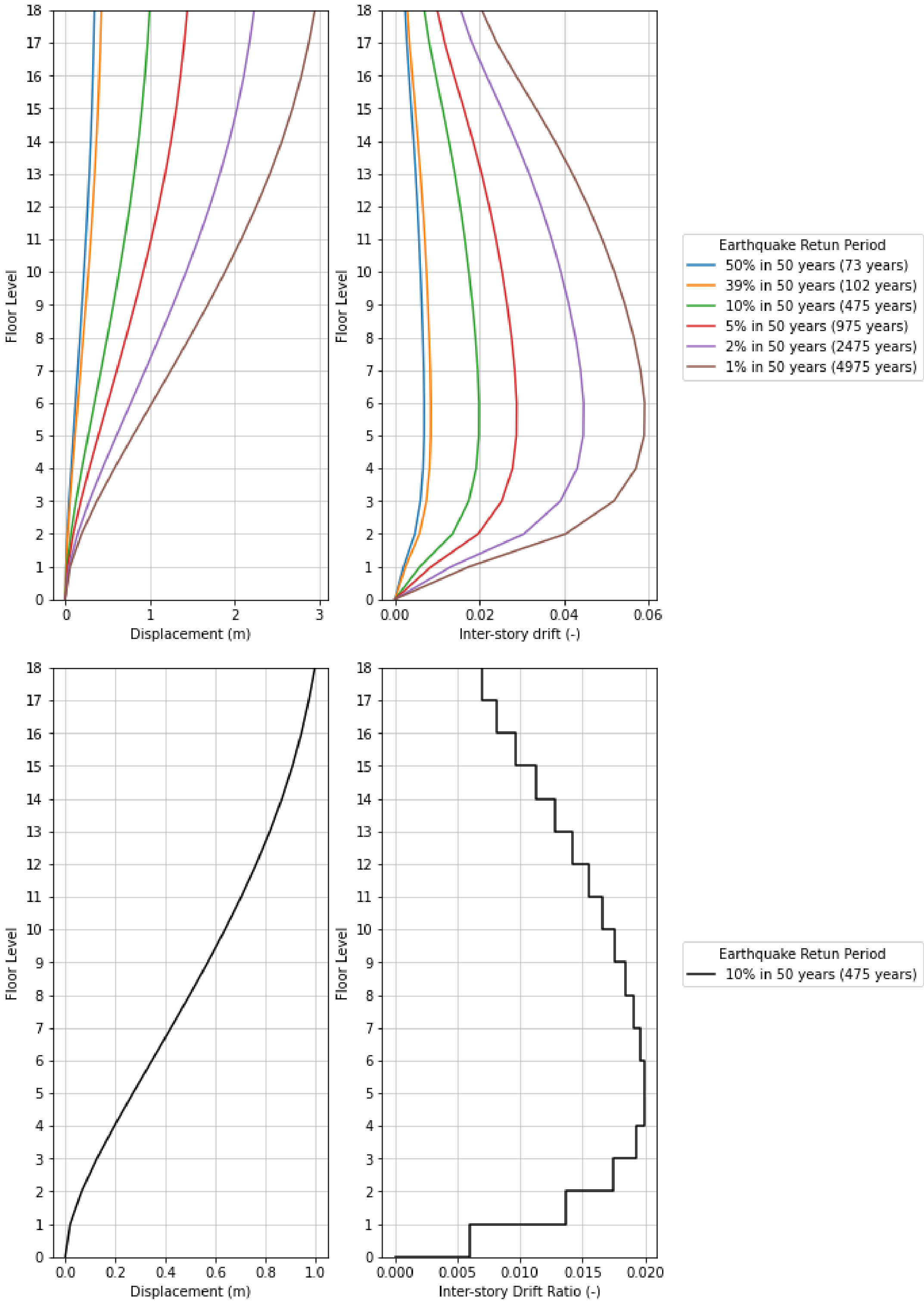

Figure 4.11: Inter-story drift ratio and displacement

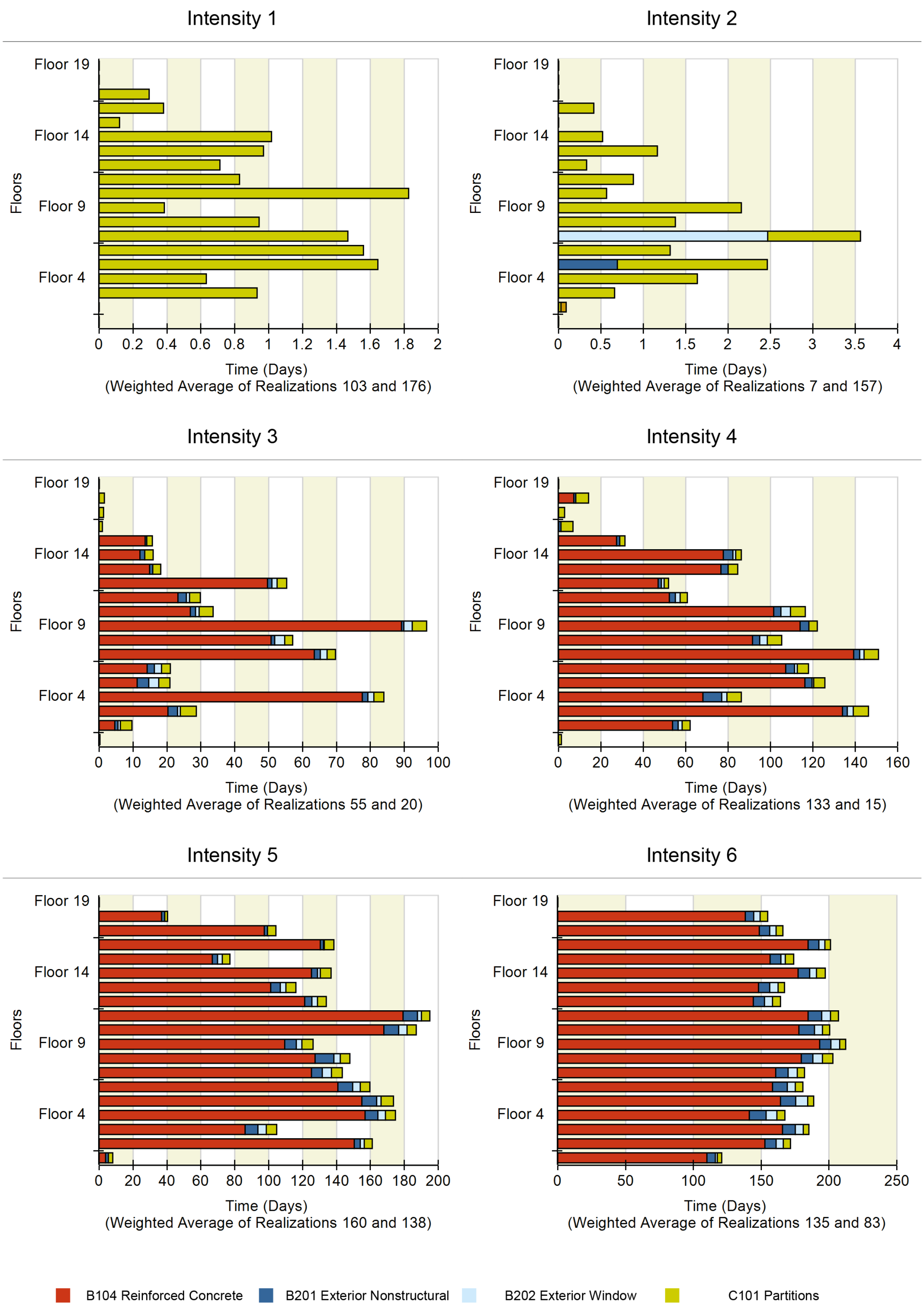

Figure 4.12: Intensity-based results from PACT

4.7 Calculate Performance

4.7.1 Case Study Facade

The analysis utilized a facade package consisting of B2011.121 (wooden frame with panel sheathing) and B2022.201 (unitized curtain wall). Figure 4.13 shows the fragility curve for the case study facade.

Fragility ID	Damage State	Description	Median Demand	Total Dispersion	Fragility Curve
B2011.121	Exterior Wall - Light framed wood walls with structural panel sheathing, gypsum wallboard and hold-downs				
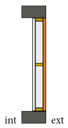 int ext	DS1	Slight separation of sheathing or nails which come loose.	0.015	0.26	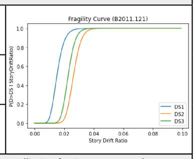
	DS2	Permanent rotation of sheathing, tear out of nails or sheathing.	0.0262	0.16	
	DS3	Fracture of studs, major sill plate cracking.	0.0226	0.17	
B2022.201	Curtain Walls - Unitized curtain wall (also generic unitized curtain wall), Config: Symmetric insulating glass units (dual-pane, equal-thickness IGU), Lamination: Not laminated, Glass Type: Full tempered, Details: 1-1/4 in. (32 mm) FT IGU [1/4 in. (6 mm) inner and outer panes], 4-sided SSG, VHBTM SGTTM;				
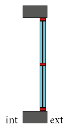 int ext	DS1	Gasket seal failure.	0.026	0.45	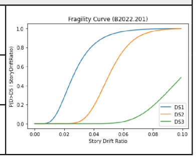
	DS2	Glass cracking.	0.05	0.25	
	DS3	Glass falls out.	0.1	0.25	

Figure 4.13: Fragility curve for the case study facade

4.7.2 Analyze Resilience Loss

The post-earthquake losses of an entire building can be calculated using PACT. PACT estimates repair costs, repair times, casualties, and environmental impacts across 200 realizations. The resulting output can be further processed and filtered by performance groups, number of floors, and other factors.

Although the repair of both structural and nonstructural components of a building may be related, only the functionality and economic loss of the facade component (one of two types of performance groups within the nonstructural component category) were extracted and analyzed to form a specific resilience curve for the facade.

Loss Function

When functionality is lost due to an earthquake, the resulting loss in performance can be calculated based on the required repairs. The severity of the loss determines the extent of the necessary repairs. Repair cost divided by replacement cost new (RCN) is referred to as damage factor or fractional loss. The quality function can be expressed using the fractional loss:

$$Q(t) = 1 - \frac{RepairCost}{ReplaceCost} \tag{4.9}$$

This indicates that if there is no facade repair cost, the functionality is at 1. However, if the facade repair cost equals the replacement cost, the functionality drops down to 0, indicating a failure of the functionality.

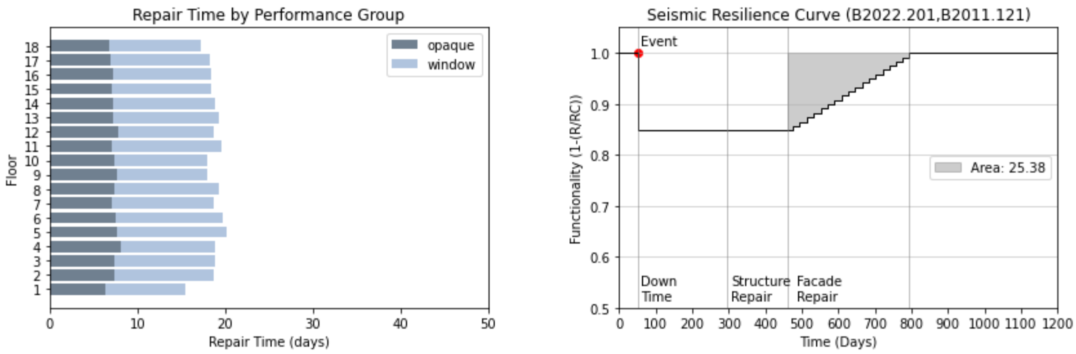

Figure 4.14: Seismic Resilience Curve

Using the PACT intensity-based results, the repair cost for each floor of each performance group was calculated. The mean repair cost per floor out of 200 realizations was then determined. The total repair cost per floor for the facade components B2011.001a and B2022.201 was defined as the sum of their individual repair costs.

The total replacement cost was determined as a proportion of the facade replacement cost out of building replacement. Not necessarily a replacement cost, but the construction cost from the literature was used as an estimate of the cost. For a unitized system that covers the entire building envelope, the estimated cost is 20-30% of the total building cost (Klein, 2013). From the previously defined replacement cost of the whole building, which is $2,187,900, $656,370 (30%) was defined as the total replacement cost.

The resilience loss for each floor was calculated by determining the repair cost per floor and the total replacement cost, and then plotted on the resilience curve as shown in Figure 4.14. The resilience loss corresponds to the filled area between full functionality 1 and $Q(t)$, and is expressed in functionality*day units:

$$\text{Resilience Loss} = \int_{t_0}^{t_1} [1 - Q(t)]dt \tag{4.10}$$

Here t_0 denotes the beginning of the facade repair process, and t_1 denotes the time at which full functionality of the facade components is restored. The total time required for repairing this facade package was 334 days.

Loss Time

The resilience curve is a function of time, and the timeline after a functionality drop due to a disruptive event would be as follows: the repairment won't start right away. Instead, there will be downtime until the repair starts, which will vary depending on the project. As the repair begins, depending on the repair plan, the repairment of building components will be conducted in serial time or in parallel time. The structural repairment comes first in the whole schedule, and therefore, it is assumed that for this project, facade repairment will follow after the structural repairment is finished.

In summary, the whole resilience curve is divided into three sectors: downtime, structural repair time, and facade repair time from the outbreak of an earthquake until the full recovery of the system. This corresponds to full functionality loss of the facade during the downtime and structural repair time, and proportional functionality loss per floor of the facade during the facade repair time.

Downtime is the time required to perform repairs to a building to allow re-occupancy or restore functionality (Almufti & Willford, 2013). It includes the delay between the earthquake event and the start of repairs. In Section A4.3 of REDi report (Almufti & Willford, 2013), a methodology for assessing downtime is presented, which provides an overview of the total downtime calculation. The factors that can impede downtime include engineering mobilization and review, financing, contractor mobilization, and permitting. Using the median delay time of 35 weeks (246 days) for these impeding factors in Table 8, the total downtime for this project was calculated.

Structural repairs were scheduled simultaneously, with the repair time for the floor requiring the most extensive repairs considered the total repair time for the entire structure. Facade repairs were scheduled sequentially, with repair time per floor correlating with functionality recovery per floor. The incremental steps in the resilience curve indicate that as repairs are made to a floor, after the repair time has passed, the functionality is recovered to the extent of the previously lost functionality of that floor.

4.7.3 Analyze Economic Loss

Based on the PACT intensity-based results, the repair cost for every floor of each performance group was calculated. Next, the repair cost per floor for facade components B2011.001a and B2022.201 were summed for all 18 stories. The total repair cost for this facade package was $639,636.

4.7.4 Facade Seismic Resilience

The functionality and economic losses were calculated for three intensities of hazards: intensity 1 (Figure 4.15(a)), an earthquake with a return period of 73 years; intensity 3 (Figure 4.15(b)), with a return period of 475 years; and intensity 5 (Figure 4.15(c)), with a return period of 2475 years. The loss in functionality, measured in functionality-days, was 11.26, 25.37, and 48.20, respectively. The loss cost (in dollars) was 427,575, 639,636, and 873,743, respectively.

The results indicate that as intensity increases, total resilience loss and economic loss also increase. Furthermore, the proportion of repair time between opaque and window components varies across different floors for different intensities. For intensity 1, it can be inferred that the damage occurred in more floors of the opaque component than the window component. However, if damage did occur, the window component required more repair time, indicating its higher resistance to intensity 1 but longer repair time if necessary.

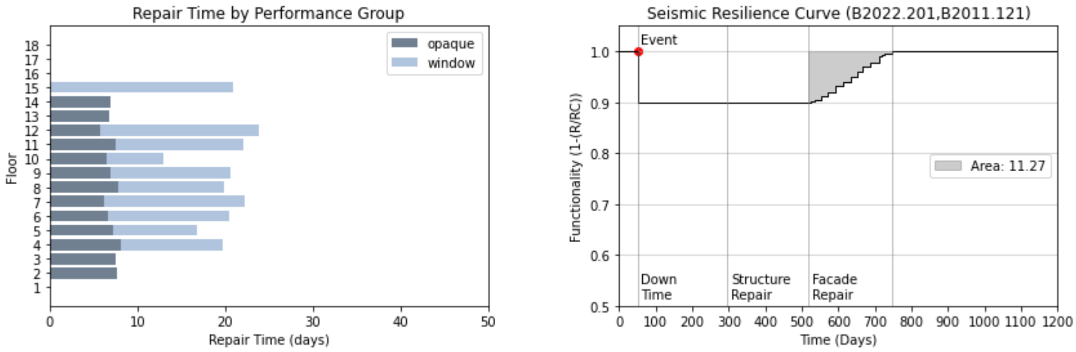

(a) Intensity 1

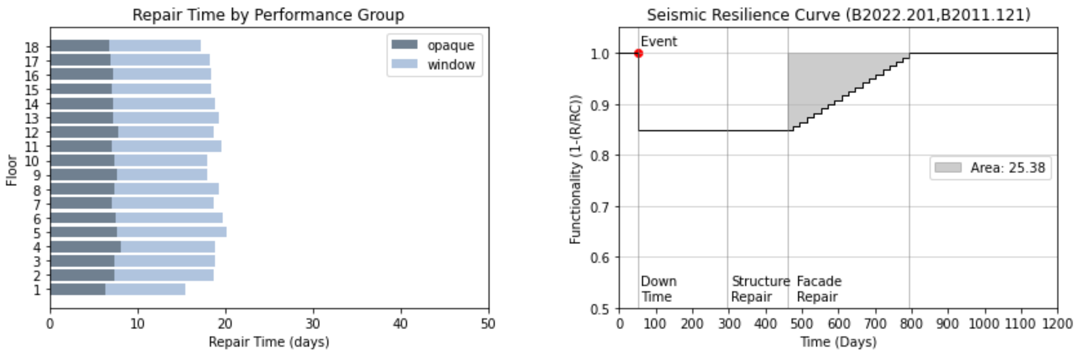

(b) Intensity 2

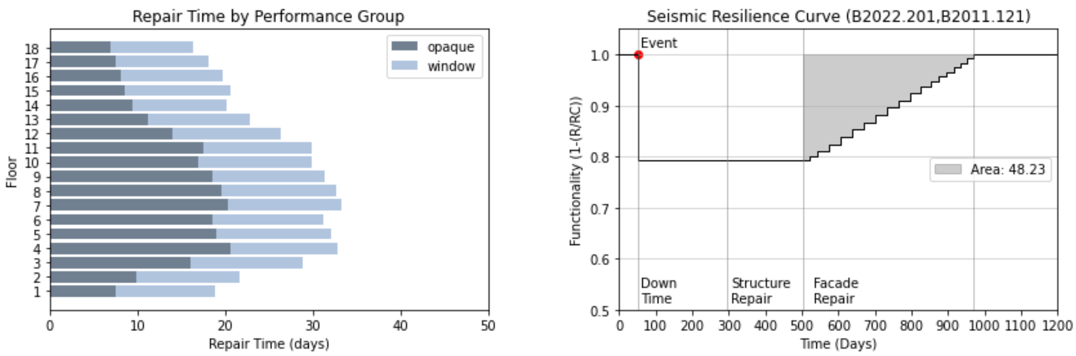

(c) Intensity 3

Figure 4.15: Facade seismic resilience

5 Quantification of Thermal Resilience

5.1 Select Assessment Type and Performance Measure

This case study evaluates the indoor thermal performance of a building during an extreme weather event. Specifically, it examines the impact of a heatwave, which increases the outdoor temperature by 5 degrees Celsius and lasts for 7 consecutive days. The indoor thermal performance is measured using the damage intensity measure SET. The hours and extent during which the observed SET exceeds the SET threshold describe the loss in functionality. Finally, the thermal resilience of the facade package is evaluated using thermal resilience metrics.

5.1.1 Damage Intensity Measure

The RELi 2.0 Rating System is a resilience-based rating system developed by the Market Transformation to Sustainability (MTS) and its RELi Collaborative. In RELi 2.0 Appendix B (USGBC, 2018), options are provided for establishing thermal safety and ensuring habitable temperatures within buildings. The rating system takes into account a building's capability to passively maintain thermally safe conditions during a power outage that lasts four days during the peak summertime of a typical meteorological year. Standard effective temperature(SET) is presented as one of the paths for demonstrating thermal safety compliance. The SET metric is used because it takes into account both relative humidity and mean radiant temperature. It is considered a more relevant metric than dry-bulb temperature for defining livable conditions in buildings that have limitations in space-conditioning systems. In RELi, the thermal safety temperatures for SET are stated as not exceeding 5°C SET-days (120 °C SET-hours) above 30°C SET for residential buildings, and 10°C SET-days (240 °C SET-hours) above 30°C SET for non-residential buildings.

SET Definition

In ASHRAE 55 (2017), SET is defined as : the temperature of an imaginary environment at 50% RH, ¡0.1 m/s air speed, and tr = ta, in which the total heat loss from the skin of an imaginary occupant with an activity level of 1.0 met and a clothing level of 0.6 clo is the same as that from a person in the actual environment, with actual clothing and activity level.

EnergyPlus uses the Pierce Two-Node model developed by Gagge to calculate Standard Effective Temperature. Calculating SET requires meteorological and physiological parameters, such as air temperature, water vapor pressure, wind velocity, radiative temperature, occupant clothing level, and metabolic rate.

SET Threshold

ASHRAE 55 (2017) introduces occupant thermal environment surveys to assess comfort conditions within an acceptable range. The survey uses the ASHRAE seven-point thermal sensation scale, ranging from cold, cool, slightly cool, neutral, slightly warm, warm, to hot (PTS=-3, PTS=-2, PTS=-1, PTS=0, PTS=1, PTS=2, PTS=3).The equation for the relationship between Predicted Thermal Sensation (PTS) and Standard Effective Temperature (SET) was derived by Gao et al. (2015) and is as follows:

$$PTS = 0.25SET - 6.03, R^2 = 0.998 \tag{5.1}$$

Using the PTS scale, a PTS value of 0 indicates a neutral comfort condition, with a SET value of 24.12°C. A PTS value of 1 indicates a slightly warm condition, with a SET value of 28.12°C. A PTS value of 2 indicates a warm condition, with a SET value of 32.12°C. Ji et al. (2023) utilized the aforementioned values to define three threshold values: $SET_{comfort}$, SET_{alert}, and SET_{emer}, for examining building resilience during summertime heat events. The research used the SET threshold values to assign different penalty coefficients and found that the threshold values were appropriate as a performance indicator for analyzing multi-building zones with different retrofit strategies.

For this research, the limit states for fragility analysis are set at 24°C for Limit State 1, 28°C for Limit State 2, and 32°C for Limit State 3. Between LS 1 and LS 2, indoor comfort is neutral. At LS 2, discomfort begins, and LS 3 is a more severe threshold where discomfort increases. In the following fragility analysis, thermal comfort is defined as the functionality of the system, where exceeding the comfort threshold results in a loss of system functionality.

5.1.2 Thermal Resilience Metrics

Thermal resilience is measured in terms of functionality and economic loss reduction. The ability to reduce damage exposure is expressed in terms of time and extent (degree hours) that the Standard Effective Temperature (SET) is within the discomfort range, which is above the comfort limit and below the critical level. The ability to recover to a habitable state is expressed in terms of the time and extent (degree hours) it takes for SET to return to the comfort limit.

5.2 Define Component Fragility

5.2.1 Fragility Function

Assessments of heat vulnerability related to building aspects are rare and often simplified, relying solely on the age of the building or the presence of air conditioning (Szagri & Szalay, 2022). Szagri and Szalay (2022) used fragility and hazard curves to determine the probability of overheating during heatwave periods. The fragility curve of six different building typologies was assessed using a maximum likelihood method, assuming a lognormal cumulative distribution function. The fragility curve shows the conditional probability of overheating.

Maximum Likelihood Fitting Procedure

The maximum likelihood method is a fitting procedure that determines the parameters of a distribution (fragility function) that are most pobable to generate the observed data. Baker (2015) provides approaches for fitting fragility functions with minimal structural analyses required. The fragility function is assumed to follow a lognormal cumulative distribution, which can be expressed mathematically as follows: :

$$P(C \mid IM = x) = \Phi\left(\frac{\ln(x/\theta)}{\beta}\right) \tag{5.2}$$

where $P(C \mid IM = x)$ is the probability that the structure will collapse at intensity measure $IM = x$; $\Phi()$ denotes the standard normal cumulative distribution function (CDF); θ denotes the median value of the probability distribution; and β denotes the logarithmic standard deviation.

The likelihood of not only the observed data, but also the entire data to be observed, is the product of individual likelihoods. The probability of observing z_j collapses out of n_j analyses with $IM = x_j$ can be given by the binomial distribution:

$$Likelihood = \prod_{j=1}^{m} \begin{matrix} n_j \\ z_j \end{matrix} \; p_j^{z_j}(1-p_j)^{n_j - z_j} \tag{5.3}$$

The objective of fragility fitting is to obtain the highest probability of having produced the observed data by maximizing the likelihood function. The variables that maximize this function can be found by solving for the values of θ and β in the following equation:

$$\{\hat{\theta}, \hat{\beta}\} = \underset{\theta,\beta}{\arg\max} \prod_{j=1}^{m} \left(\begin{matrix} n_j \\ z_j \end{matrix} \; \Phi\left(\frac{\ln\left(x_j/\theta\right)}{\beta}\right)^{z_j} \left(1 - \Phi\left(\frac{\ln\left(x_j/\theta\right)}{\beta}\right)\right)\right)^{n_j - z_j} \tag{5.4}$$

5.2.2 Fragility Analysis

Shoebox Model

An example shoebox model was used to illustrate the calculation of various component fragility functions. The shoebox represents a typical floor, the 10th floor, located in the middle of a 19-floor building. The floor plan of the shoebox model is shown in Figure 5.1.

The analysis used weather data from TUR-IZ_Izmir_172190_TMYx as the base climate setting. The simulation ran for the full range of weather data, which is 8760 hours (one year). The SET temperature of Zone2, one of four parameter zones on the south-facing side, was measured throughout the year.

Three Factor Experiment

To measure a facade's contribution to the SET of a building, facade components with different thermal properties were tested. The thermal properties were defined by three factors: heat transmittance (U-value), heat capacity, and admitted solar radiation (SHGC).

In situations where outdoor air is warmer than indoor air, typically in the summer, the main load to address is the cooling load. One way to reduce the cooling load is to prevent heat

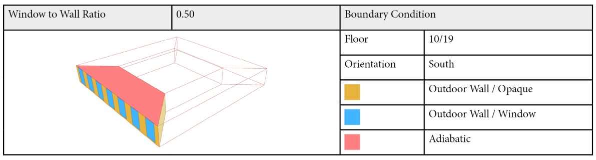

Figure 5.1: Shoebox model for fragility analysis

transfer from the exterior to the interior. Under these circumstances, a facade with thermal properties that have a low U-value, high heat capacity, and low SHGC is assumed to be better performing. This is the case when the facade is very insulative, stores much heat, or has less solar radiation coming in. On the contrary, a facade with thermal properties that have a high U-value, low heat capacity, and high SHGC would be the worse performing facade. This is equivalent to a greenhouse where there is an active transfer of heat between the exterior and interior.

Figure 5.2 shows the parameter domain of facade components that were tested for their thermal fragility. It is important to note that not all material types possess all three thermal properties. While all glazing materials contain these properties, opaque materials lack the property of solar heat gain. Six components were tested in total: two for a full glazing facade and four for a full opaque facade. The tested components are placed on a 2D plane, with one performing better and one performing worse in terms of thermal properties, while the other two thermal properties remain fixed. For example, W0.05T01 has a U-value of 0.5 W/m²K, while W0.05T02 has a U-value of 2.3 W/m²K. The heat capacity value is fixed at 0.4 J/K, and the SHGC value is not applicable.

A combination of opaque wall and window wall was tested to evaluate the combined effect of two different material types on thermal fragility. The better-performing opaque material and better-performing window material were combined to form a facade type like W0.50T01 and W0.50C01. Conversely, worse-performing components were also combined, resulting in W0.05T02 and W0.05C02.

Fragility Function

Fragility functions were created for three limit states (LS1 = 24°C, LS2 = 28°C, LS3 = 32°C) using outdoor air temperature as the intensity measure. Exceeding these limits is expected to cause the system to collapse, resulting in a failure to maintain a comfortable indoor thermal environment. The objective of the fragility analysis is to determine the probability of the indoor thermal environment (SET) exceeding the limit state at a given outdoor air temperature. This can be formulated as follows:

$$P(C \mid IM = x_j)_{observed} = \frac{number\, of\, hours\, when\, IM = x_j}{number\, of\, hours\, per\, day} \tag{5.5}$$

In this context, the intensity measure x_j corresponds to the daily mean outdoor air temperature. The probability of SET reaching the limit state, given the intensity level x_j is represented by P. This probability can be expressed as the number of hours in a day during which SET exceeds the limit state, divided by the total number of hours in the day. Assuming that this probability follows a lognormal distribution, maximum likelihood method to derive fragility functions for facades with varying thermal properties.

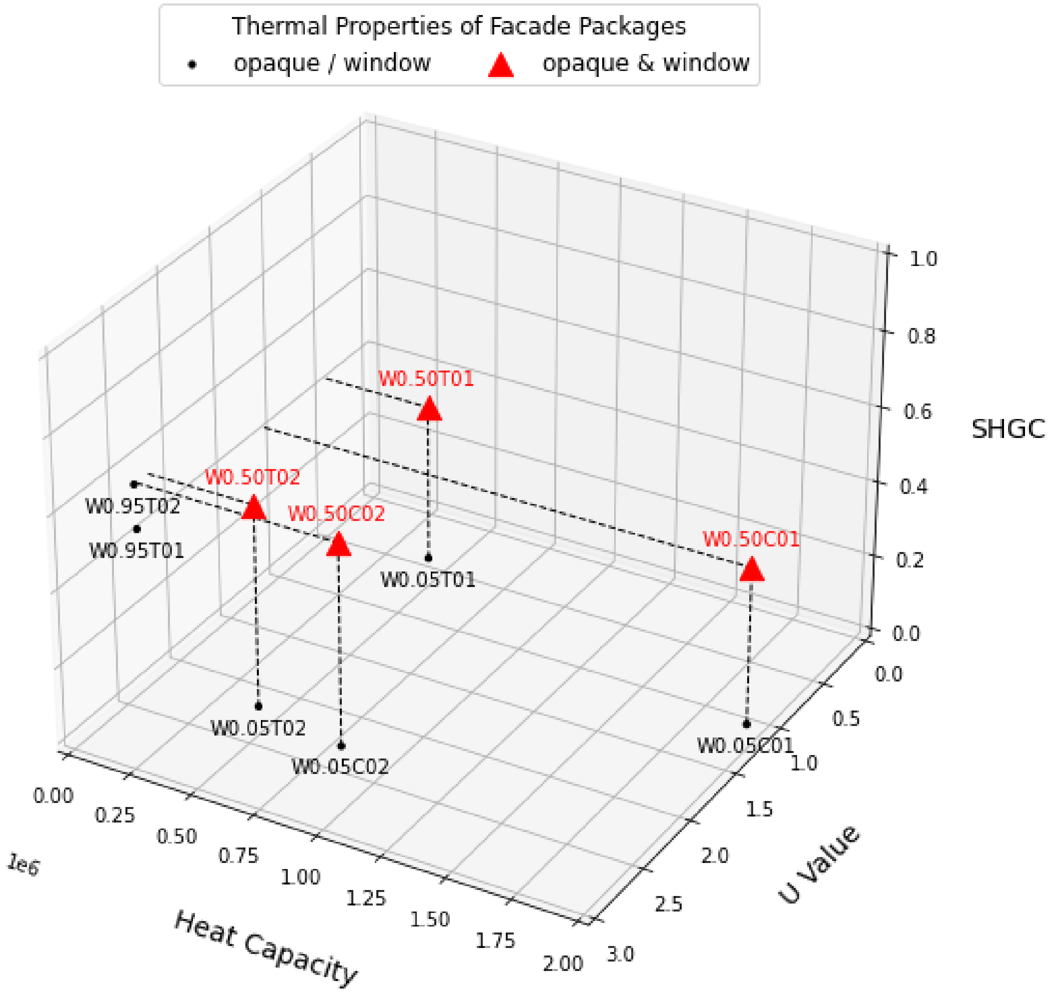

Figure 5.2: Parameter domain for testing fragility

5.2.3 Thermal Fragility Specifications

Figure 5.3, 5.4, 5.5 displays fragility curves for ten different facade types at SET limits of 24°C, 28°C, and 32°C. The depicted facades have exterior walls that are either fully opaque or fully glazed with windows. Figure 5.6, on the other hand, shows a combination of opaque and glazing, with a window-to-wall ratio of 0.5.

For all the fragility curves in Figure 1, the maximum likelihood method resulted in the initial guess parameter (median value of 0.8 and dispersion of 0.5) for LS1 and LS2 fragility functions. This indicates that the fitting procedure was unable to find a fragility function that could be tested as the data contains too little information for SET being over LS1 and LS2. In light of these missing results, the fragility curves of LS3 were compared among the tested facade types.

Thermal Fragility Specifications - Opaque / Window

Based on the fragility curve W0.05T01, which corresponds to a fully opaque facade with double layers of insulation, there is approximately a 15% chance that the SET will exceed LS3 (32 °C) when the average daily outdoor temperature is 24 °C. Similarly, for the fragility curve W0.05T02, which represents a less insulative facade, the probability is also around 15% at the same outdoor temperature. However, when the outdoor temperature rises to 32°C, the facade with less insulation (W0.05T02) has twice the probability of exceeding the LS3 compared to the fully insulated facade (W0.05T01). This suggests that at moderate temperatures, the level of insulation is less significant, whereas at high temperatures, the insulation layer makes a notable difference in maintaining a separate indoor thermal condition from the outdoor environment.

Facade systems with similar insulative values but different heat capacities were compared. Concrete walls (W0.05C01, W0.05C02) showed a lower probability of exceeding LS3 compared to composite walls with insulation layers (W0.05T01, W0.05T02) at an outdoor temperature of 32°C. The U-value for W0.05C02 is 2.35 kWh, while the U-value for W0.05T02 is 2.21; these values are very similar. However, the concrete wall has about a 10% lower probability of exceeding LS3. This can be explained by the thermal lagging effects of materials with high heat capacity. It can also be inferred that the effect of heat capacity increases at higher outdoor temperatures.

Compared to the opaque wall, the window fragility curves (W0.95T01, W0.95T02) generally had a higher probability of exceeding the limit state at both moderate and high temperatures. This can be explained by solar heat gain. Windows with higher solar heat gain coefficient (W0.95T02) and those more resistant to solar heat gain (W0.95T01) exhibited distinct fragility curves for different limit states. Therefore, a direct comparison was not possible.

Thermal Fragility Specifications - Opaque & Window

When the opaque wall and window are combined half and half, as shown in Figure 5.6, the difference that was observable between the composite wall and concrete wall became less apparent. Obviously, the solar heat gain from the 50% of the window flattened out the performance in a more vulnerable way.

SHOEBOX THERMAL ZONE

Window to Wall Ratio	0.05	Boundary Condition	
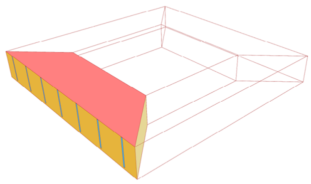		Floor	10/19
		Orientation	South
			Outdoor Wall / Opaque
			Outdoor Wall / Window
			Adiabatic

FACADE PACKAGE

Opaque		Window		Fragility Curve (W0.05T01)		
Typical Insulated Exterior Mass Wall-R12		Generic Double Pane		Limit State	Median	Dispersion
U value	0.49	U value	2.36	L1 = 24	0.8	0.5
SHGC	N/A	SHGC	0.42	L2 = 28	0.8	0.5
Heat Capacity	428,228	Heat Capacity	N/A	L3 = 32	1.3	0.53
int 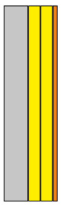 ext				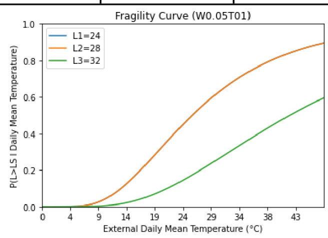		
Opaque		Window		Fragility Curve (W0.05T02)		
Typical Insulated Exterior Mass Wall-R6		Generic Double Pane		Limit State	Median	Dispersion
U value	2.24	U value	2.36	L1 = 24	0.8	0.5
SHGC	N/A	SHGC	0.42	L2 = 28	0.8	0.5
Heat Capacity	428,228	Heat Capacity	N/A	L3 = 32	0.90	0.21
int 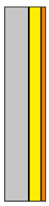 ext				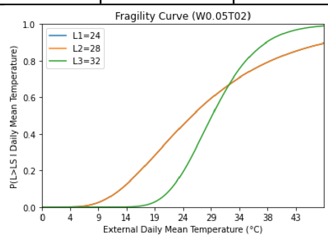		

Figure 5.3: Thermal fragility curves - Opaque - Uvalue

SHOEBOX THERMAL ZONE

Window to Wall Ratio	0.05	Boundary Condition	
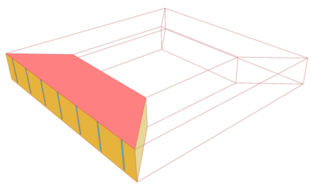		Floor	10/19
		Orientation	South
			Outdoor Wall / Opaque
			Outdoor Wall / Window
			Adiabatic

FACADE PACKAGE

Opaque		Window		Fragility Curve (W0.05C01)		
(custom) Exterior Mass Wall Multiple		Generic Double Pane		Limit State	Median	Dispersion
U value	1.12	U value	2.36	L1 = 24	0.8	0.5
SHGC	N/A	SHGC	0.42	L2 = 28	0.8	0.5
Heat Capacity	1950,787	Heat Capacity	N/A	L3 = 32	1.77	0.65
int 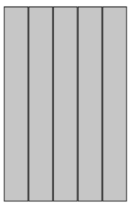 ext				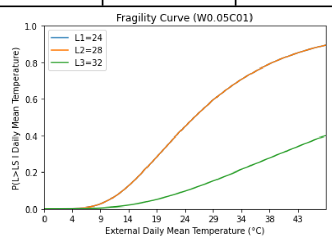		

Opaque		Window		Fragility Curve (W0.05C02)		
(custom) Exterior Mass Wall		Generic Double Pane		Limit State	Median	Dispersion
U value	2.35	U value	2.36	L1 = 24	0.8	0.5
SHGC	N/A	SHGC	0.42	L2 = 28	0.8	0.5
Heat Capacity	808,867	Heat Capacity	N/A	L3 = 32	1.00	0.30
int 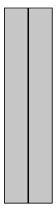 ext				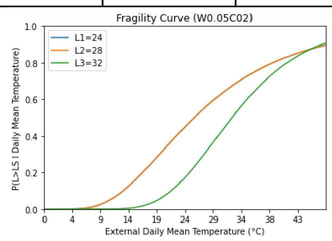		

Figure 5.4: Thermal fragility curves - Opaque - Heat Capacity

SHOEBOX THERMAL ZONE

Window to Wall Ratio	0.95	Boundary Condition	
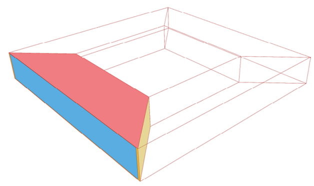		Floor	10/19
		Orientation	South
			Outdoor Wall / Opaque
			Outdoor Wall / Window
			Adiabatic

FACADE PACKAGE

Opaque		Window		Fragility Curve (W0.95T01)		
Typical Insulated Exterior Mass Wall-R12		Generic Double Pane 6mm Generic Window Air Gap 13mm Generic Clear Glass 6mm		Limit State	Median	Dispersion
U value	0.49	U value	2.36	L1 = 24	0.8	0.5
SHGC	N/A	SHGC	0.42	L2 = 28	0.50	0.51
Heat Capacity	428,228	Heat Capacity	N/A	L3 = 32	0.8	0.5
		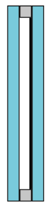 int ext		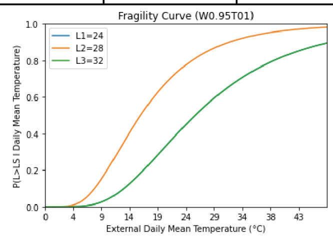		

Opaque		Window		Fragility Curve (W0.95T02)		
Typical Insulated Exterior Mass Wall-R12		Planibel Clearlite (AGC) 6mm Generic Window Air Gap 13mm Generic Clear Glass 6mm		Limit State	Median	Dispersion
U value	0.49	U value	2.37	L1 = 24	0.8	0.5
SHGC	N/A	SHGC	0.54	L2 = 28	0.8	0.5
Heat Capacity	428,228	Heat Capacity	N/A	L3 = 32	0.74	0.76
		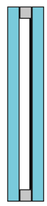 int ext		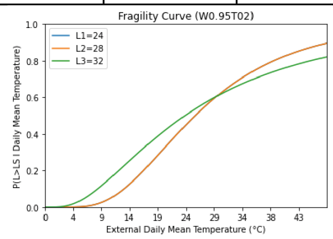		

Figure 5.5: Thermal fragility curves - Window - SHGC

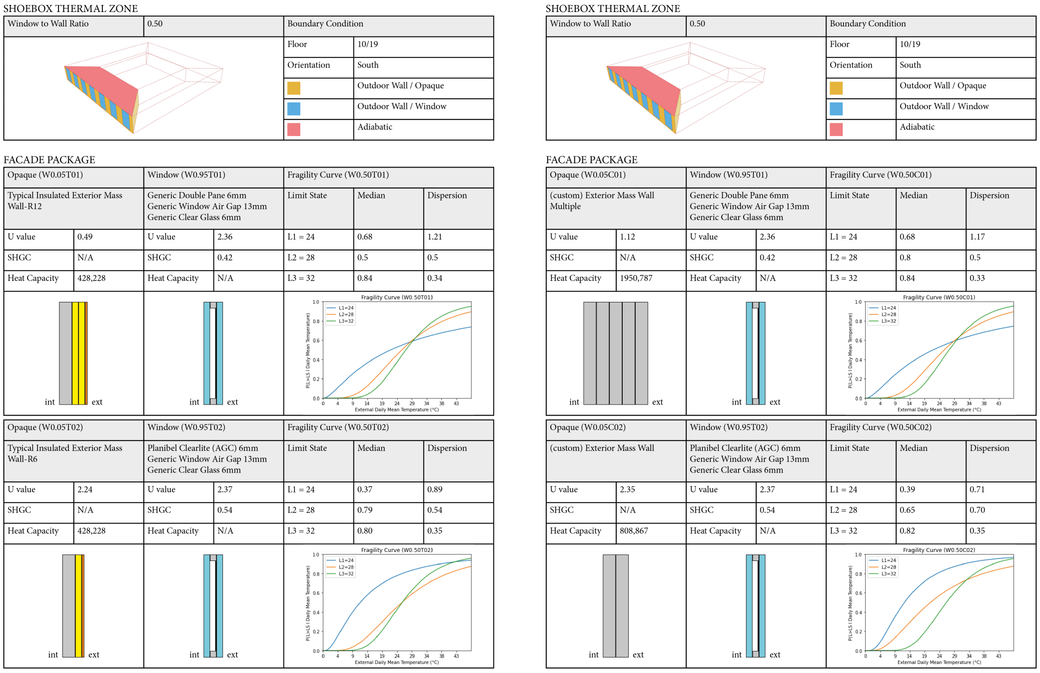

Figure 5.6: Thermal fragility curves - Opaque & Window

5.3 Assemble Building Performance Model

5.3.1 Building Information

Multi Thermal Zone

The building has a floor plan of 22.5m by 22.5m and 18 stories, with a height of 3m per story. The thermal zone was divided based on the guidelines provided by ASHRAE Standard 90.1 Appendix G. It suggests dividing the thermal zone into a core and a perimeter zone, and then further dividing the perimeter zone based on orientation. The perimeter zone depth is five meters.

As shown in Figure 5.7, each floor was divided into five thermal zones. Each zone represents a node within a thermal network. The thermal zone is usually aligned with the spatial subdivision of the floor plan. For this research, an open plan layout was used, so the inter-zone wall was set to have a U value of 3.24 W/m²K. Although not as much as a completely lumped mixed air volume, it still allows for quite a high degree of air mixing between the zones. The boundary condition between floors is adiabatic, which means they are thermally separate. To reduce computational load and focus only on the relevant floors, the energy simulation was conducted separately for each floor.

The simulation was carried out for the entire building, but to observe the direct impact of the facade on the SET temperature, the SET temperature of the node in Zone 2, which is a

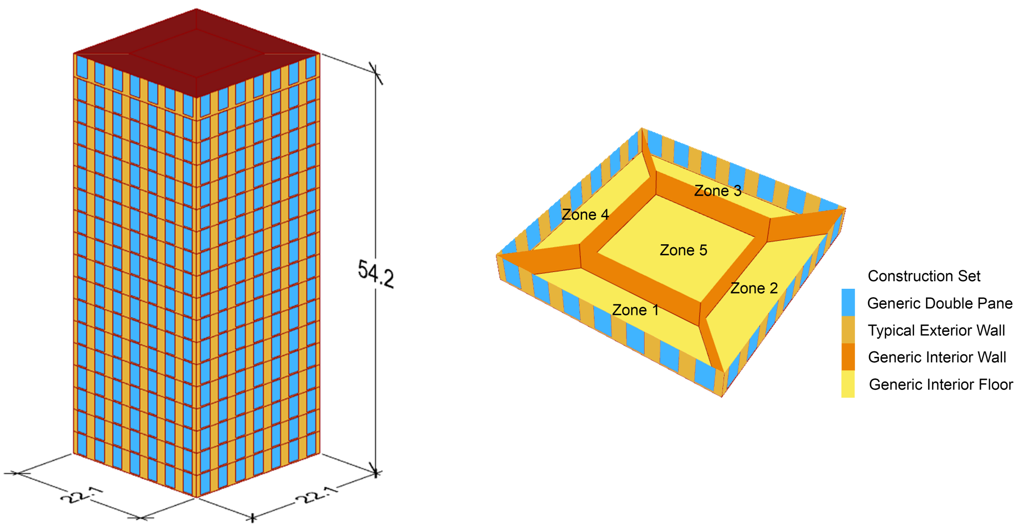

Figure 5.7: 18-story office building and thermal zones of a typical floor

south-oriented parameter zone, was examined.

Window to Wall Ratio

The window-to-wall ratio was fixed at 0.5, meaning that out of the total 270 m² of facade surface per floor, 135 m² was allocated for opaque wall and 135 m² for window. To ensure that all parameter zones had the same configuration, the facade pattern was developed so that opaque and window sections were placed next to each other in a stripe pattern. Either an opaque or window wall can span the entire story height, instead of having the window placed within the frame of an opaque wall. This design decision was made because the seismic fragility database lacked data on framed windows, and it was necessary to make the set of facades equivalent for modeling purposes.

Building Program

A 'MediumOffice Building' was selected from the Honeybee Building Program library. The program for medium office buildings includes the following preset values and schedule for the simulation: Occupancy - 0.071 people/m², Lighting - 10 W/m², Electric Equipment - 7.5 W/m², Infiltration - 0.000227 m³/s-m², and Setpoint - Heating 21°C, Cooling 24°C.

Building Construction Set

The base construction set was created using the ASHRAE Climate Zone 4, ASHRAE 90.1 2019 building vintage, and the Mass construction type. The opaque wall was designed using the exterior_subset, and the window was designed using the subface_subset. Table 1 provides details on the construction layers, with Layer 1 representing the exterior facing layer and Layer 4 representing the interior facing layer. The materials, except the glazing component Planibel Clearlite, were taken and modified from the Honeybee material library. Planibel Clearlite is a glass product from AGC that provides high light transmission to let in more natural light. The glass material specifications were taken from the product catalogue.

Table 5.1: Facade construction set

Fragility ID	Layer 1	Layer 2	Layer 3	Layer 4
		Typical Insulated Exterior Mass Wall-R12		
W0.05T01	Stucco	Concrete	Insulation-R10	Gypsum
thickness (m)	0.0253 m	0.2032 m	-	0.0127 m
		Typical Insulated Exterior Mass Wall-R6		
W0.05T02	Stucco	Concrete	Insulation-R4	Gypsum
thickness (m)	0.0253 m	0.2032 m	-	0.0127 m
		Exterior Mass Wall Double		
W0.05C01	Stucco	Concrete	Concrete	Gypsum
thickness (m)	0.0253 m	0.0826 m	0.6096 m	0.0127 m
		Exterior Mass Wall Single		
W0.05C02	Stucco	Concrete	Concrete	Gypsum
thickness (m)	0.0253 m	0.2032 m	0.2032 m	0.0127 m
		Generic Double Pane Low-E		
W0.95T01	Low-e Glass	Air Gap	Clear Glass	
thickness (m)	0.006	0.0127	0.006	
		Generic Double Pane Planibel		
W0.95T02	Planibel Clearlite	Air Gap	Clear Glass	
thickness (m)	0.006	0.0127	0.006	

Building Service Systems

The Ideal Load Air System object from Honeybee Energy was used to condition zones. This HVAC system cools or heats air to a zone in sufficient quantity to meet the zone load or up to its limits, in an 'ideal' manner. The Ideal Loads Air System calculates the thermal energy required to fulfill the zone's thermal energy demand without specifying HVAC.

The HVAC system was sized based on the DDY file of the specified weather data TUR-IZ-Izmir-Adnan.Menderes.Univ.172190-TMYx. The sizing parameters included 78 design days and a multiplication factor of 1.25 for peak heating load and 1.15 for peak cooling load in each zone.

When evaluating a facade's ability to maintain survivable indoor conditions, the Ideal Air System needs to be modified to a certain extent. With the Ideal Air System, the building will meet setpoints regardless of the actual load. However, this approach cannot accurately reflect the facade's contribution to the SET temperature output. To address this issue, the cooling limit was set to 70% of the maximum cooling capacity, instead of auto-sizing the system. For Zone 2, the maximum total cooling capacity for the Ideal Loads Air System Design is 11,442.57 W. We set the cooling capacity limit of the HVAC system to 8,009.8 W, which is 70% of the cooling capacity. This means that the cooling system will not operate if the cooling demand exceeds this limit.

The windows of the building cannot be opened, meaning there is no natural ventilation. The room is only ventilated through a mechanical ventilation system, which is set to have an air change rate per hour (ACH) of 3. This is a reference value from ASHRAE 2022 for typical office buildings. Instead of operating the mechanical ventilation according to the occupancy schedule, the zone is set to be ventilated hourly, mainly to let out internal heat at night. Even when the cooling system is unavailable, the mechanical ventilation is still operated (this explains why cooling energy is still consumed even when the cooling is unavailable). This setting turned out to be important at times to regulate the SET temperature from exceeding outdoor temperature due to overheating when the cooling was unavailable for a certain time. Nighttime ventilation helps to cool down the system and stabilize the building's thermal condition on a daily basis.

5.4 Construct Building Numerical Model

5.4.1 Dynamic Energy Model

Energy Model with/without Cooling System during Heatwave

The purpose of the energy simulation is to assess the facade component's ability to mitigate the impact of heatwave. Therefore, it's best to eliminate other operational factors that contribute to the standard effective temperature (SET) in the model. However, without any additional cooling measures, the SET will either converge to the exterior temperature or exceed it. This creates an unrealistic indoor thermal condition that makes it impossible to differentiate between indoor conditions with and without a heatwave for the indoor temperature will remain overheated throughout all periods. To address this issue, mechanical cooling with a capacity limit was introduced, while passive cooling measures remained unavailable.

The energy simulation was conducted for two cases: one where the cooling system is operational, and one where the cooling system is unavailable only during a heatwave. Two simulations were conducted for a single building/facade configuration, under different operational conditions, in order to quantify the extra energy consumption caused by a heatwave. This extra energy consumption during a heatwave can be calculated as an energy cost, which indirectly implies the recovery cost (cost of returning the SET to a comfortable state).

Figure 5.8 shows the flowchart of the energy model with heatwave events. The flowchart consists of three main streams of energy simulation. The first energy model calculates the design cooling capacity based on normal weather data (without heatwaves). This design capacity is used as the base cooling system sizing for the other two energy models.

The Energy Model 2 uses weather data (EPW file) with heatwave applied, and the system sizing (DDY file) without heatwave. This reflects a system that is designed based on normal historical weather data with fewer anomalies like heatwaves. The cooling energy consumption during the heatwave period will therefore reflect the energy consumed to diminish the increased cooling load.

Energy Model 3 is modeled similarly to Energy Model 2, except the system is set to be unavailable during the heatwave schedule. As a result, subtracting the cooling energy consumption from Energy Model 2 by 3 will result in the added energy consumption during a heatwave, accounting for the 'recovery cost'.

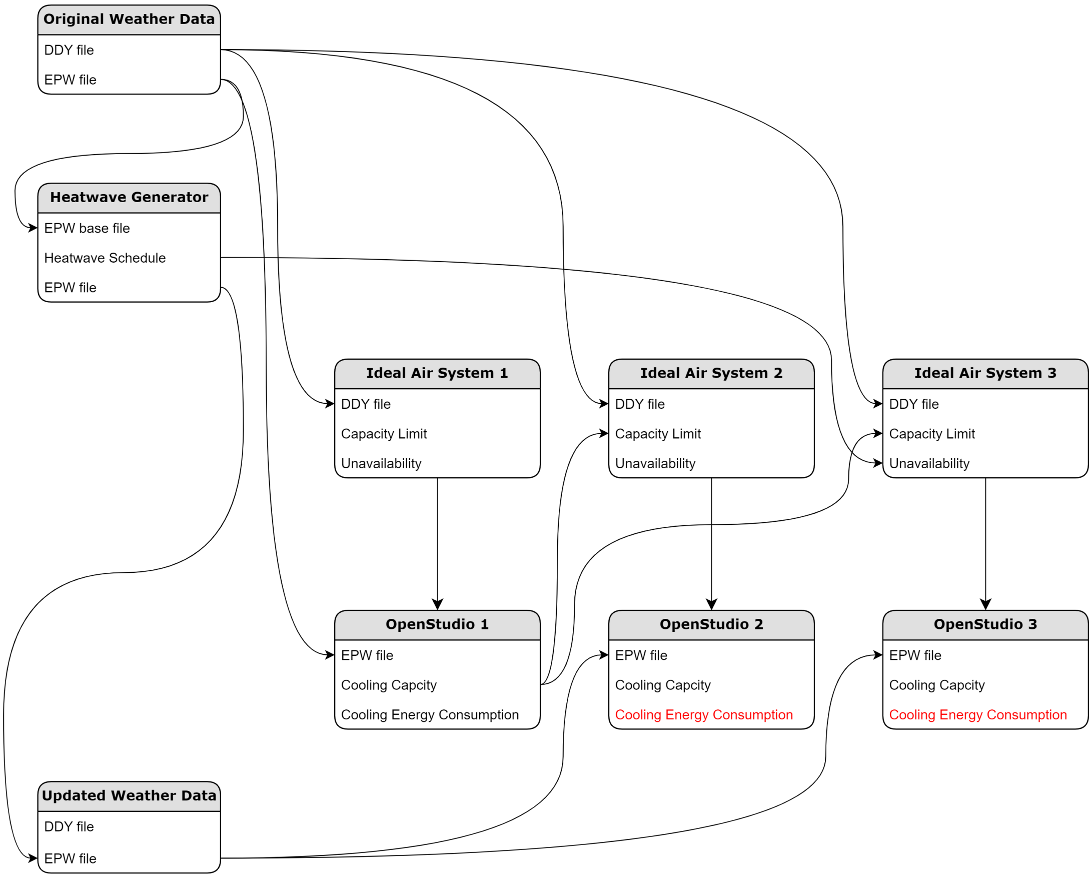

Figure 5.8: Flowchart of the energy model with heatwave events

5.5 Define Thermal Hazard

5.5.1 Heatwave

Definition of Heatwave

The World Meteorological Organization (WMO) defines a heat wave as a period during which the daily maximum temperature exceeds for more than five consecutive days the maximum normal temperature by 5 degrees Celsius, the normal period being defined as 1961–1990.

However, caution should be exercised when comparing or modeling heatwaves due to differences in local climatological conditions affecting their behavior. Recent studies have focused on heatwave detection models, with research examining specific driving factors in different regions (Hulley et al., 2020). Flores-Larsen et al. (2022) proposed a method that uses Ouzeau's model to detect heatwaves and capture their impact on the indoor environment. Ouzeau's model characterizes heatwaves by their duration (number of days), intensity (maximum mean daily temperature), and severity (mean daily temperature above threshold). Indoor overheating degree was used to classify heatwaves according to their impact on the indoor environment. Currently, there are no agreed-upon international protocols for heatwaves, as heatwave detection models vary across regions. To make the tool applicable for assessing different regions with a single method, a methodology for generating heatwave conditions was proposed in the research. In this method, heatwaves are generated by referring to the definition of WMO, based on TMY data.

Heatwave Generation

The weather data, TUR-IZ-Izmir-Adnan.Menderes.Univ.172190-TMYx, was used as the base for applying the heatwave. The data covers the period 1989-2021. Information on a typical spring week on April 29th, an extremely hot week on July 29th, and a typical summer week on August 26th was obtained from the EnergyPlus Design Day (DDY) file. These three weeks were used to apply the heatwave. For a 7 day duration, dry bulb temperature was increased by 5°C.

By definition, a heatwave is an extreme climatic event that is relative to the compared weather. As shown in Figure 5.9, the maximum temperature during a heatwave in a typical spring week is around 30°C, while in an extremely hot week, it is around 40°C. The intensity of a heatwave is not indicated by the absolute temperature, but rather by the discrepancy from the normal temperature. Heatwave was applied to these three weeks with different maximum temperatures to also include the heaetwave in the intermediate season. Additionally, these typical weeks from the DDY file are used for sizing the heating/cooling system in EnergyPlus simulation. If a heatwave is applied to a building with a mechanical system sized based on weather data without considering heatwaves, the system will be overloaded. To simulate such a condition, the typical three weeks were selected for applying heatwave.

The dry bulb temperature in the base weather data was replaced with the heatwave temperature and the newly generated weather file was saved as a separate epw file. To accurately model a heatwave event, climate indicators such as global solar radiation, wind speed, and relative humidity must be considered together. However, in this case, only the air temperature was modified, which could result in some inaccuracies.

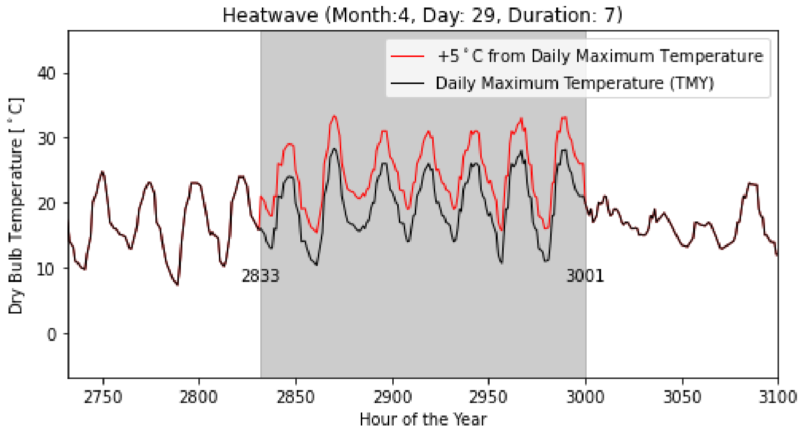

(a) Typical spring week

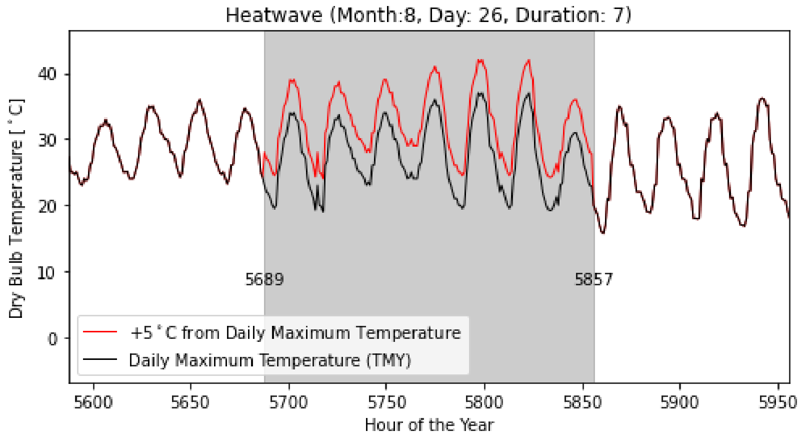

(b) Typical summer week

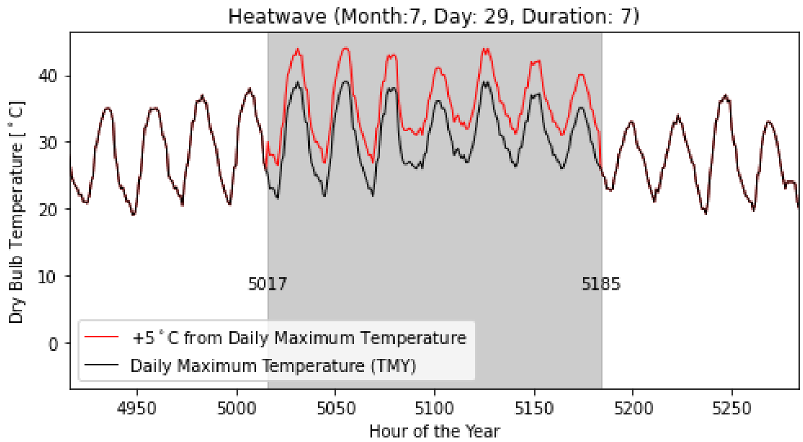

(c) Extremely hot week

Figure 5.9: Heatwave generation based on DDY file

5.6 Analyze Building Response

5.6.1 Indoor Thermal Condition during Heatwave

Figure 5.10 displays the Standard Effective Temperature (SET) during a heatwave for two energy models: one with cooling and one without cooling available, except during the heatwave.

For energy model 1, the SET is maintained at 25°C during the day and around 28°C during unoccupied periods before the heatwave. However, during the first two days of the heatwave, the SET fails to maintain 25°C during occupied periods. Afterward, the SET is more stable but still follows the outdoor temperature's peaks. This illustrates the indoor thermal condition (building response) when exposed to the heat.

In energy model 2, the SET is almost equal to the exterior temperature during a heatwave, as no cooling measures are applied. At the beginning and end of the heatwave, there is over a 20°C difference between the minimum and maximum SET. This suggests that the cooling system's peak load during a heatwave will occur at the very beginning and end of the period, accounting for a significant portion of the total energy consumption during that time.

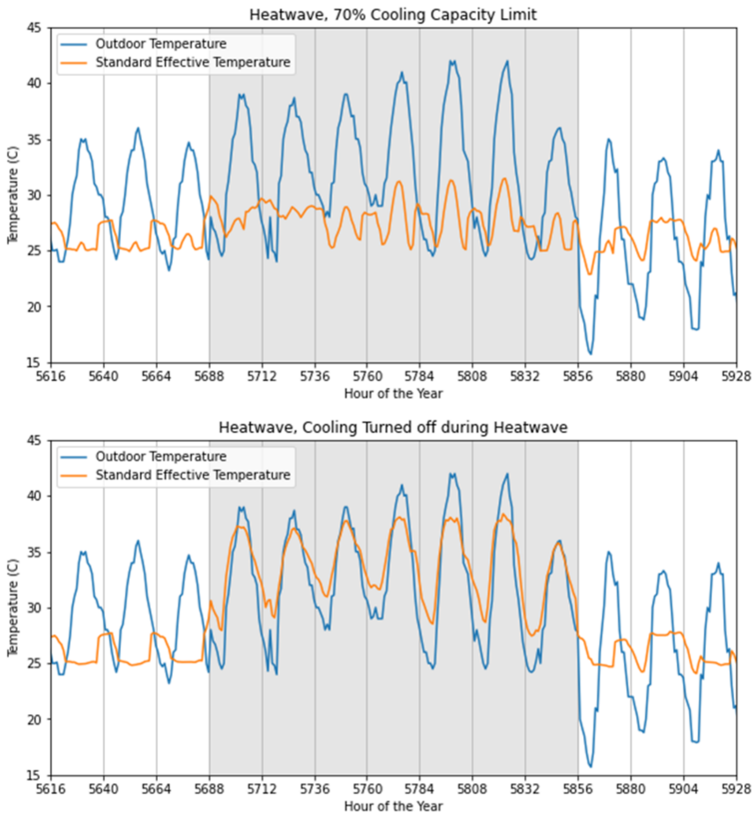

Figure 5.10: SET during heatwave

5.7 Calculate Performance

The analysis used the Facade package with the W0.50T01 fragility curve, which consists of a composite wall with concrete and insulation (W0.05T01) and a double-pane window (W0.95T01). The window-to-wall ratio was set to 0.5. This means that, for each floor, half of the surface is covered with an opaque composite wall, while the other half is covered with a transparent window. The facade package, shown in Figure 5.11, was applied to the building to calculate its resilience performance.

Opaque (W0.05T01)		Window (W0.95T01)		Fragility Curve (W0.50T01)		
Typical Insulated Exterior Mass Wall-R12		Generic Double Pane 6mm Generic Window Air Gap 13mm Generic Clear Glass 6mm		Limit State	Median	Dispersion
U value	0.49	U value	2.36	L1 = 24	0.68	1.21
SHGC	N/A	SHGC	0.42	L2 = 28	0.5	0.5
Heat Capacity	428,228	Heat Capacity	N/A	L3 = 32	0.84	0.34
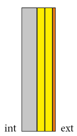		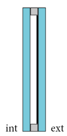		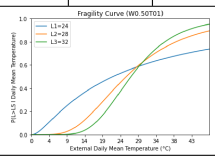		

Figure 5.11: Thermal fragility curve for the case study facade

5.7.1 Analyze Resilience Loss

Bucking et al. (2022) simulated building performance during a winter storm power outage. The quality function is defined by the equation:

$$Q(t) = \begin{cases} 1 & \text{if } T(t) \geq T_\gamma \\ 0 & \text{if } T(t) \leq T_\alpha \\ \frac{T(t)}{T_\gamma - T_\alpha} & \text{otherwise} \end{cases} \tag{5.6}$$

If the indoor air temperature $T(t)$ falls below T_a = 0°C, it is considered as a failure, with quality function being 0. If $T(t)$ is above T_r = 20°C, it implies acceptable recovery with quality function 1. For indoor air temperatures in between 0°C and 20°C, linear interpolation is used.

The mathematical formulation of the quality function in this research was adapted from an assessment of indoor environment quality by Bucking et al. (2022). While Bucking's assessment accounted for cold hazard, this research accounts for heat hazard, and as a result, the inequality signs were switched:

$$Q(t) = \begin{cases} 1 & \text{if } SET(t) \leq SET_{comf} \\ 0 & \text{if } SET(t) \geq SET_{alert} \\ \frac{SET_{alert} - SET(t)}{SET_{alert} - SET_{comf}} & \text{otherwise} \end{cases} \tag{5.7}$$

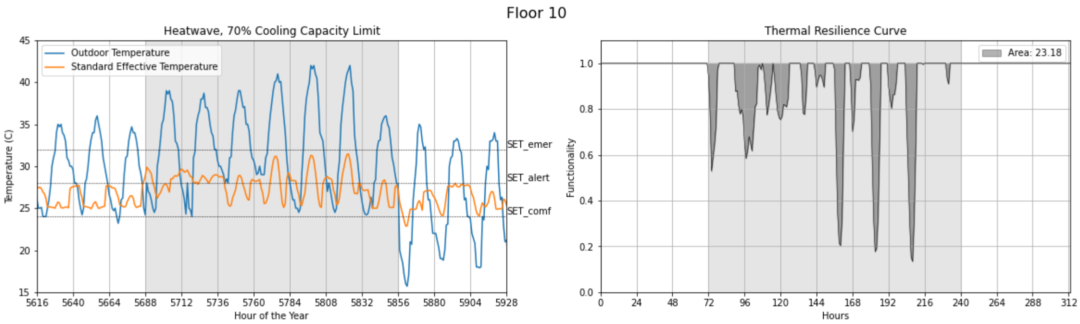

Figure 5.12: Thermal Resilience Curve

If the standard effective temperature $SET(t)$ is above SET_{alert} = 28°C, it is considered as a failure, with a quality function of 0. If $SET(t)$ is below SET_{comf} = 24°C, it lies within the comfortable range, with a quality function of 1. The quality function is a linear interpolation of SET between 24°C and 28°C.

Figure 5.12 shows the functionality curve during a heatwave. The thermal functionality curve has the characteristic that, without any repairs, the system self-recovers over time. This is mainly due to fluctuations in the outdoor air temperature. As the temperature drops at night, the SET temperature also drops, and the lost functionality is recovered. The loss of resilience can be measured by the expected degradation in quality over time, as defined by Bruneau and Reinhorn (2006), with the following formula:

$$\text{Resilience Loss} = \int_{t_0}^{t_1} [1 - Q(t)]dt \tag{5.8}$$

The resilience loss corresponds to the filled in area between full functionality 1 and $Q(t)$. It can be understood that a lower value of the area indicates lower resilience loss, meaning a more resilient system.

5.7.2 Analyze Economic Loss

The economic loss was calculated based on the loss of energy load, which is the difference in cooling energy consumption between the energy model with cooling operation during a heatwave and the model without cooling during a heatwave. The energy model with cooling operation resulted in 510.27 kWh of zone total cooling energy, which cost 128.84€ when the electricity tariff of 0.2525 €/kWh is applied. On the other hand, the energy model without cooling resulted in 404.78 kWh of total cooling energy, which cost 102.20€. The difference between the two, which is 26.63 €, is the final loss cost outcome.

5.7.3 Facade Thermal Resilience

The functionality and economic losses were calculated for three representative floors: the bottom and top floors, and the middle 10th floor. Figure 5.13 shows the resilience curve of three floors. The loss in functionality (measured in functionality-hours) was 23.52, 23.18, and 16.57 for floors 1, 10, and 18, respectively. The loss cost (in €) was 26.23, 26.63, and 47.16 for floors 1, 10, and 18, respectively. The values for the representative floors were added, resulting in a total loss of 63.27 functionality-hours and 100.04 €.

According to the results, the top floor has the lowest resilience loss but the highest economic loss. Based on the definition of resilience loss from Bruneau and Reinhorn (2006), a lower resilience loss should indicate a more resilient system. However, in this case, that is not true. This is because the resulting SET has fewer hours of resilience loss due to the removal of overheated loads by cooling under its maximum capacity. While achieving better seeming resilience performance, the cost of using the cooling system is high, as indicated by the opposite loss result for cost. Although it may not be intuitive, in terms of facade thermal resilience, a more resilient facade system indicates higher resilience loss with lower economic loss. This indirectly suggests that the building's indoor conditions were controlled to a certain extent with less help from mechanical cooling.

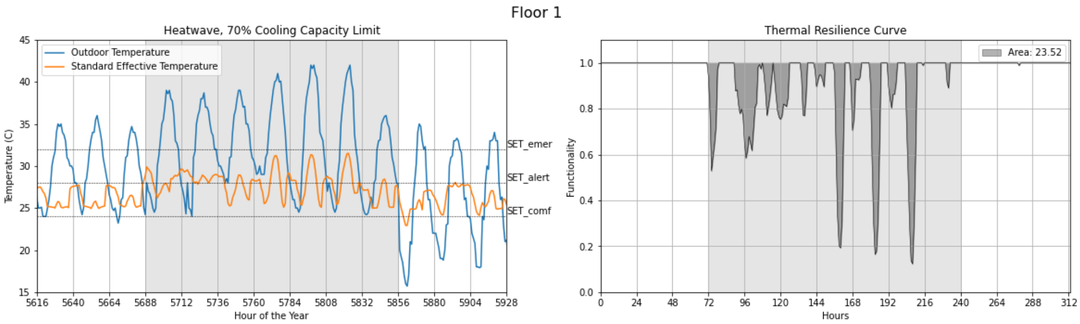

(a) Floor 1

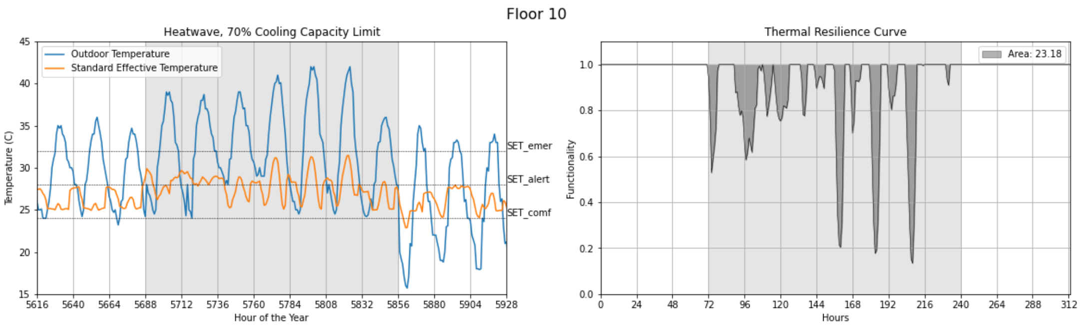

(b) Floor 10

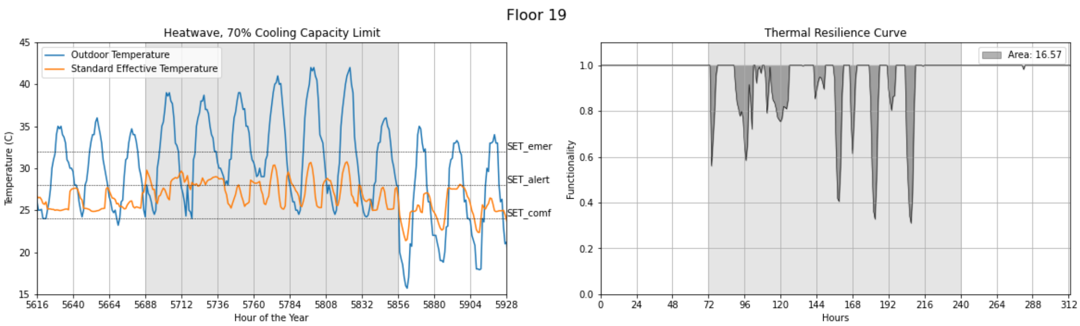

(c) Floor 18

Figure 5.13: Facade thermal resilience

6 Multi-attribute Decision Making

6.1 Decision Making in Early Design Stages

The first objective of the design tool is to enable the selection of a facade system that is more resilient to multiple hazards. A multi-criteria analysis that includes two criteria for seismic resilience and two criteria related to thermal resilience is implemented. The values for the four individual criteria are combined into one overall resilience value for each facade system. This value can then be compared across different facade systems.

6.1.1 Method: Multi-attribute analysis

The resilience of a facade system was measured in terms of resilience loss and economic loss. For seismic resilience, resilience loss was quantified by the total time of functionality loss (unit: days) and the degree of functionality loss (unit: value between 0 and 1). Economic loss was quantified by the total cost of repairment (unit: dollars). The time period for these values spanned from the outbreak of the event to the completion of repairs for the facade system. To evaluate thermal resilience, resilience loss was quantified by the total time of functionality loss (unit: hours) and the degree of functionality loss (unit: value between 0 and 1). Economic loss was quantified by the cost (unit: euros) of eliminating discomfort through mechanical cooling. The range of the values was refined during the seven-day heat event in the summer.

A radar chart, as shown in Figure 6.1, presents the values of the aforementioned criteria for facade package A01. As the multi-criteria have different scales, the radar chart displays the normalized values within their respective categories. The filled-in area of the radar chart represents the overall resilience characteristics of a facade package. The area value is calculated using un-normalized, real values from the table on the right. A lower area value indicates lower loss in terms of resilience and economics, resulting in higher overall resilience.

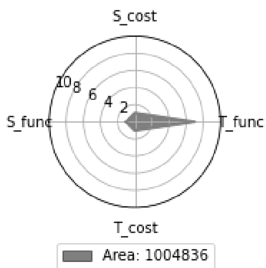

package	A01
S func	25.37
S cost	639761.17
T func	63.27
T cost	100.04

Figure 6.1: Radar chart with multi attributes

6.1.2 Selecting the Most Resilient Facade System

The radar plots in Figure 6.2 present the multi-criteria resilience results for facade packages under the same base building and hazard condition. The base setting assumed an 18-story building in Izmir that is at risk of experiencing an earthquake with a 10% probability of exceedance in 50 years (return period of 475 years) and a predicted heatwave with a maximum daily mean temperature increase of 5 degrees Celsius for 7 consecutive days.

The filled-in areas of radar charts were compared to determine which facade package is most suitable for a specific location with a certain hazard intensity. When making a decision based on the highest combined resilience, the infill system is the preferred choice. The infill system, which includes packages C and D, occupies a smaller area on the radar chart, indicating higher combined resilience when compared to the cladding system (packages A and B). However, when the facade packages have an equivalent combined resilience value, such as categories C and D, additional reasoning is necessary for selecting the design. For instance, building usage can be an additional criterion for selection. If the building is a hospital, minimizing thermal resilience loss would be prioritized over cost, and therefore package D would be selected instead of package C. This accounts for situations where compromising on indoor comfort is not an option. Another criterion to consider is the availability of a mechanical cooling system. While package D provides a more habitable space, it requires cooling through the system, which may not be available if the system is at capacity or nonexistent. In such cases, package D is automatically ruled out, leaving C as the best option for the given conditions.

<table>
<tr><th colspan="4">Component Fragility</th><th>Multi Attribute Facade Resilience</th></tr>
<tr><th colspan="2">Opaque</th><th colspan="2">Window</th><th rowspan="2">Functionality Loss (S_func, T_func)
Economic Loss (S_cost, T_cost)</th></tr>
<tr><th>Seismic</th><th>Thermal</th><th>Seismic</th><th>Thermal</th></tr>
<tr><td>B2011.121</td><td>W0.05T01</td><td>B2022.201</td><td>W0.95T01</td><td>Package A01</td></tr>
<tr><td colspan="4"></td><td>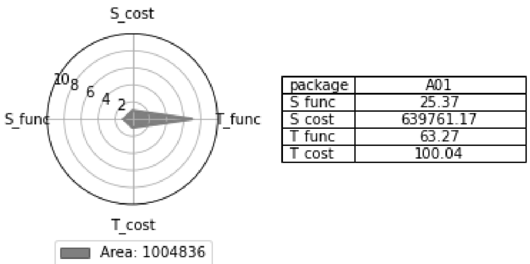
</td></tr>
<tr><td>B2011.121</td><td>W0.05C01</td><td>B2022.201</td><td>W0.95T01</td><td>Package B01</td></tr>
<tr><td colspan="4">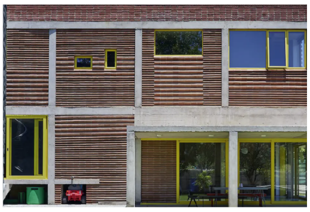</td><td>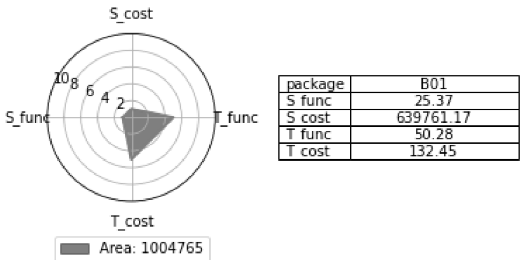
</td></tr>
<tr><td>B2011.302a</td><td>W0.05T01</td><td>B2022.011</td><td>W0.95T01</td><td>Package C01</td></tr>
<tr><td colspan="4">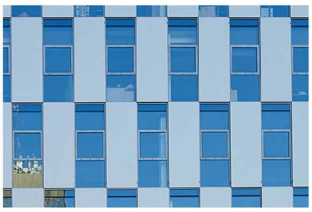</td><td>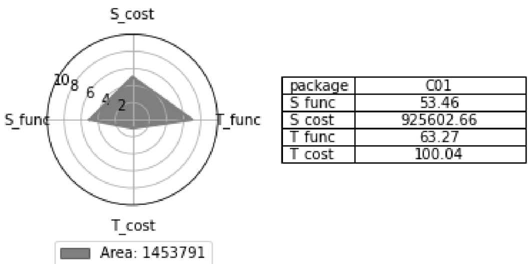
</td></tr>
<tr><td>B2011.302a</td><td>W0.05C01</td><td>B2022.011</td><td>W0.95T01</td><td>Package D01</td></tr>
<tr><td colspan="4">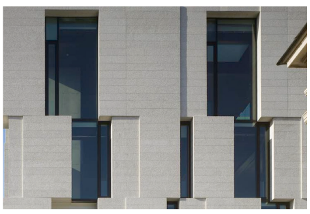</td><td>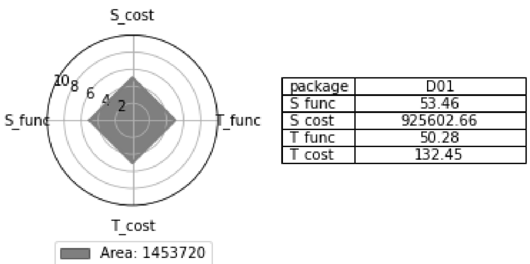
</td></tr>
</table>

Figure 6.2: Multi-attribute facade resilience

6.2 Strategies for Facade Retrofitting

Making decisions based on the highest combined resilience can be useful in situations where there are multiple possible options for facade systems. This is especially true in the early phases of design when quickly narrowing down options is more important. However, in situations where a system is already defined, such as in the case of a retrofit, it can be more useful to know how to improve performance based on the existing system.

6.2.1 Method: Fragility-based Decision Tree

To set up a facade package with enhanced performance, the fragility curves of the facade components in the database were compared with a standard intensity measure. A decision tree was then created, combining components with different damage probabilities.

Figure 6.3(a) shows seismic fragility curves for damage state 1 of eight different facade components. The intersection of the fragility curves at the point where intensity measure (inter-story drift) is 0.02 is marked. For example, the B2022.2021 facade component with an inter-story drift of 0.02 is estimated to have 27% damage. This difference in damage probability is then compared among the facade components.

Thermal fragility curves for limit state 3 (32°C) of six different facade components are shown in Figure 6.3(b). The intersection points indicate the probability of reaching the limit state when the intensity measure (mean outdoor temperature) is 28°C. W0.05C01, a thick concrete facade with high heat capacity, has a 13% probability of damage, whereas W0.05C02, a relatively thinner concrete facade, has a 32% probability of damage.

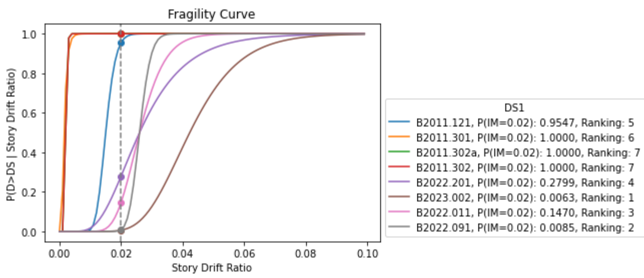

(a) seismic fragility curves

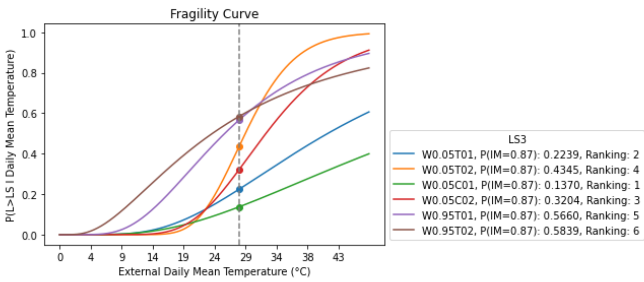

(b) thermal fragility curves

Figure 6.3: Comparison of fragility curves

Figure 6.4 illustrates how a decision tree is formed for a facade package. Facade package A01 is a combination of seismic fragility curves B2011.121, B2022.201, and thermal fragility curves W0.05T01, W0.95T01. Facade package A02, on the other hand, is a combination of fragility curves with higher damage probabilities compared to those selected for A01. This indicates that if an existing facade's component is A02, A01 can be used as a facade retrofitting strategy to decrease all aspects of seismic and thermal damage probabilities.

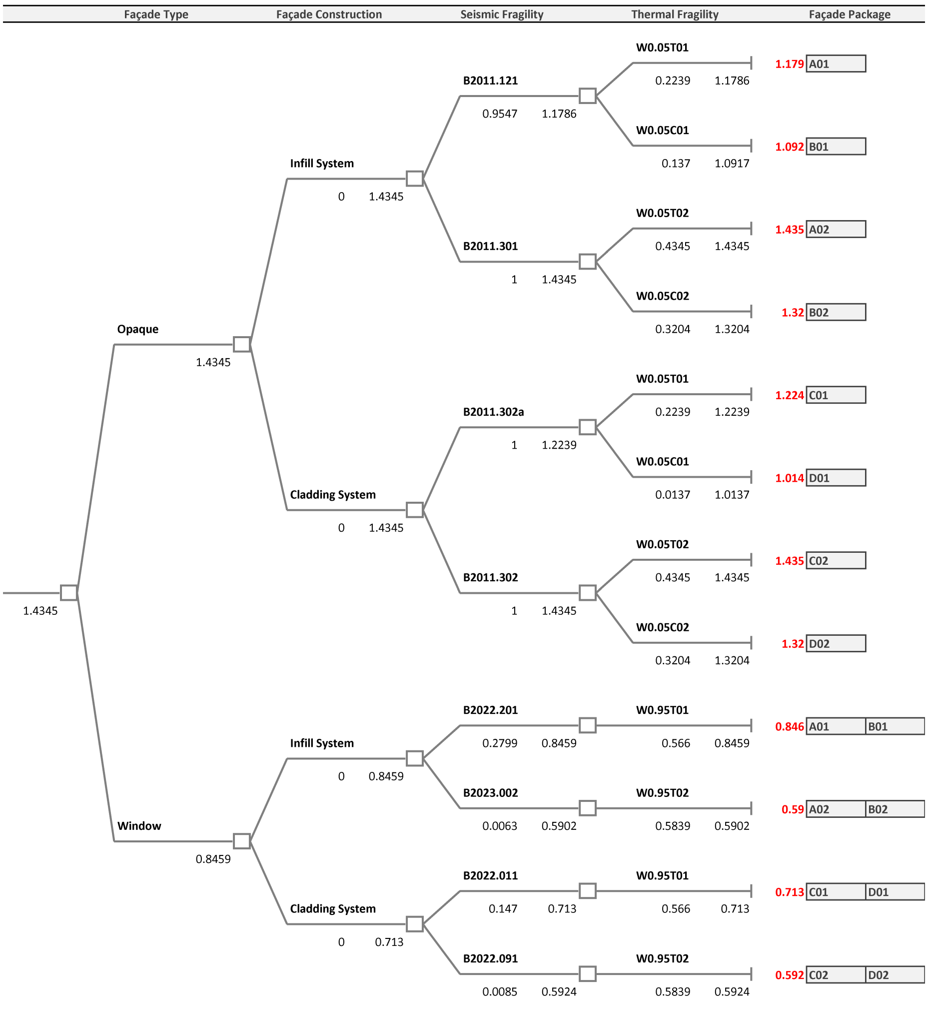

Figure 6.4: Facade package design tree

6.2.2 Configuring a system for improved resilience performance

A demonstration of how a facade package can be formed to configure a facade system for improved resilience performance is illustrated in Figure 6.5. By choosing a facade component with higher resistivity, both resilience and economic loss are reduced, resulting in improved resilience attributes. It should be noted that the thermal resilience loss is plotted as increased for the improved facade package, which is actually not the case. The thermal cost is decreased for the improved facade package, as less cooling energy is consumed. Although counterintuitive, when reading the values, it is recommended to focus on the three attributes: seismic resilience loss, seismic economical loss, and thermal economical loss.

Figure 6.6 includes a facade package of A02, B02, C02, D02 and Figure 6.7 includes a facade package of A01, B01,C01,D01. The facade package of Figure 6.7 is formed in a way that there's a decrease in the damage probability for all the opaque and window components within the package. As a result, both the combined resilience value (the area within the radar chart) and the individual values of the resilience attributes are improved.

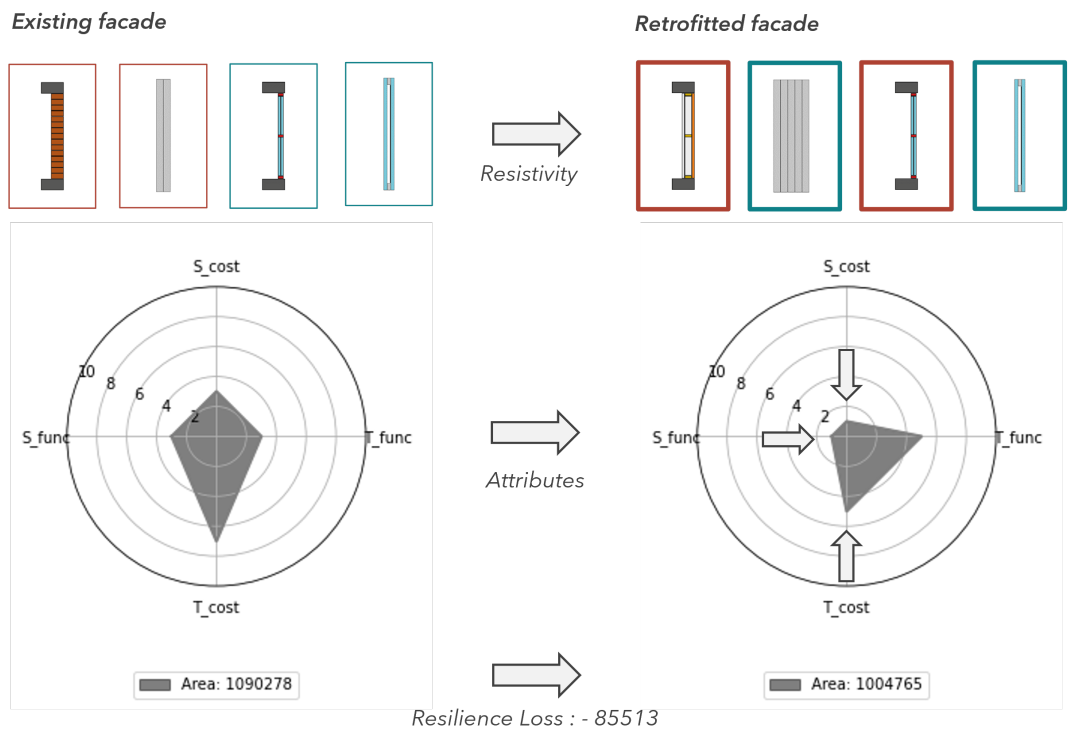

Figure 6.5: Resilience-based Retrofit Strategy

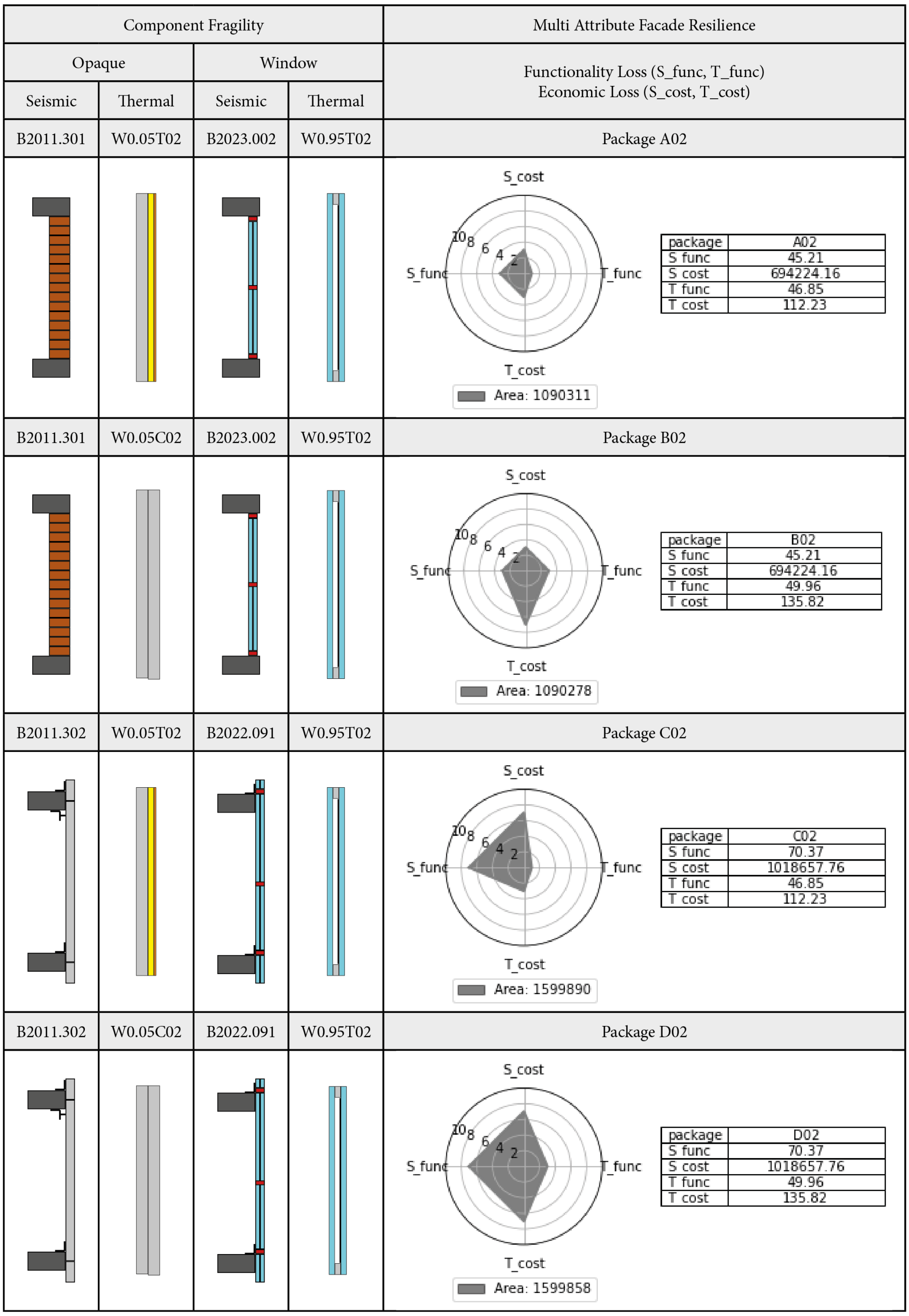

Figure 6.6: Facade packages with original performance

Component Fragility				Multi Attribute Facade Resilience	
Opaque		Window		Functionality Loss (S_func, T_func) Economic Loss (S_cost, T_cost)	
Seismic	Thermal	Seismic	Thermal		
B2011.121	W0.05T01	B2022.201	W0.95T01	Package A01	
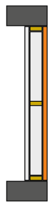	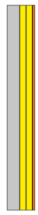	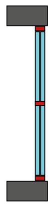		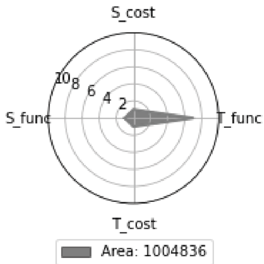	package A01 S func 25.37 S cost 639761.17 T func 63.27 T cost 100.04
B2011.121	W0.05C01	B2022.201	W0.95T01	Package B01	
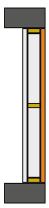	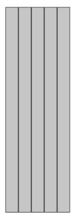	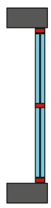	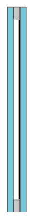	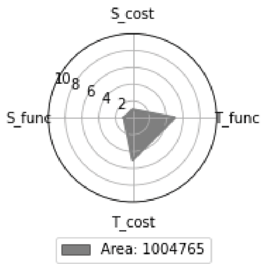	package B01 S func 25.37 S cost 639761.17 T func 50.28 T cost 132.45
B2011.302a	W0.05T01	B2022.011	W0.95T01	Package C01	
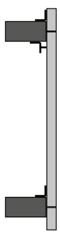	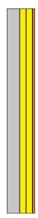	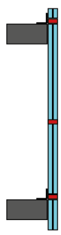	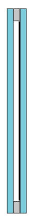	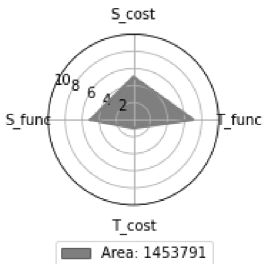	package C01 S func 53.46 S cost 925602.66 T func 63.27 T cost 100.04
B2011.302a	W0.05C01	B2022.011	W0.95T01	Package D01	
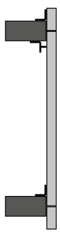	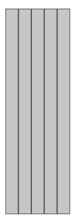	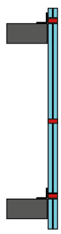	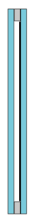	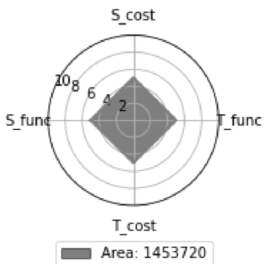	package D01 S func 53.46 S cost 925602.66 T func 50.28 T cost 132.45

Figure 6.7: Facade packages with improved performance

7 Conclusion

7.1 Discussion and Conclusions

With the increasing number and diversity of disruptive events imposed on the built environment, it is becoming more important to identify a system's resilience. Quantifying resilience is crucial because it enables effective preparation, recovery, and adaptation to the uncertainties that lie ahead.

This study focuses on the resilience of building facades, which play an integral role in a building's various functions, including environmental, structural, and operational performance. Facades contribute significantly to the total building damage, yet their resilience is not sufficiently addressed in current discourse. The main research question aims to address the research gap, which is:

> **What methodology can be developed to assess the resilience of facade systems under multiple hazards and integrate into the facade design process?**

To address the research question, this study developed a methodology with two main objectives: 1) evaluating the resilience of facades and 2) integrating this methodology into the facade design process. The following section presents the effectiveness of the proposed methodology, resilience-based facade design framework, in achieving these key objectives.

7.1.1 Assessing Facade Resilience

Which functional layer of the facade is measured for resilience?

Quantifying resilience involves a comprehensive evaluation of a system's vulnerability, resistance, robustness, and recovery. In this research, facade resilience was defined in a simplified manner, as the ability of a facade system to resist impact and recover to its original functional state. The resilience performance of the facade was evaluated based on its structural functionality (including structural stability and repairability) and thermal functionality (ability to maintain indoor thermal conditions at a comfortable state and recover back to comfort when necessary). The factors were assessed by modeling a case study building and conducting a simulation under disruptive events, using different facade systems.

How to assess the seismic resilience of a facade system?

A seismic hazard with a 475-year return period was assumed. Inter-story drift was used as a demand parameter to indicate the impact of the seismic hazard on the facade of each floor. Seismic performance assessment was conducted following the FEMA P-58 methodology. The calculation tool/fragility database PACT was used for probabilistic calculations and accumulation of losses. Functionality loss was calculated as the fraction of repair cost and replacement cost of the facade. Economic loss was calculated based on the total repair cost of the facade.

As a result, it was possible to assess the facade systems of four different facade packages, consisting of opaque and window components. The number of facade packages to be simulated relied mainly on the availability of fragility, repair measure, and repair cost data from the PACT repository. While the repository contained sufficient data on curtain walls, the information on masonry infill systems and concrete cladding systems were collected from literature.

How to assess the thermal resilience of a facade system?

A heatwave was defined as a heat hazard, with an increase of 5°C in the daily maximum outdoor temperature for 7 consecutive days. To indicate the impact of the heat hazard on the facade, an hourly outdoor air temperature was used as a demand parameter. To evaluate thermal performance, a dynamic thermal simulation was conducted using EnergyPlus. This simulation measured indoor thermal conditions during a heatwave, using the standard effective temperature (SET) as an intensity measure. Functionality loss was calculated as the degree-hours when the SET is above the comfort limit. Economic loss was calculated as the additional cost of cooling energy consumed during a heatwave, considering it as the cost of recovering the SET to a fully functional state.

The study successfully evaluated the facade systems of four distinct packages, which included both opaque and window components. However, certain assumptions made during the assessment of thermal resilience require further validation. In this research, the indoor thermal condition was used as an indirect measure of the facade's thermal state during heatwaves, since there is currently no defined metric or threshold for evaluating the facade's thermal condition. To assess the direct impact of heatwaves, mechanical cooling was used to maintain consistent indoor baseline conditions before, during, and after the heatwave. By using mechanical cooling during the heatwave, however, the degree of resilience loss was calculated to be lower when there was increased heat transfer due to the facade's thermal properties. As the cooling load increased, the mechanical cooling system had to work harder until it reached its capacity limit. Therefore, a facade that exhibited greater resistance to heat resulted in a higher resilience loss value. On the other hand, the economic loss accurately reflected the situation, as a more heat-resistant facade led to lower losses due to reduced cooling demand.

7.1.2 Assessing Facade Resilience to Multi Hazard

The study focused on assessing the resilience of building facades when exposed to seismic and heat hazards. It was assumed that these hazards would not occur simultaneously, enabling separate evaluations of the facade's resilience under seismic and thermal conditions. To evaluate the effect of seismic hazards on facade damageability, a finite element model from OpenSees and vulnerability assessment from PACT were employed. For assessing the impact of heat hazards on indoor thermal conditions, a thermal model from EnergyPlus was utilized.

Regarding seismic resistance, it was observed that precast concrete cladding with different connection types behaved as distinct systems, exhibiting varying degrees of damage. However, from a thermal perspective, these systems were considered as a single entity, accounting for the thermal properties of the concrete material only. To integrate the assessment data, a facade package was developed, comprising one structural model and one thermal model. This approach allowed for the generation of 16 facade packages through combinations of the four available models for each aspect. Consequently, it was possible to obtain an assessment value for a facade in relation to multiple hazards. However, it is important to note that the method employed in this study could not assess the combined effects of hazards on the facade, such as structural damage caused by thermal expansion.

7.1.3 Metrics for Comparing the Resilience of Facade Systems

To ensure a systematic evaluation of various facade types and incorporate the assessment into the design process, it is necessary to establish evaluation metrics for facade systems with different resilience values. Doing so will help identify a range of favorable facade systems and determine which design parameters contribute significantly to overall resilience.

In this research, the fragility curve of each component was adopted as a metric. For seismic fragility analysis, fragility functions in the form of lognormal cumulative distributions were used. The median value and logarithmic standard deviation value were extracted from the PACT fragility database. An intensity measure of maximum story drift (2%) was applied to compare the probability of reaching a damage state for different facade systems. Higher probabilities of damage indicate less favorable design choices. For thermal fragility analysis, fragility curves were generated using the maximum likelihood fragility function fitting method. An intensity measure of the SET alert threshold (28°C) was used to compare the probability of reaching the limit state.

A decision tree was constructed to evaluate and compare the resilience of facade packages with different combinations of 'probability of exceedance' values obtained from the fragility curve. This approach allows for the formulation of facade packages with varying fragility values. It is important to note that the fragility value will change depending on how the intensity measure is specified. The intensity measure should be defined and referenced according to the code-defined acceptable range to address this issue.

7.1.4 Implementing Resilience-based Facade Design

The resilience assessment produced a set of performance indicators, such as resilience loss and economic loss, which were used as decision-making criteria. A radar chart was utilized to visually represent these four attributes for each facade package. This information was used to make informed decisions during two distinct stages of building design.

During the early design phases, it is beneficial to quickly narrow down options. When considering the multifunctionality of a system and its ability to withstand multiple hazards, making an early-phase decision ensures a holistic approach and minimizes unnecessary iterations across multiple facade-related domains in later stages. This objective is accomplished by selecting a facade package with the highest combined attribute value. Such a choice indicates the least combined loss and signifies relative resilience compared to other facade packages under consideration.

In situations where a system is already defined, such as in retrofitting projects, knowing how to enhance performance based on the existing system becomes more valuable. A decision tree was employed to configure a facade package with a lower probability of damage. For instance, if the existing system consisted of facade components with a second level of seismic and thermal performance, another system incorporating facade components with a first level of seismic and thermal performance was configured. Swapping different facade components allowed for the configuration of an overall improved system. Furthermore, this method also facilitated partial improvements based on the specific weights of importance specified by the project.

7.2 Future Research Needs

This research has developed an initial framework for resilient facade design through the utilization of quantitative resilience assessment. The subsequent focus of this study will primarily revolve around enhancing the framework by addressing its current limitations and broadening its applicability through the management of larger datasets.

The quantified resilience outcomes can be heavily influenced by the metrics and performance measures used in the assessment. Therefore, the framework's performance measures are examined to ensure that they accurately measure the intended attributes (validity), address the most critical factors (relevance), and are applicable to different contexts (flexibility). First, the limitations of the current method are addressed, and a possible approach is suggested. Figure 7.1 summarizes the performance measures used in the framework and indicates the sector where further research is required.

Validity

SET Threshold for mechanically conditioned spaces

- he thermal safety threshold defined by RELi and the comfort PTS scale developed by ASHRAE both consider the Standard Effective Temperature (SET) in naturally conditioned spaces. This passive habitability assumes that no HVAC system is present or power outages occur. However, a hybrid habitability should be considered to determine a line where appropriate material selection and HVAC sizing result in an increased thermal resilience.
- This research examines hybrid habitability by using HVAC systems with a cooling capacity limit in conjunction with facade systems of varying thermal properties. Naturally conditioned spaces have a wider range of tolerable temperatures. Therefore, in these spaces, the ”neutral comfort” state of the Predicted Mean Vote (PMV) scale of 24°C was used as the threshold for ”overheating.” However, this value is assumed and requires validation. When determining the PMV value thresholds for overheating in mechanically conditioned spaces, the cooling set point temperature of 24°C and a 70% cooling capacity limit must also be taken into consideration.

SET Threshold outside the comfort range

- This research uses the predicted thermal sensation (PTS) scale to determine the threshold value of SET. The PTS scale primarily assesses the comfort range, without considering conditions beyond habitable limits. As distance from the comfort threshold increases, loss also increases linearly. Currently, there is no upper limit that indicates failure. To accurately define the limit states of SET and its association with facade failure, it is crucial to develop a threshold value that encompasses conditions outside

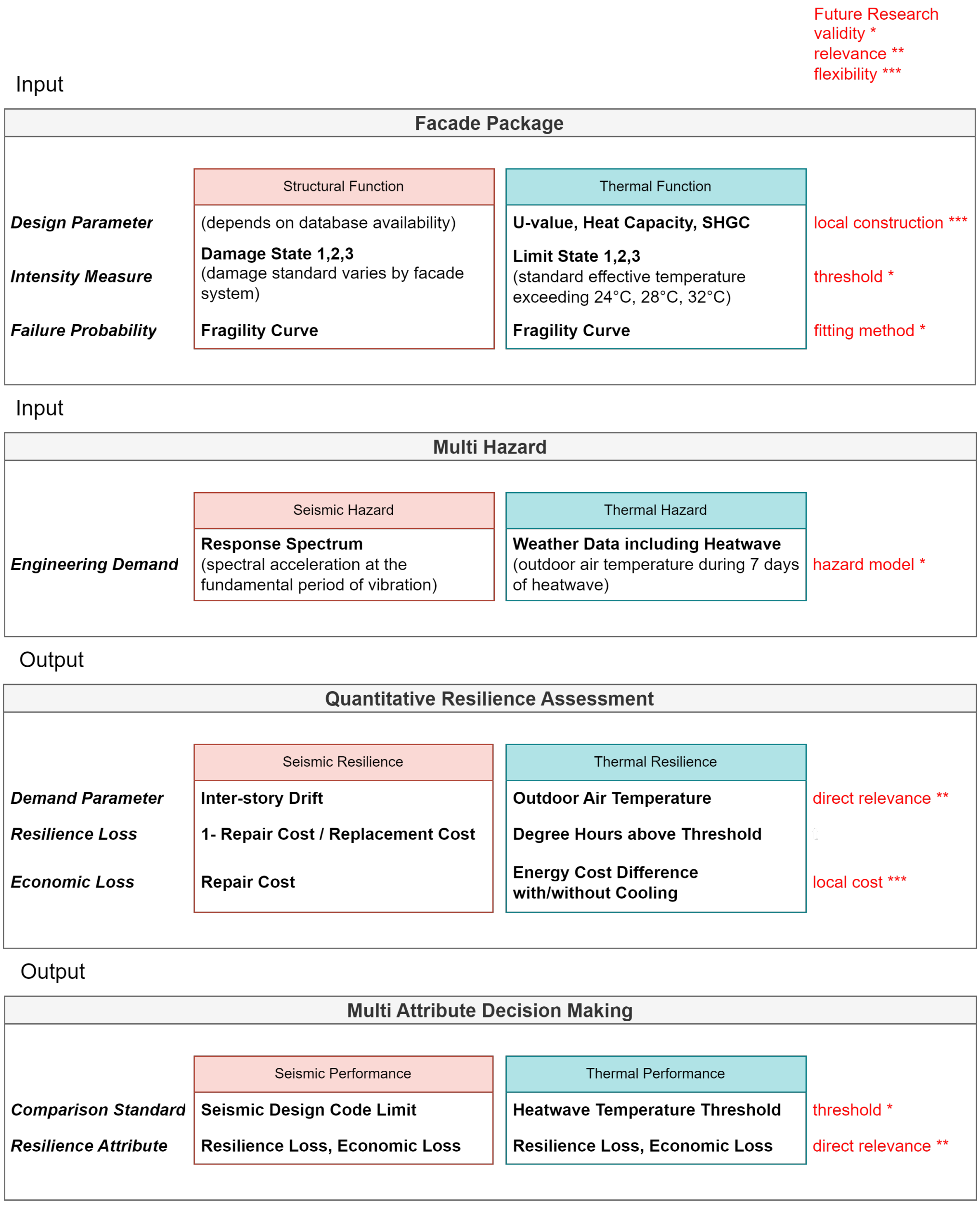

Figure 7.1: Framework performance measures

the comfort zone and accounts for potential system failures. This requires a definition of the failure of thermal control capability in terms of SET values.

Validation of thermal fragility function

- The fragility fitting method (maximum likelihood fitting) employed in creating thermal fragility curves has demonstrated stability for the limit state of SET 32°C. However, it has encountered difficulties in fitting the fragility curves for the other two limit states. Therefore, it is necessary to evaluate the suitability of the fragility fitting method for generating accurate and reliable fragility curves in those cases. Alternative methods or modifications to the fitting procedure should be explored to ensure robustness and consistency in curve creation across different limit states.
- Using the daily mean outdoor temperature as the demand parameter raises concerns about its ability to capture the dynamic nature of indoor thermal conditions. A single temperature value cannot account for temperature peaks or shifts that occur throughout the day. By considering multiple temperature readings at different time intervals, a more accurate representation of the dynamic thermal conditions can be obtained.

Hourly weather data from heat hazard model

- The generated weather data, which includes heatwave days, does not account for uncertainty or realistic simulation of heatwave events. A heatwave is defined as an average temperature exceeding certain threshold for certain days, which the heat hazard model is also based on. A daily average temperature is too sparse as an input for a dynamic thermal simulation that generates an hourly output. That's why in this research the generated weather data has a consistent 5°C difference throughout 168 hours, which does not reflect real weather conditions where temperature differences fluctuate. Future research is needed to take probability-based heat hazard models and generate an hourly weather data file.

Threshold values for comparing failure probabilities

- The allowable story drift limit of 2% from ASCE 7-10 was used as the threshold value for comparing failure probabilities in the seismic fragility function. However, this limit is not specific to the RC dual system used in this research, so a more precise threshold value should be applied.
- The level of damage being compared is comparable when comparing fragility curves based on different definitions of damage states. For example, damage state 2 in a stud wall indicates a tear-out of nails and sheathing, while damage state 2 in a curtain wall represents glass cracking. Therefore, it is recommended to compare fragility functions based on the same definitions of damage states or similar levels of damage states.
- A threshold outdoor temperature of 28°C, which is the Met Office's heatwave threshold, was used to compare the failure probabilities of thermal fragility functions. However, this value may not accurately indicate a heatwave, as it is based on UK climate conditions. It is important to note that heatwave thresholds not only differ by climate zone, but also change over time. With climate change, heatwave threshold values are increasing, which should be considered when determining the appropriate threshold value.

Relevance

Direct relevance between demand parameter and intensity measure

- The probability of the seismic demand parameter, inter-story drift, reaching the damage state is measured using the fragility function. In this function, the demand parameter and intensity measure have a direct relation. However, for the thermal fragility function, the outdoor air temperature (demand parameter) and the SET limit state (intensity measure) are not necessarily in direct relation. As a result, it's not possible to distinguish the resistance to heat of different components if they experience the same outdoor temperature and resulting SET. Therefore, using the indoor surface temperature as a demand parameter, which has gone through heat transfer of the exterior wall, could potentially be a better representation of the causative demand for reaching SET. If the indoor surface temperature is used as the demand parameter, a standard threshold value indicating the heat risk should also be identified through statistical studies.

Thermal resilience loss directly due to facade system

- Seismic resilience loss is directly proportional to economic loss, as the extent of damage from an event is taken into account when calculating repair costs. Conversely, thermal resilience loss is inversely proportional to economic loss. Within the cooling capacity limit, when the cooling load increases, the cost of cooling also increases, but the resulting resilience loss decreases because the cooling load is removed by cooling. This inconsistency in the representation of loss between seismic and thermal can be overcome by applying a higher capacity limit.

Flexibility

Fragility functions for local facade construction

- The range of facade design options should reflect the typical construction type used in the location to ensure availability and reduce embodied carbon. Increasing the number of data points will allow for optimizing design parameters based on resilience objectives.
- The FEMA P58 fragility function database contains relatively sufficient information on stick system curtain walls, but lacks data on unitized glazing systems. Additionally, experimental testing of the seismic behavior of prefabricated facade systems, ranging from lightweight to heavyweight and including diverse connection types, is necessary to establish fragility functions for these systems.
- The effective thermal resistance value varies by climate zone, and the range of these values should be the baseline for examining facade systems. R-values for specific climate zones and building types can be determined by referencing ASHRAE 90.1. Once this is done, it can be determined whether a high-performance building envelope with good insulation and airtightness for a given location contributes to overheating.

Pricing tariff based on locations

- Resilience and economic loss are the two primary decision-making attributes. The calculation of resilience loss takes into account many location-related factors, such as the intensity of seismic hazards and weather data. Economic loss should also reflect location effects. The seismic repair cost from FEMA P58 is based on US statistical data, which means that cost factors for Europe are necessary if the location is in Europe. In this research, the energy cost is calculated using a single electricity tariff for all of Europe. However, it should reflect the different tariffs of countries and cities because they can differ significantly. This cost also varies by building type and time of day, so it should also be taken into account.

The framework does not aim to find a universally applicable, single resilient facade system. Instead, its goal is to identify facade systems that perform well in the specific context of their placement. As a result, the framework should consistently incorporate the unique aspects of each project. This requires implementing the framework in various types of case study buildings and locations, or by utilizing alternative measures to evaluate the resilience of the current case study building. Only then can the assessment methodology be used to set standards or requirements for resilient facades.

8 Reflection

Societal Impact

Resilience is a topic that is gaining more attention in practice, as a response to the increasing frequency of climate-induced disruptive events on a global scale that affect not only the built environment, but also a wide range of economic and social aspects. The recent trend in resilience is a shift towards a proactive approach to risk management, with a consensus that the likelihood of climate change is certain, and that the built environment should anticipate and prepare for future risks. This graduation project aims to address the increasing demand for dealing with engineering uncertainties by developing a practical tool that can provide prompt and specific design solutions to the problem. As the research in this area is relatively new, the project aims to fill a knowledge gap in dealing with multi-hazard problems and measuring resilience at the building level.

Graduation Process

The studio topic is "Digital building design tools for climate resilient structures". As a subset of the studio topic, I have chosen to focus on quantification of resilience, specifically of facade under hazard of natural disaster and extreme weather event. This project aligns with the Structural Design and Facade & Product Design chairs within the Building Technology track and requires a multidisciplinary approach, incorporating knowledge from structural and facade design, building physics, and risk management methodologies from earthquake engineering. Utilizing knowledge gained during my master's program and resources from my mentor's ongoing research, the project aims to deliver an integrated approach through the interdisciplinary environment of the AET faculty.

Upon reflecting on the original approach and goal of the thesis project, the primary objective was to create a novel framework that combines keywords such as "multi-hazard approach," "facade resilience," and "resilience-based design," which had not been previously explored. This objective was successfully achieved. However, the absence of an existing methodology posed an additional challenge in both developing and evaluating the framework. The most difficult task involved establishing a consistent methodology that could encompass these two distinct subjects. The field of seismic engineering has well-established methodologies for risk assessment and resilience quantification. In contrast, thermal resilience, particularly at the building component scale, is a relatively new and emerging topic with no established methodology. To overcome this challenge, I adapted the methodology used in seismic risk assessment to address the thermal aspect, despite the disparities in properties and measures. For instance, I generated a thermal fragility curve and used it to assess thermal resilience, providing new insights from a facade perspective.

Throughout the process, my focus became too heavily centered on developing the framework and establishing a digital workflow. Fortunately, my mentors reminded me of the core purpose of the framework and emphasized the importance of its applicability. From the beginning, I was challenged to consider the implications of quantifying the resilience of a facade system and how this information contributes to the decision-making process.

These questions prompted me to incorporate this line of thinking into the framework's development from the early stages, rather than treating it as an afterthought. This approach significantly influenced the selection of simulation outputs and served as a validation check to ensure the relevance and utility of the results. Considering these factors, I am satisfied with the current outcome of the framework.

Transferability

The framework is designed to assist engineers in making design decisions for multi-hazard problems. However, if the user wants to precisely adjust the design parameters and see the results accordingly, or if an analysis on an urban scale is required, major adjustments must be made to the framework, particularly regarding fragility functions. While the components are defined as fragility functions, which are useful for analyzing the combined performance of an integrated facade system, they are not very efficient when dealing with many individual parameters.

Another aspect that needs to be addressed is the transferability of knowledge and all the information contained within the framework. While the research mainly used Python as a common scripting language for analysis, the use of many separate existing tools makes the current framework less fluid. More effort can be invested in developing an integrated data platform that allows for interoperability. Furthermore, the framework should be able to communicate not only with specific target users but also with non-experts. This would broaden the applicability of the research and gather external feedback for further development. Just as cost was used as one of the resilience loss indicators, the inputs and outputs should be structured with tangible indicators that are understandable for the general audience.

Bibliography

Almufti, I., & Willford, M. (2013). *REDi ™ Rating System Resilience-based Earthquake Design Initiative for the Next Generation of Buildings* (tech. rep.).

American Society of Civil Engineers. (2010). Seismic Design Requirements for Nonstructural Components. In *Asce 7-10: Minimum design loads for buildings and other structures* (p. 608).

ASCE. (2010). ASCE 7-10: Minimum Design Loads for Buildings and Other Structures.

ASHRAE 55. (2017). ASHRAE Standard 55-2017 Thermal Environmental Conditions for Human Occupancy.

Attia, S., Levinson, R., Ndongo, E., Holzer, P., Berk Kazanci, O., Homaei, S., Zhang, C., Olesen, B. W., Qi, D., Hamdy, M., & Heiselberg, P. (2021). Resilient cooling of buildings to protect against heat waves and power outages: Key concepts and definition. *Energy and Buildings*, *239*, 110869. https://doi.org/10.1016/J.ENBUILD.2021.110869

Attia, S., Rahif, R., Corrado, V., Levinson, R., Laouadi, A., Wang, L., Sodagar, B., Machard, A., Gupta, R., Olesen, B., Zinzi, M., & Hamdy, M. (2020). Framework to evaluate the resilience of different cooling technologies. https://doi.org/10.13140/RG.2.2.33998.59208

Baird, A., Palermo, A., & Pampanin, S. (2013). Controlling Seismic Response using Passive Energy Dissipating Cladding Connections. *2013 NZSEE Conference*.

Baird, A., Palermo, A., Pampanin, S., Riccio, P., & Tasligedik, A. S. (2011). Focusing on reducing the earthquake damage to facade systems. *Bulletin of the New Zealand Society for Earthquake Engineering*, *44*(2), 108–120. https://doi.org/10.5459/bnzsee.44.2.108-120

Baker, J. W. (2015). Efficient Analytical Fragility Function Fitting Using Dynamic Structural Analysis. https://doi.org/10.1193/021113EQS025M

Baniassadi, A., & Sailor, D. J. (2018). Synergies and trade-offs between energy efficiency and resiliency to extreme heat – A case study. *Building and Environment*, *132*, 263–272. https://doi.org/10.1016/J.BUILDENV.2018.01.037

Bedon, C., & Amadio, C. (2018). Numerical assessment of vibration control systems for multi-hazard design and mitigation of glass curtain walls. *Journal of Building Engineering*, *15*, 1–13. https://doi.org/10.1016/J.JOBE.2017.11.004

Beers, P. E. (2011). Wind Risk Assessments for Cladding and Glazing in Critical Facilities.

Bianchi, S., Ciurlanti, J., Overend, M., & Pampanin, S. (2022). A probabilistic-based framework for the integrated assessment of seismic and energy economic losses of buildings. *Engineering Structures*, *269*, 114852. https://doi.org/10.1016/J.ENGSTRUCT.2022.114852

Bianchi, S., & Pampanin, S. (2022). Fragility Functions for Architectural Nonstructural Components. *Journal of Structural Engineering*, *148*(10). https://doi.org/10.1061/(ASCE)ST.1943-541X.0003352

Brundtland, G., & Khalid, M. (1987). *World Commission on Environment and Development: Our Common Future* (Vol. 4). Oxford University Press, https://doi.org/10.1080/07488008808408783

Bruneau, M., & Reinhorn, A. (2006). Overview of the Resilience Concept.

Bruneau, M., Chang, S. E., Eguchi, R. T., Lee, G. C., O'Rourke, T. D., Reinhorn, A. M., Shinozuka, M., Tierney, K., Wallace, W. A., & Von Winterfeldt, D. (2019). A Framework to Quantitatively Assess and Enhance the Seismic Resilience of Communities. *https://doi.org/10.1193/1.1623497*, *19*(4), 733–752. https://doi.org/10.1193/1.1623497

Bucking, S., Rostami, M., Reinhart, J., & St-Jacques, M. (2022). On modelling of resiliency events using building performance simulation: a multi-objective approach. *Journal of Building Performance Simulation*, *15*(3), 307–322. https://doi.org/10.1080/19401493.2022.2044906

Building Seismic Safety Council. (2003). *FEMA 450:2003* (tech. rep.). www.bssconline.org

Cardone, D., & Perrone, G. (2015). Developing fragility curves and loss functions for masonry infill walls. *Earthquake and Structures*, *9*(1), 257–279. https://doi.org/10.12989/eas.2015.9.1.257

Charleson, A. (2008). *Seismic design for architects : outwitting the quake*. Architectural Press.

Chiu, G. L., & Chock, G. Y. (1998). Multihazard Performance Based Objective Design for Managing Natural Hazards Damage. *IFAC Proceedings Volumes*, *31*(28), 159–164. https://doi.org/10.1016/S1474-6670(17)38490-2

Ciurlanti, J., Bianchi, S., Palmieri, M., & Pampanin, S. (2019). FEASIBILITY STUDY OF LOW-DAMAGE TECHNOLOGY FOR HIGH-RISE PRECAST CONCRETE BUILDINGS. *Earthquake risk and engineering towards a resilient world*.

de Rubeis, T., Nardi, I., Muttillo, M., & Paoletti, D. (2020). The restoration of severely damaged churches – Implications and opportunities on cultural heritage conservation, thermal comfort and energy efficiency. *Journal of Cultural Heritage*, *43*, 186–203. https://doi.org/10.1016/J.CULHER.2019.11.008

European Comitee for Standardisation. (1998). *EN 1998-1:2004/AC:2009 - Eurocode 8: Design of structures for earthquake resistance - Part 1: General rules, seismic actions and rules for buildings* (tech. rep.). Brussels, Belgium. https://standards.iteh.ai/catalog/standards/cen/b72212d1-f818-46ed-8d30-86442dc67cf1/en-1998-1-2004-ac-2009

Favoino, F., Chalumeau, A., & Aquaronne, A. (2022). Facade Resilience Evaluation Framework: A Qualitative Evaluation Tool To Support Resilient Facade Design Decision Making. https://www.facadetectonics.org/papers/facade-resilience-evaluation-framework

FEMA P-58. (2018). Seismic Performance Assessment of Buildings Volume 1-Methodology. *Federal Emergency Management Agency*. www.ATCouncil.org

Flores-Larsen, S., Bre, F., & Hongn, M. (2022). A performance-based method to detect and characterize heatwaves for building resilience analysis. *Renewable and Sustainable Energy Reviews*, *167*. https://doi.org/10.1016/J.RSER.2022.112795

Flores-Larsen, S., & Filippín, C. (2021). Energy efficiency, thermal resilience, and health during extreme heat events in low-income housing in Argentina. *Energy and Buildings*, *231*, 110576. https://doi.org/10.1016/J.ENBUILD.2020.110576

Gao, J., Wang, Y., & Wargocki, P. (2015). Comparative analysis of modified PMV models and SET models to predict human thermal sensation in naturally ventilated buildings. *Building and Environment*, *92*, 200–208. https://doi.org/10.1016/J.BUILDENV.2015.04.030

Hamdy, M., Carlucci, S., Hoes, P. J., & Hensen, J. L. (2017). The impact of climate change on the overheating risk in dwellings—A Dutch case study. *Building and Environment*, *122*, 307–323. https://doi.org/10.1016/J.BUILDENV.2017.06.031

Homaei, S., & Hamdy, M. (2021a). Quantification of Energy Flexibility and Survivability of All-Electric Buildings with Cost-Effective Battery Size: Methodology and Indexes. *Energies 2021, Vol. 14, Page 2787*, *14*(10), 2787. https://doi.org/10.3390/EN14102787

Homaei, S., & Hamdy, M. (2021b). Thermal resilient buildings: How to be quantified? A novel benchmarking framework and labelling metric. *Building and Environment*, *201*. https://doi.org/10.1016/J.BUILDENV.2021.108022

Hulley, G. C., Dousset, B., & Kahn, B. H. (2020). Rising Trends in Heatwave Metrics Across Southern California. *Earth's Future*, *8*(7). https://doi.org/10.1029/2020EF001480

Jami, M., Rupakhety, R., Elias, S., Bessason, B., & Snæbjörnsson, J. T. (2022). Recent Advancement in Assessment and Control of Structures under Multi-Hazard. *Applied Sciences 2022, Vol. 12, Page 5118*, *12*(10), 5118. https://doi.org/10.3390/APP12105118

Ji, L., Shu, C., Laouadi, A., Lacasse, M., & Wang, L. ((2023). Quantifying improvement of building and zone level thermal resilience by cooling retrofits against summertime heat events. *Building and Environment*, *229*. https://doi.org/10.1016/j.buildenv.2022.109914

Joyner, M. D., & Sasani, M. (2018). Multihazard Risk-Based Resilience Analysis of East and West Coast Buildings Designed to Current Codes. *Journal of Structural Engineering*, *144*(9). https://doi.org/10.1061/(asce)st.1943-541x.0002132

Katal, A., Mortezazadeh, M., & Wang, L. ((2019). Modeling building resilience against extreme weather by integrated CityFFD and CityBEM simulations. *Applied Energy*, *250*, 1402–1417. https://doi.org/10.1016/J.APENERGY.2019.04.192

Klein, T. (2013). *Integral Façade Construction Towards a new product architecture for curtain walls*. Architecture; the Built Environment.

Mathew, P., Sanchez, L., Lee, S. H., & Walter, T. (2021). Assessing the Energy Resilience of Office Buildings: Development and Testing of a Simplified Metric for Real Estate Stakeholders. *Buildings 2021, Vol. 11, Page 96*, *11*(3), 96. https://doi.org/10.3390/BUILDINGS11030096

Mckay, A. E., Jones, C. A., Conrath, ; E., & Davis, C. (2015). *Multi-Hazard Design of Facades: Important Considerations of Wind and Seismic Interaction with Blast Requirements* (tech. rep.).

Milovanovic, B., Bagaric, M., Gaši, M., & Stepinac, M. (2022). Energy renovation of the multi-residential historic building after the Zagreb earthquake – Case study. *Case Studies in Thermal Engineering*, *38*, 102300. https://doi.org/10.1016/J.CSITE.2022.102300

Nardini, V., & Doebbel, F. (2016). Performance-Based Concept for Design of Structural Silicone Joints in Façades Exposed to Earthquake. In C. Louter, F. Bos, & J. Belis (Eds.), *Challenging glass 5 – conference on architectural and structural applications of glass*.

National Research Council. (2012). The Nation's Agenda for Disaster Resilience. In *Disaster resilience: A national imperative* (pp. 1–244). National Academies Press. https://doi.org/10.17226/13457

O'Brien, W., & Bennet, I. (2016). Simulation-Based Evaluation of High-Rise Residential Building Thermal Resilience. *ASHRAE Transactions; Atlanta*, *122*, 455–468.

Ouyang, Z., Spence, S. M. J., & Asce, A. M. (2020). A Performance-Based Wind Engineering Framework for Envelope Systems of Engineered Buildings Subject to Directional Wind and Rain Hazards. https://doi.org/10.1061/(ASCE)

Ozkan, A., Kesik, T., Yilmaz, A. Z., & O'Brien, W. (2019). Development and visualization of time-based building energy performance metrics. *Building Research and Information*, *47*(5), 493–517. https://doi.org/10.1080/09613218.2018.1451959

Padgett, J., & Kameshwar, S. (2016). Supporting Life Cycle Management of BridgesThrough Multi-Hazard Reliability and RiskAssessment. In P. Gardoni & J. LaFave (Eds.), *Multi-hazard approaches to civil infrastructure engineering* (1st ed., pp. 41–58). Springer.

Patel, D., & Amin, J. A. (2015). Evaluation of Shear Wall-RC Frame Interaction of High-rise Buildings using 2-D Model Approach. *JOURNAL OF MATERIALS AND ENGINEERING STRUCTURES*, *2*, 111–119.

Patterson, M., Kensek, K., & Noble, D. (2017). Supple Skins: Considering the Relevance, Scalability, and Design Strategies for Façade System Resilience. *71*(1), 34–45. https://doi.org/10.1080/10464883.2017.1260919

Pomianowski, M., Heiselberg, P., & Zhang, Y. (2013). Review of thermal energy storage technologies based on PCM application in buildings. *Energy and Buildings*, *67*, 56–69. https://doi.org/10.1016/J.ENBUILD.2013.08.006

Ramakrishnan, S., Wang, X., Sanjayan, J., & Wilson, J. (2017). Thermal performance of buildings integrated with phase change materials to reduce heat stress risks during extreme heatwave events. *Applied Energy*, *194*, 410–421. https://doi.org/10.1016/J.APENERGY.2016.04.084

Sailor, D. J. (2014). Risks of summertime extreme thermal conditions in buildings as a result of climate change and exacerbation of urban heat islands. *Building and Environment*, *78*, 81–88. https://doi.org/10.1016/J.BUILDENV.2014.04.012

SHARE. (2013). ESHM13 The 2013 European Seismic Hazard Model: key components and results. https://doi.org/10.1007/s10518-015-9795-1

Siu, C. Y., O'Brien, W., Touchie, M., Armstrong, M., Laouadi, A., Gaur, A., Jandaghian, Z., & Macdonald, I. (2023). Evaluating thermal resilience of building designs using building performance simulation – A review of existing practices. *Building and Environment*, *234*, 110124. https://doi.org/10.1016/J.BUILDENV.2023.110124

Sun, H., Calautit, J. K., & Jimenez-Bescos, C. (2022). Examining the regulating impact of thermal mass on overheating, and the role of night ventilation, within different climates and future scenarios across China. *Cleaner Engineering and Technology*, *9*, 100534. https://doi.org/10.1016/J.CLET.2022.100534

Sun, S., Kensek, K., Noble, D., & Schiler, M. (2016). A method of probabilistic risk assessment for energy performance and cost using building energy simulation. *Energy and Buildings*, *110*, 1–12. https://doi.org/10.1016/J.ENBUILD.2015.09.070

Szagri, D., & Szalay, Z. (2022). Theoretical fragility curves A novel approach to assess heat vulnerability of residential buildings. *Sustainable Cities and Society*, *83*. https://doi.org/10.1016/J.SCS.2022.103969

The Rockefeller Foundation & Arup. (2014). *City Resilience Index, Understanding and measuring city resilience* (tech. rep.).

Theodosiou, T. G., Tsikaloudaki, A. G., & Bikas, D. K. (2014). Thermal Bridging Analysis on Cladding Systems for Building Facades. http://lbcp.civil.auth.gr

UNDDR. (2020). *Hazard Definition & Classification Review (Technical Report)* (tech. rep.). https://doi.org/10.13140/RG.2.2.28232.34561

United Nations. (2022). *The Sustainable Development Goals Report* (tech. rep.).

US Department of Defense. (2018). *United Facilities Criteria (UFC) DoD Minimum Antiterrorism Standards for Buildings* (tech. rep.).

USGBC. (2018). Rating Guidelines for Resilient Design + Construction RELi 2.0 I RELi 2.0.

Vailati, M., Monti, G., & Di Gangi, G. (2017). Earthquake-Safe and Energy-Efficient Infill Panels for Modern Buildings. In *Geotechnical, geological and earthquake engineering* (pp. 233–261). Springer, Cham. https://doi.org/https://doi.org/10.1007/978-3-319-62099-2{_}12

Wang, Q., Chen, H., Wang, Y., & Sun, J. (2013). Thermal shock effect on the glass thermal stress response and crack propagation. *Procedia Engineering*, *62*, 717–724. https://doi.org/10.1016/J.PROENG.2013.08.118

White, L. M., & Wright, G. S. (2020). ASSESSING RESILIENCY AND PASSIVE SURVIVABILITY IN MULTIFAMILY BUILDINGS. www.ibpsa.us

World Bank. (2017). *EH_GLOBAL_VITO_100 Development of a hazard screening protocol for Extreme Heat (Selection# 1228917)* (tech. rep.).

Wûest, T., & Luible, A. (2016). Increased thermal induced climatic load in insulated glass units. *Journal of Facade Design and Engineering*, *4*(3-4), 91–113. https://doi.org/10.3233/FDE-161146

Zhang, C., & Kazanci, O. B. (2021). Resilient cooling strategies – A critical review and qualitative assessment. *Energy and Buildings*, *251*, 111312. https://doi.org/10.1016/J.ENBUILD.2021.111312